**Ana Marta Correia Alves Diniz**

*Mestre em Bioorgânica*

# Multiresponsive Supramolecular Systems for Information Processing at the Molecular Level

Dissertação para obtenção do Grau de Doutor em Química Sustentável

Orientador: Professor Doutor Fernando Pina, Professor Catedrático, FCT-UNL
Co-orientador: Professor Doutor A. Jorge Parola, Professor Associado, FCT-UNL

Júri:

Presidente: Prof. Doutor Fernando Manuel Anjos Henriques

Arguente(s): Prof. Doutora Laura Rodríguez Raurell
Prof. Doutor Nathan David McClenaghan

Vogais: Doutor José Paulo da Silva

FACULDADE DE CIÊNCIAS E TECNOLOGIA
UNIVERSIDADE NOVA DE LISBOA

**Dezembro de 2013**

**Multiresponsive Supramolecular Systems for Information Processing at the Molecular Level**

To my parents
Aos meus pais

*"Nothing happens unless first we dream"*

Carl Sandbug

# Acknowledgments

There are times like these that make us look back and realize that four years, we thought they would be an eternity, actually spent running. It is a significant time and the people who accompanied me along this amazing journey are not so few. I want to thank them all.

The first person I would like to thank is Dr. César Laia. In the many hours spent in the flash photolysis during my Masters and in the several conversations we had you encouraged me to an idea, that it has been just a dream: to persist in research and to do a PhD. A thank from the heart César, for sowing the seed, for sharpening my curiosity, for all the incentives and discussions.

My special thanks to my patient bosses Fernando Pina and Jorge Parola, each unique in his own way, for believing in me with an immeasurable patience because, yes I know, I'm a first class annoying student. For the patience, guidance, advice and directions throughout this work as well for the friendship, a big thank you. You've made me grow as a scientist, as a colleague, as a student, as a friend. Thanks to Professor Pina, the Great Chief, who taught me to love and care the 406 as if it was my home. I have to confess that the most productive times were with him, my big boss, always demanding results from yesterday. But if on one hand I complained about the level of demand, I must say they were always rewarding times. Thanks to Little Chief Professor Jorge, who encouraged me and stood by me in my ups and the downs. It was incredible to see his belief, more than mine, that certain syntheses were possible. Several times we were both proved wrong. Many were the hours we spent in front of NMR spectra, where new ideas or new possible ways almost always arose. For the patience, advice, guidance throughout all projects, a big thank you.

Thanks to Dr. JC Lima, equally important in my growth as a person but mainly in what concerns my future. He made me believe that we are all adults and peers, and the incompatibility of doing a PhD and teach simultaneously existed only in my head. Besides teaching me the basics when my brain refused to recall the times of degree, repeatedly told me to organize, process and reflect on the data before a collective discussion.

Thanks to Raquel Gomes and André VP for the good times, friendship and especially for the precious advises. You were those who followed me at the beginning of this journey.

Several generations of "young people" suffered me in the lab. Raquelita is the only one who followed me all the way. Roommate in conferences, buddy in the late hours in the lab, confident in times of need and peer in times of scientific discussions. Thank you for being who you are, just a simple girl, but most of all for being always there. Aidinha e Rita, far but closer to the heart, long cigars and short hours revealed and helped grow a beautiful and long friendship. Thank you both for the conscience that I usually leave home, the advices and for

always being there. Angela's "good morning happiness" is missed every day, but being on a similar journey to mine in another part of the globe entitled her to be excused. Yoann Leylet, one of the two unique French guys that I can bear. Thank you for your friendship, support, incentive, especially for the good mood you brought daily to the lab.

The one and only João Avó. How is it possible to be so different and so alike? I've watched you grow, you've watched me grow, it has been a pleasure. Useless things I've learned with you and precious ones, too. Late hours and weekends spent "Breaking Bad" led to what I like to call, a beautiful awkward friendship. I would work with you anytime, anywhere. ☺

Ritinha, or Engenheira Ana Rita Almendra. One of the recent acquisitions and losses of the photochemistry group. She arrived with all her pride, but she conquered us all. She turned out to be a beautiful, intelligent, critical and argumentative girl but most of all, a good friend.

Dr. Artur Moro, the real buddy through graduation and now at the end of my PhD. Thank you for the partnership and collaboration, but especially for the good talks and laughs.

A special thanks to Dr. Luis Cabrita, just for being who you are! You're a big asset to any group!

A younger and recent generation, Joana, Noémi, Neuza, Andreiinha, Sandrinha, Tiago, Tati and the list go on…. Thank you for the good mood and for nurturing the mum in me. With your love, support and nagging you've all made every day more bearable.

To all colleagues of the photochemistry and supramolecular group, Leti, Márcia, Sandra, Karolina, Nuno, Luis and so on... for the good times we have been and the group for the technical, financial, physical and psychological support!! To the gang from Conservation, especially to Ana Isabel and Vanessa, but also to the undefined scientist Andreia Ruivo, you're priceless! Much obliged for your friendship!

I acknowledge Dr. Nathan McClenaghan for accepting me for a short-term period in Institut des Sciences Moléculaires at the University of Bordeaux and for his inputs about my work. I would like to thank especially Arnaud for the accommodation and Dr. HP Jacquot for all his ideas, support and encouragement. Thank you for not letting me give up!

Finally to all my friends who accompanied me on this journey, thank you just for being there. Specially to David, Val and Rita, since the first day of graduation, 13 years ago….with highs and lows, you've been always there for me.

Ao Luis, por todos estes anos em que sofreste o meu mau feitio. Pela companhia, pela alegria e pela tristeza…. pela força para continuar, por acreditares em mim mesmo quando eu não o fazia. Obrigada, mm!

E por fim, a quem mais devo, ao meu irmão e aos meus pais. Pela minha educação, pelo apoio incondicional, mas principalmente por todo o Amor, obrigada!

Ana

# Resumo

O processamento de informação ao nível molecular requer sistemas capazes de se interconverter entre diversos estados através de estímulos específicos. Os sais de flavílio (2-fenil-1-benzopirílio) constituem uma família versátil de moléculas que ilustra o conceito de sistemas multiestados/multiresponsivos. Do complexo sistema de reações químicas dos flavílios, diferentes formas podem ser obtidas exibindo diversas propriedades por acção de estímulos externos, tais como pH e luz.

O trabalho de investigação elaborado no âmbito desta dissertação de doutoramento teve como objectivo a síntese e estudo de sistemas covalentes supramoleculares multiresponsivos, tendo por base uma unidade flavílio acoplada a unidades redox reversíveis ou unidades coordenantes. Pretende-se deste modo aumentar o número de estímulos disponíveis no complexo sistema dos flavílios, incluindo electrões e metais, além dos protões e fotões.

Num estudo inicial, dois novos sais benzopirílio com grupos complexantes de iões metálicos foram sintetizados e caracterizados (capítulo 2). O estímulo elétrico foi introduzido com uma unidade redox, o viologénio (capítulo 3) e por fim, acoplou-se unidades de flavílio a unidades redox e fotoactivas, complexos de polipiridina Ru(II) (capítulo 4).

Tendo em conta a sua possível aplicação como compostos modelo de memórias ópticas, espera-se conseguir com a introdução destas novas unidades à unidade de flavílio, um maior número de estados, que possibilitem uma maior funcionalidade e versatilidade.

PALAVRAS-CHAVE: Flavílios, Química Supramolecular, Multiestados, Fotocromismo

# Abstract

Information processing at the molecular level requires systems able to move between several states under control of specific inputs. Flavylium salts (2-phenyl-1-benzopyrylium salts) analogues of naturally occurring anthocyanin dyes, are a versatile family of molecules that illustrates the multistate/multiresponsive concept. On the basis of the pH and light dependent network of chemical reactions of the flavylium network, different forms can be obtained by external stimuli exhibiting different properties.

The research work developed in the framework of this PhD thesis aimed the synthesis and study of multiresponsive covalently linked supramolecular systems, based on a flavylium unit coupled redox-active and/or metal-complexing moieties. It is intended to increase the number of stimuli in the complex network of flavylium, including electrons and metal ions besides protons and photons (flavylium).

In an initial study, two new benzopyrylium salts with directly attached metal-complexing groups were synthesized and characterized (Chapter 2). The electrical stimulus was introduced with a viologen (Chapter 3) and finally redox- and photoactive units such as Ru(II) polypyridyl complexes (Chapter 4) are discussed.

Regarding their possible applications as model compounds to optical memories, it is expected to achieve with these new systems a larger number of states, which allow increased functionality and versatility.

KEYWORDS: Flavylium, Supramolecular Chemistry, Multistate, Photochromism.

# Abbreviation List

| | |
|---|---|
| A | Absorbance |
| a.u. | Arbitrary unit |
| $C_0$ | Total concentration of species |
| *c* | Speed of light |
| CMC | Critical micelle concentration |
| CMT | Critical micelle temperature |
| COSY | Correlation spectroscopy |
| CTAB | Cetyl trimethylammonium bromide |
| δ | Chemical shift |
| ε | Molar absorption coefficient |
| $\Phi_i$ | Quantum yield for a given process *i* |
| F | Fluorescence |
| $I_0$ | Light intensity emitted by irradiation source at a selected wavelength |
| I | Intensity of emission |
| IC | Internal Conversion |
| ISC | Intersystem crossing |
| J | Coupling constant |
| $k_j$ | Rate constant for a given process *j*, e. g. , $k_{nr}$ = rate constant for non radiative processes |
| λ | Wavelength |
| $\lambda_{em}$ | Emission wavelength |
| $\lambda_{exc}$ | Excitation wavelength |
| $\lambda_{irr}$ | Irradiation wavelength |
| $\lambda_{max}$ | Wavelength of maximum emission or absorption |
| $\bar{\nu}$ | Wavenumber |
| η | Viscosity |
| $\eta_i$ | Efficiency for a given process *i* |
| NMR | Nuclear magnetic resonance spectroscopy |
| NOESY | Nuclear Overhauser effect spectroscopy |
| PSS | Photostationary state |
| T | Temperature |
| $\tau_l$ | Lifetime for a given process *l* |
| U.V.-Vis | Ultraviolet-Visible spectroscopy |

| | |
|---|---|
| $\mathbf{AH_2^{2+}}$ | Protonated amino flavylium cation |
| $\mathbf{AH^+}$ | Flavylium cation |
| **A** | Quinoidal base |
| $\mathbf{A^-}$ | Ionized quinoidal base |
| **B** | Hemiketal |
| **Cc** | *Cis*-chalcone |
| $\mathbf{Cc^-}$ | Ionized *cis*-chalcone |
| **Ct** | *Trans*-chalcone |
| $\mathbf{Ct^-}$ | Ionized *trans*-chalcone |
| $\mathbf{CtH^+}$ | Protonated amino *trans*-chalcone |
| **CB** | Conjugated bases (**A**, **B**, **Cc** and **Ct**) |
| | |
| $K_{a+}$ | Equilibrium constant for the deprotonation of $\mathbf{AH_2^{2+}}$ |
| $K_{a(1)}$ | Equilibrium constant for the deprotonation of $\mathbf{AH^+}$ |
| $K_{a2}$ | Equilibrium constant for the deprotonation of **A** |
| $K_{Ct+}$ | Equilibrium constant for the deprotonation of $\mathbf{CtH^+}$ |
| $K_{Ct(1)}$ | Equilibrium constant for the deprotonation of **Ct** |
| $K_h$ | Equilibrium constant for the hydration of $\mathbf{AH^+}$ |
| $K_t$ | Equilibrium constant for the tautomerization of the **B** |
| $K_i$ | Equilibrium constant for the isomerization of **Cc** |
| $K'_a$ | Apparent equilibrium constant between $\mathbf{AH^+}$ and **CB** |
| $k_a$ | Kinetic constant for the direct deprotonation reaction (formation of **A**) |
| $k_{-a}$ | Kinetic constant for the inverse deprotonation reaction (the protonation of **A**) |
| $k_h$ | Kinetic constant for the direct hydration reaction |
| $k_{-h}$ | Kinetic constant for the inverse hydration reaction (the dehydration of **B**) |
| $k_t$ | Kinetic constant for the direct tautomerization reaction |
| $k_{-t}$ | Kinetic constant for the inverse tautomerization reaction |
| $k_i$ | Kinetic constant for the direct isomerization reaction |
| $k_{-i}$ | Kinetic constant for the inverse isomerization reaction |
| $k_{-i+}$ | Kinetic constant for the inverse isomerization reaction (of $\mathbf{CtH^+}$) |

# Index

# Figure Index

# Table Index

# CHAPTER I. Introduction

# I. Introduction

We find ourselves living the age of technology. The demand for ever-faster and ever-smaller machines with higher capacity has paved the way for the miniaturization of technology. While physicists and engineers seek to manipulate progressively smaller pieces of matter, always confronted with the intrinsic limitations of working below the micrometer scale,[1,2,3] chemists work at the molecular level in an effort to minimise some of these limitations.

A machine at the molecular level can be defined as a set of molecular components designed to perform mechanical-like movements in response to an appropriate external stimulus.[4] The idea of a machine at the molecular level emerged in 1959 by Nobel Prize R. P. Feynman[5] with his known sentence "There is Plenty of Room at the Bottom." By the early 70's, with the emergence of a new line of research field - Supramolecular Chemistry – new directions have emerged in the design and construction of machines and devices at the nanometer scale. [1]

## I.1. Supramolecular chemistry

Supramolecular Chemistry was defined by Lehn as a non-covalent interaction: "As there is a field of molecular chemistry based on the covalent bond, there is a field of supramolecular chemistry, the chemistry of molecular assemblies and of the intermolecular bond" or "the chemistry beyond the molecule".[6] Supramolecular chemistry studies chemical species of greater complexity, "*supermolecules"*. They have features different from the sum of their individual components and can be characterized by several types of interactions, such as metal ion coordination, electrostatic forces, hydrogen bonding, van der Waals interactions or even donor-acceptor interactions.[6]

Based on the non-covalent interactions of biological processes, the beauty of which weak interactions that through self-assembly and self-organization originate supramolecular structures like our DNA and all information within, supramolecular chemistry is the art of growing complexity by assembling molecules whose interactions give rise to new characteristic properties of the ensemble, not present in the individual components. This is an interdisciplinary scientific area that covers chemical, physical and biologic features of chemical species of higher complexity.

One of the basic functions of supramolecular chemistry is molecular recognition. Molecular recognition is the energy and/or information that comes from binding a substrate to a given receptor. This requires a "pattern recognition process through a structurally well-defined set of intermolecular interactions"[6], residing on complementarity between the substrate and the

receptor in terms of both geometry and energetics. This complementarity will ensure the selectivity of the substrate/receptor interaction.

As such, molecular recognition "implies the (molecular) storage and (supramolecular) read-out of the molecular information" just like in biologic systems. With appropriate manipulation of these interactions, molecular recognition and storage of information can be achieved, resembling biological systems, making supramolecular chemistry an information science.[7] All these facts led to the concept of programmed supramolecular systems, enabling the construction of molecular devices.

The definition of supramolecule implies the identification of molecular moieties with individual properties assembled in such a way that leads to the appearance of new properties of the ensemble. The molecular units are usually connected non-covalently, as above referred. It is therefore a complex system comprising individual molecular units with defined properties.[8] The same definition can also be extended to covalently linked systems provided that they meet specific conditions, such as their molecular moieties having well defined and easily identified properties,[9] see Figure I.1.

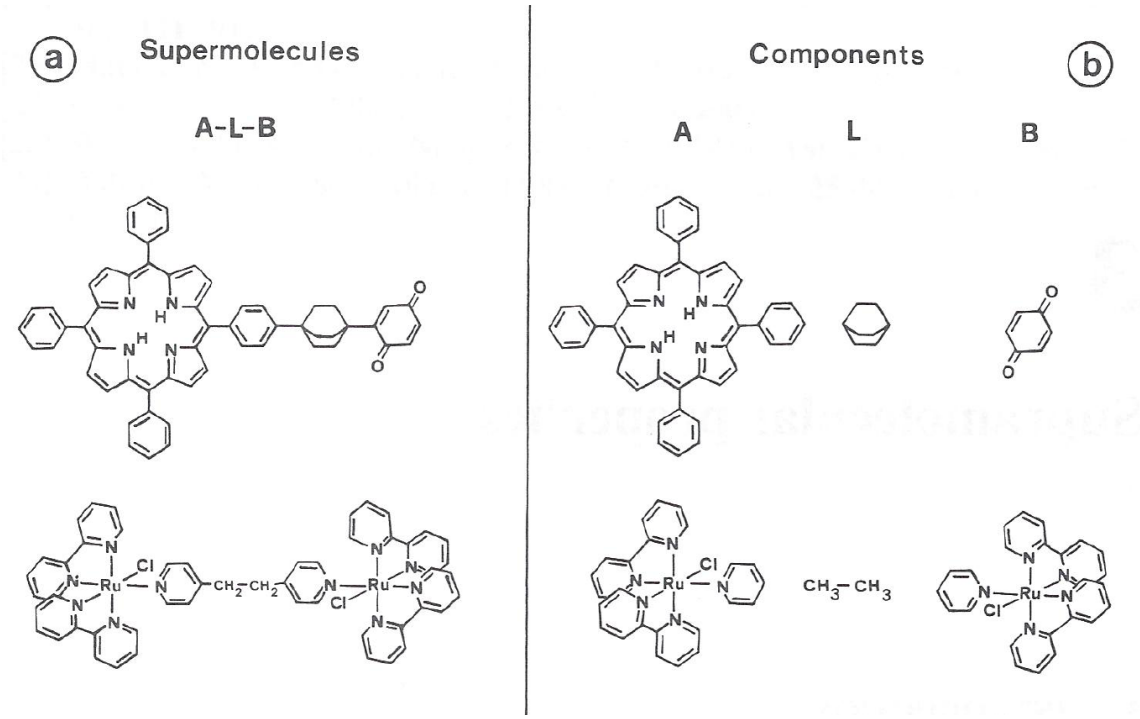


**Figure I.1 –** Covalently linked supermolecules (a) and their components (b).[9]

In the systems above depicted it is easy to understand the supramolecular covalent concept where each system contains molecular moieties having distinct properties, including

those of spectroscopic, photophysical, photochemical and even redox nature, which are covalently linked through spacers, extending the concept of molecule to supermolecule.[9]

The usual supramolecular approach is a vertical one, where complexity is reached through a bottom-up strategy,[2] from nano or subnano-scale objects (atoms or molecules) to build up nanostructures.[3] But "definitions have a clear, precise core but often fuzzy borders"[6] as referred by Lehn and, being chemists, already at the bottom it is possible to increase the complexity of a system by using a horizontal approach. By conceiving molecules with several available states reversibly transformed between them and controlled by external stimuli with each state having different properties, we can find ourselves at the bottom opening new ways at the horizontal supramolecular chemistry or molecular metamorphosis, Scheme I.1.[10]

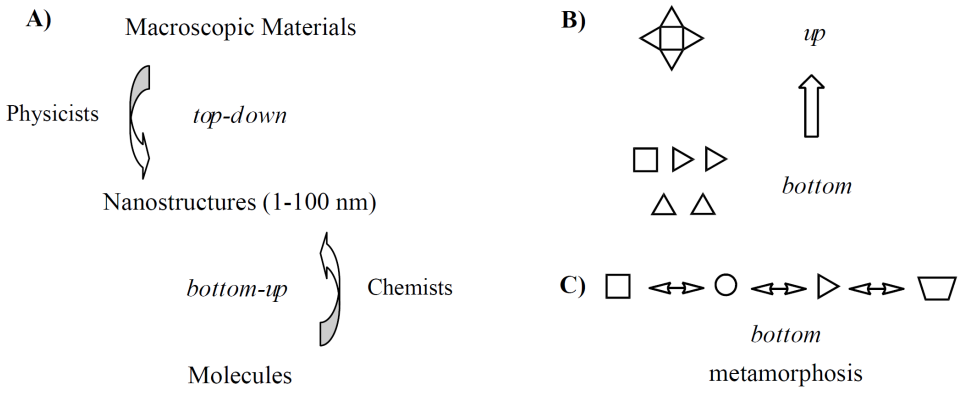


**Scheme I.1 - A**) Bottom-up vs top-down approach;[1] B) C) Bottom-up and metamorphosis approach.[11]

The supramolecular concept can be extended to other supramolecular functions, such as the case of supramolecular photochemistry where covalently linked devices "made up of distinct but interacting components" which retain the characteristics that identify each individual component, add information and versatility to the whole system. [6]

## I.1.1. *Supramolecular photochemistry*

The definition of photochemical molecular devices was introduced in the NATO Workshop on Supramolecular Photochemistry in 1987 in Italy[2] as "An appropriate assembly of molecular components capable of performing light-induced functions can be called a photochemical molecular device (PMD)." PMD's can perform relevant functions regarding to information exchange such as (i) generation and migration of electronic energy, (ii) photoinduced vectorial transport of electric charge, (iii) photoinduced conformational changes, and (iv) control and tuning of photochemical and photophysical properties.[12]

The main requirement for the construction of a molecular device is the possibility that the system may exist in at least two different states that may be interconverted as a result of a reversible chemical transformation caused by an external stimulus.[1] This is the reason why the most commonly studied components of supramolecular devices are photochemically or redox active molecular moieties, which are able to undergo several different processes upon light absorption or electron capture or loss, respectively.[8]

The most well known bi-stable molecules are photochromic compounds that can be reversibly interconverted, where at least one of the reactions is induced by light, as in the case of organic photoreceptors.[1] In these systems we *write* the information while irradiating at the wavelength of a state, which originates another state, and we *read* the newly formed state, for instance, by absorption or emission spectroscopy.

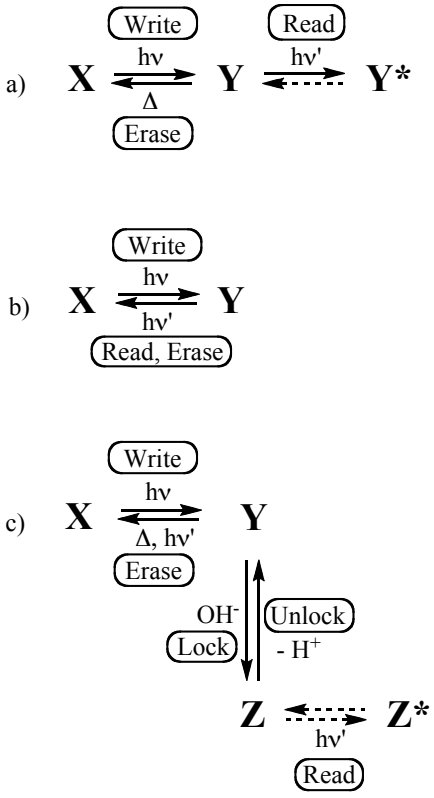


**Scheme I.2 -** Schematic representation of the behavior of three types of photochromic systems. a) The photochemical reaction of the form X reverts by thermally in the dark. b) The photochemical reaction of the form X reverts only through light excitation of the form Y. c) The form Y which reverts to X through light excitation, can be transformed by means of a second stimulus (such as an acid/base reaction) into another form Z, which is stable toward light excitation and, when necessary, can be reconverted to Y.[1,13]

Some photochromic compounds change colour by light excitation and revert to its initial state when not exposed to light, more or less slowly depending on the compound. They are classified as T-type thermally reverted (Scheme I.2a) and are ineffective for storing information, once the written information is spontaneously cleared with time. Photochromic compounds that do not revert thermally to the initial state but also suffer reversible

photoreaction are classified as P-type (Scheme I.2b). These compounds present a problem; the light used to read information leads to conversion to the initial state, leading to the loss of information.[1]

One way of solving these drawbacks is by using a compound with two reversible processes, which can be controlled by different external stimuli. In these systems (Scheme I.2c) light is used for writing, converting X to Y, and then a second stimulus converts Y in Z locking the system and allowing it to read without destroying the information. These systems are always reversible when necessary. Addition of base unlocks the system reverting Z to Y and finally to X through light.

Such systems, write-lock-read-unlock-erase, can be the basis of a molecular optical memory.[1]

## I.2. Flavylium salts

The aim of this subsection is to introduce flavylium salts, briefly starting by a historical background and proceeding with thermodynamics, kinetics, photochemistry and some reported applications of these multistate molecules.

### I.2.1. *Structure of flavylium salts and historical background*

Flavylium salts are constituted by a basic skeleton of 2-phenyl-1-benzopyrylium and have the same basic chromophore (Scheme I.3) as anthocyanins, anthocyanidins and deoxyanthocyanins, which constitute the flavonoid class of natural compounds. They are biosynthesized through a combination of the shikimate pathway and the acetate pathway[14], whose crucial enzyme is *chalcone synthase*.[15]

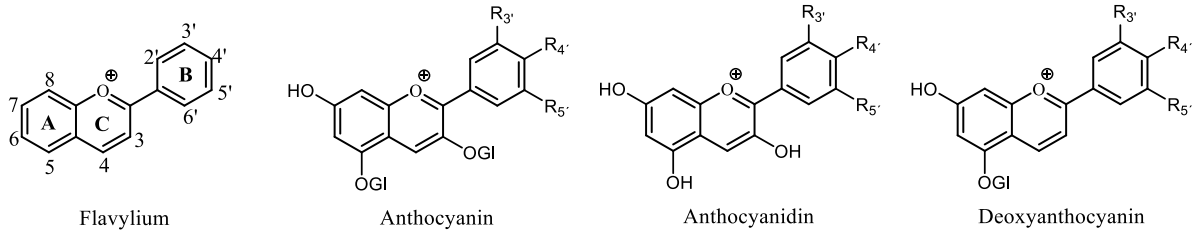


**Scheme I.3 –** Anthocyanin compounds and the flavylium chromophore (GI = glycoside).

In anthocyanidins hydroxyl groups are always present in positions 3, 5, 7 and 4', a direct consequence of the biosynthetic pathway[14] and due to their instability are usually found in plant tissues glucosylated at the 3-*O*-position.[16] On the contrary, the so-called deoxyanthocyanins

corresponding to anthocyanidins lacking the hydroxyl in position 3, are quite stable in solution, and have been isolated from mosses and ferns.[16] Anthocyanins (from the Greek words for flower and blue) are the ubiquitous dyes known in nature responsible for most of natural colour on flowers and fruits from the blue, purple to magenta and reds.[17] They are polyhydroxy and polymethoxy *O*-glycosylated in position 3 (monoglycoside) and sometimes also in position 5 (diglycosides) or less frequently in position 7[18] derivatives of 2-phenyl-1-benzopyrylium salts.[17]

The basic structure of anthocyanins was clarified in the early nineties by Richard Willstätter who deduced the structures of pelargonidin, cyanidin and delphinidin and also introduced the term "anthocyanidins" to describe sugar free anthocyanins.[19,20,21] It was in the mid-twenties of the XX century that R. Robinson first published the synthesis of these compounds.[22,23]

Anthocyanins have been investigated for long in order to understand the chemistry behind these remarkable molecules. They have been consumed by man and animals for many centuries without undesirable physiological effects, and being the largest group of soluble pigments in water they have been widely used as colorants in food industry, in place of traditional pigments (e.g. azo dyes).[17,24] Another significant property of anthocyanins is their antioxidant activity, preventing neural and cardiovascular illnesses, cancer and diabetes, among other.[25]

Synthetic flavylium, possessing the same basic structure as anthocyanins and having identical network of chemical reactions in aqueous solution have also been widely investigated in applications on the food industry,[26] cosmetic[27,28] and more recently as models of optical memories.[29]

## I.2.2. *Network of reactions*

Flavylium salts in aqueous solution exhibit a complex network of chemical reactions that can be carried out by pH and/or light excitation.[1] Their physicochemical properties are heavily dependent on substituents and these transformations are usually accompanied by colour changes.[30] Scheme I.4 depicts the several equilibriums.

The flavylium cation ($\mathbf{AH^+}$) is the thermodynamically more stable species at very acid pH's, and intensely coloured. When the pH is increased two processes occur in parallel, a deprotonation that leads to the quinoidal base **A**, also stained (responsible form for blue shades in Nature, conferred by anthocyanins), and a hydration in the C2 carbon leading to the formation of hemiketal $\mathbf{B_2}$ (colourless). The hydration in position 4 leading to the formation of hemiketal $\mathbf{B_4}$ occurs usually in very low extension. The hydration reaction is slower than deprotonation, but the hemiketal ultimately leads to the more thermodynamically stable **Ct** species at neutral pH values. The hemiketal tautomerizes leading to the formation of a *cis* chalcone (**Cc**), which can isomerise to the *trans* chalcone (**Ct**). In basic media, ionized species

can be formed, the anionic **Ct** (**Ct$^{n-}$**) species and also **Cc** (**Cc$^{n-}$**) species. The distribution of the molar fractions of all species will depend on the degree of substitution and the nature of the substituent.

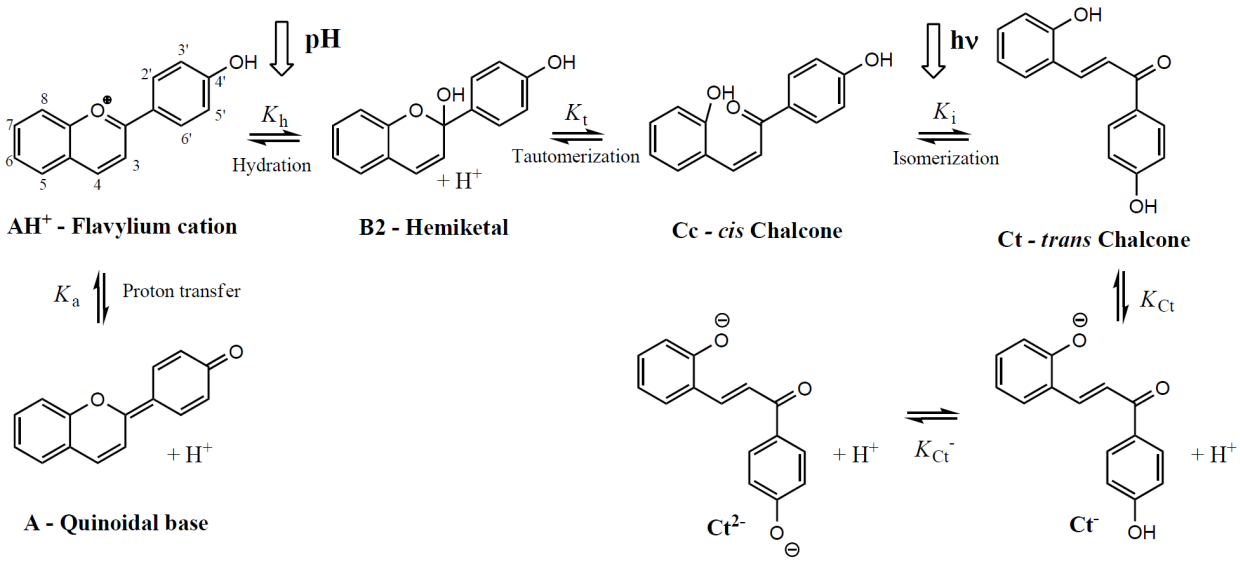


**Scheme I.4 –** Network of chemical reactions of 4'-hydroxyflavylium

The flavylium network took a few decades to be completely clarified. After callestephin chloride isolated by Willstätter and the synthetic pelargonidin 3-monoglucoside chloride prepared by Robinson, it was Sondheimer the first to make quantitative measurements of the pH dependent UV-Vis absorption and to determine the equilibrium constant between the flavylium cation and the hemiketal.[31,32] Jurd went forward to more basic pH's demonstrating the reversibility of the system between pH 1 and 12, also isolating crystalline chalcones but without specifying whether he considered *cis* and/or *trans* chalcones in the network of reactions.[33,34]

Timberlake was the first to refer spectral changes with light in the UV-Vis spectra of equilibrated solutions.[35] It was finally in 1969 that Jurd with the help of NMR data reported the existence of *trans* chalcones in the equilibrium, which in the presence of light were easily photo-isomerised to cis chalcones, and depending on the pH and by a non-photochemical process could cyclise to flavylium salts.[36]

Only by the end of the 1970's Brouillard and Dubois[37] proposed what it is known to date as the correct mechanistic model for the formation of the hemiketal (**B**) only through the flavylium cation, and the later in equilibrium with the quinoidal base (**A**). With several wrong conclusions published along the way, finally in 1990 Brouillard and Lang[38] described the slowest process as the *cis-trans* isomerisation and not the ring-opening-closure as Boruillard and Delaporte[39] previously said. It is noteworthy that the mole fraction distribution of the *trans*-

chalcones at the equilibrium in anthocyanins is much less that in synthetic flavylium salts. The complete elucidation on the pH dependence of malvin (anthocyanin) equilibria in water was only achieved by H. Santos *et al.*[40] in 1993.

McClelland et al. [41,42] always accurately presented the structural changes in solution for synthetic flavylium salts but only in 1994, the complete elucidation of the 2-hydroxychalcones photoisomerisation of the flavylium network was reported for the compound 4',7-dihydroxyflavylium.[43]

## I.2.3. *Thermodynamics of the network reactions*

The network of flavylium compounds in water, from acidic to neutral pH values, is accounted for by scheme I.5 - I.9.[1]

$$AH^+ + H_2O \rightleftharpoons A + H_3O^+ \qquad K_{a1} \qquad \text{Proton transfer}$$

**Scheme I.5 –** Equilibrium between $AH^+$ and A and the respective thermodynamic constant

$$AH^+ + H_2O \rightleftharpoons B_4 + H_3O^+ \qquad K_h^4 \qquad \text{Hydration}$$

**Scheme I.6 –** Equilibrium between $AH^+$ and $B_4$ and the respective thermodynamic constant

$$AH^+ + H_2O \rightleftharpoons B_2 + H_3O^+ \qquad K_h \qquad \text{Hydration}$$

**Scheme I.7 –** Equilibrium between $AH^+$ and $B_2$ and the respective thermodynamic constant

$$B_2 \rightleftharpoons Cc \qquad K_t \qquad \text{Tautomerization}$$

**Scheme I.8 –** Equilibrium between $B_2$ and Cc and the respective thermodynamic constant

$$Cc \rightleftharpoons Ct \qquad K_i \qquad \text{Isomerisation}$$

**Scheme I.9 –** Equilibrium between Cc and Ct and the respective thermodynamic constant

The species involved in the equilibrium described are the flavylium cation $\mathbf{AH^+}$, the two hemiketal forms $\mathbf{B_2}$ and $\mathbf{B_4}$ obtained from the hydration in the 2 and 4 positions respectively, the *cis*-chalcone **Cc** formed through a tautomeric process from the hemiketal $\mathbf{B_2}$ and, the *trans*-chalcone **Ct** obtained from isomerisation of the *cis*-chalcone. Usually the hydration in the 4 position occurs in a very small extent (less than 1% of $\mathbf{B_2}$)[1] and from now on is going to be neglected.

Schemes I.5 - I.9 can be substituted by a single acid-base equilibrium, Scheme I.10 in which the flavylium cation ($\mathbf{AH^+}$) is in equilibrium with the conjugate base (**CB**) witch consists

of the quinoidal base (**A**), hemiketal (**B**) and the chalcones (**Cc** and **Ct**) at acid / neutral pH with an apparent acidity constant $K'_a$, Equation I.1 and I.2.

$$AH^+ \rightleftharpoons CB + H^{+a} \qquad K_{a1}$$

**Scheme I.10 –** Equilibrium between $AH^+$ and CB and the respective thermodynamic constant

$$K'_a = \frac{[CB][H_3O^+]}{[AH^+]} \qquad \textbf{Equation I-1}$$

$$K'_a = K_a + K_h + K_h K_t + K_h K_t K_i \qquad \textbf{[CB]= [Ct] + [Cc] + [B] + [A]} \qquad \textbf{Equation I-2}$$

The mole fraction distribution of the different species is calculated as follows:

$$\chi_{AH^+} = \frac{\left[H^+\right]}{\left[H^+\right] + K'_a}; \qquad \textbf{Equation I-3}$$

$$\chi_A = \frac{K_a}{\left[H^+\right] + K'_a}; \qquad \textbf{Equation I-4}$$

$$\chi_B = \frac{K_h}{\left[H^+\right] + K'_a}; \qquad \textbf{Equation I-5}$$

$$\chi_{Cc} = \frac{K_h K_t}{\left[H^+\right] + K'_a}; \qquad \textbf{Equation I-6}$$

$$\chi_{Ct} = \frac{K_h K_t K_i}{\left[H^+\right] + K'_a} \qquad \textbf{Equation I-7}$$

Nowadays, routine procedures involving several experimental techniques, such as pH jumps followed by UV-Vis spectroscopy, NMR spectroscopy, flash photolysis and stopped flow measurements, allow the determination of most if not all the equilibrium constants[1,44,45] and will be presented and discussed further ahead.

A convenient way to represent the flavylium network is the use of an energy level diagram where the Gibbs free energy, $\Delta G^o$, of the different equilibria is represented at different pH values, Scheme 1.11A.[46] At low pH values $\mathbf{AH^+}$ is the most stable species. As pH increases the components of the conjugate base become the more stable species, the respective equilibrium concentrations depending on the relative energy level. In alternative, the network can be described through the mole fraction distribution in the equilibrium of the several species by means of equations I.5 – I.9, Scheme 1.11B.

[a] From now on, and for the sake of simplicity, the notation $H^+$ will be often used instead of $H_3O^+$.

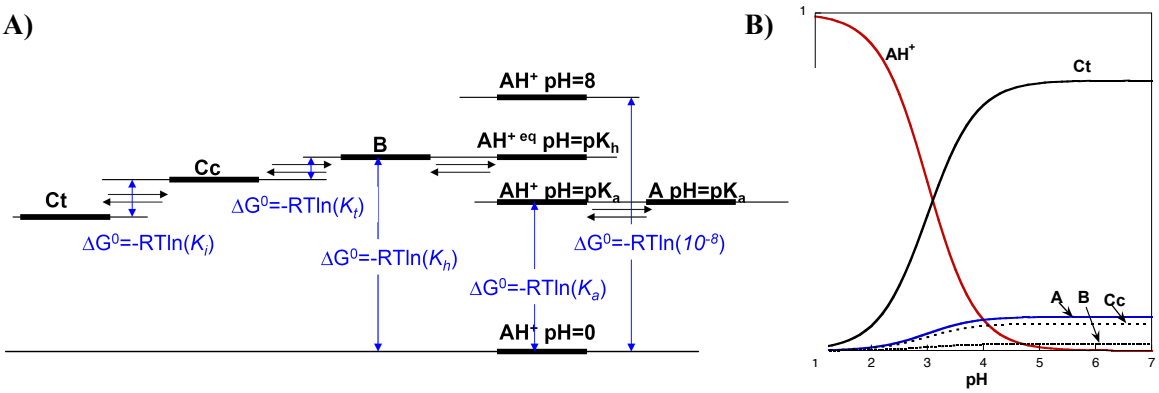


**Scheme I.11** - **A**) Construction of energy level diagrams. **B**) Example of mole fraction distribution at the equilibrium.

In cases where the rate of the thermal *cis-trans* isomerisation reaction (Scheme I.9) is much slower than the rates involved in the other equilibria, a pseudo-equilibrium can be assumed allowing to consider that $\mathbf{AH^+}$, **A**, **B** and **Cc** are equilibrated before significant appearance of **Ct**. In such cases by performing a pH jump from $\mathbf{AH^+}$ to more basic pH values, **Ct** is not detected by UV-Vis measurement after one hour or more.

In a similar way to the previous treatment, the pseudo-equilibrium can be accounted by a single acid-base equilibrium, $K^{\wedge}_a$, Scheme I.15 and Equation I.8 and I.9.[47]

$$AH^+ + H_2O \rightleftharpoons CB^{\wedge} + H^+ \qquad K^{\wedge}_a$$

**Scheme I.12** – Equilibrium between $AH^+$ and CB^ and the respective thermodynamic constant

$$K^{\wedge}_a = \frac{[CB^{\wedge}][H^+]}{[AH^+]} \qquad \textbf{Equation I-8}$$

$$K'_a = K_a + K_h + K_hK_t + K_hK_t \qquad [CB^{\wedge}] = [Cc] + [B] + [A] \qquad \textbf{Equation I-9}$$

With this treatment for the cases where pseudo-equilibrium can be defined, identical diagrams to the ones presented in Scheme 1.11 A and B can be easily obtained.

It is noteworthy that unsubstituted flavylium compounds as well as flavylium with no OH substituents share a peculiarity in the network of reactions. Despite the behaviour is the same as for those with substitution pattern; there is no formation of the quinoidal base **A** due to the impossibility of deprotonation of the $\mathbf{AH^+}$.[1]

## I.2.4. *Kinetics of the network reactions*

The kinetics involved in Scheme I.4 can be separated into four processes taking place on four different time scales: i) fast proton transfer in the microseconds timescale,[37] ii) pseudo-equilibrium between flavylium cation and hemiketal regarding the hydration in seconds to minutes timescale,[37,39] iii) ring opening and closing in sub-seconds for tautomerization,[41,42] iv) cis-trans isomerisation, the slowest process that can take seconds to days.[41,42] Using the appropriate technique it is possible in most cases to separate if not all, at least three of the four kinetic processes and measure the respective rate constants. The overall kinetic process is very dependent on the magnitude of the *cis-trans* isomerisation barrier. If the barrier is high, this kinetic process is the slowest one, which can take days.

Hydration and tautomerization constants can be obtained through a stopped-flow or a common spectrophotometer, depending on the rate of the process (which depends on pH), whereas for isomerisation processes a common spectrophotometer is enough.

The proton transfer reaction is very fast and the respective kinetics can be determined, for example, with temperature jump techniques.[37,41] As shown in literature, the system will approach the first (pseudo) equilibrium exponentially with a rate constant $k_1$ equal to the sum of the forward and backward reactions, $k_1 = k_a + k_{-a}[H^+]$.[48]

To assess the other kinetics of the system pH jumps are carried out. For example, starting from $\mathbf{AH^+}$ at very acidic pH values and making a pH jump to moderately acidic region, leads to the immediate formation of the quinoidal base **A**, as a kinetic product (not possible to follow by stopped flow techniques). Until equilibrium is reached the evolution of the system can be monitored by a common spectrophotometer and in a case of a very fast process fast by stopped flow analysis. This process occurs by the hydration reaction of $\mathbf{AH^+}$ to give **B**. The kinetic product **A** disappears with the same rate $\mathbf{AH^+}$, because this equilibrium is much faster than the other, meaning the two species behave like a single species. The tautomerization of **B** leading to **Cc** is now the following process. The rate-determining step of this process is usually the hydration and by consequence the system will approach the second equilibrium (pseudo-equilibrium) exponentially with a rate constant $k_2$ given by:

$$k_2 = \frac{\left[H^+\right]}{\left[H^+\right] + K_a} k_h + \frac{k_{-h}}{1 + K_t}\left[H^+\right] \qquad \textbf{Equation I-10}$$

Finally the rate of the slowest isomerisation leading to the final equilibrium is given by $k_3$:

$$k_3 = \frac{K_h K_t}{\left[H^+\right] + K_a^{\wedge}} k_i + k_{-i}$$ **Equation I-11**[48]

More information about the kinetics of the system can be reached if *reverse pH jumps* are performed, i. e., a solution is allowed to reach the pseudo-equilibrium ($K^{\wedge}_a$), before interference of the *trans*-chalcone, and then reacidified or even from a thermally equilibrated solution also reacidified. Using stopped flow techniques it is possible to follow this process. As the dehydration reaction depends on the proton concentration and can be made faster by increasing $[H^+]$ it is possible to observe a bi-exponential formation of flavylium cation: the first kinetics due to the dehydration (formation of $\mathbf{AH}^+$ from **B**), and the second one to the tautomerization (formation of $\mathbf{AH}^+$ from **Cc** through **B**). Indeed, stopped flow measurements are a very powerful method to assess the intricate network of reactions of flavylium cations in aqueous solution, particularly to determine $K_t$.[49,50,51,52]

When the *cis-trans* isomerisation barrier is small this process can compete with the hydration-dehydration and the overall kinetic process is more complex. In the case of the flavylium compounds bearing a 7-hydroxy substituent, the system can be described as in Equation I.12 where the hydration and the *cis-trans* isomerisation are the rate controlling steps. In other words, $\mathbf{AH}^+$ and **A** can be considered in fast equilibrium behaving as a single species, the same assumption can be made for **B** and **Cc**.

$$A \underset{}{\overset{K_a}{\rightleftharpoons}} AH^+ \underset{k_{-h}[H^+]}{\overset{k_h}{\rightleftharpoons}} B \overset{K_t}{\rightleftharpoons} Cc \underset{k_{-i}}{\overset{k_i}{\rightleftharpoons}} Ct$$ **Equation I-12**

The steady state hypothesis can be applied to the species **B** and **Cc** leading to Equation I.13 where the observed rate constant defines a bell-shaped curve as function of pH, in which $k_{-i}$ is a limit for low pH and zero an upper limit for high pH, Figure I.2 (see Supplementary Material, section VI.I, page 111).[46,53]

$$k_{obs} = \frac{\frac{\left[H^+\right]}{\left[H^+\right] + K_a} k_i K_t K_h + k_{-i}\left[H^+\right]}{\left[H^+\right] + \frac{k_i K_t}{k_{-h}}}$$ **Equation I-13**

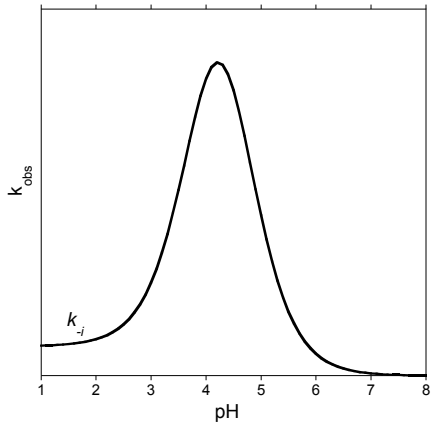


**Figure I.2–** Global rate constant as a function of pH, for the cases where there is no thermal barrier from cis-trans isomerisation.

## I.2.5. *Photochemistry*

As previously mentioned *cis* and *trans* chalcones can be reversible photo-isomerized under continuous and / or pulsed light irradiation depending on the temperature and pH of the irradiated solution.[1] The different work time scale allows understanding the photochemical behaviour of the system.

An example of continuous irradiation of an equilibrated **Ct** solution of unsubstituted flavylium and its dependence with pH can be found in Fig I.3. The spectral variations at pH=2 (Fig. I.2A) and pH= 5.2 (Fig. I.2B) observed under irradiation with 313 nm light are the reverse of those observed in the thermal reactions upon pH jumps of $\mathbf{AH}^+$ solutions at pH = 1 to the referred pH's. At acid pH the only photoproduct is $\mathbf{AH}^+$ while at more basic pH values **Cc** is formed. Moreover, if **Cc** absorbs at the wavelength of irradiation, at a certain point the back photoisomerisation starts to take place. [54]

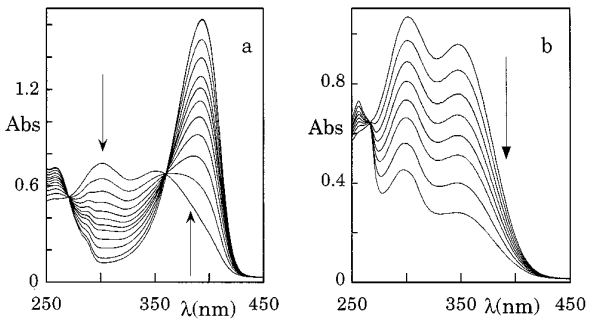


**Figure I.3** - Spectral variations observed upon continuous irradiation (313 nm) of dark equilibrated aqueous solutions of the **Ct** of unsubstituted flavylium as a function of time (initial time increments = 30 s); a) pH = 2.0; b) pH =5.2.[54]

It is possible to calculate the isomerisation quantum yield from the initial irradiation points, as the variation in absorption of the photoproduct versus time of irradiation is still linear, according to Equation I.14:

$$\Phi = \frac{V_{sol}\dfrac{\Delta A_{\lambda obs}}{b\Delta\varepsilon_{\lambda obs}}}{\Delta t I_0 (1-10^{-A_{\lambda irr}})} \qquad \textbf{Equation I-14}$$

in which, $V_{sol}$ is the volume of the solution in L, $\Delta t$ is the time interval, $b$ is the optical path, $\lambda_{obs}$ refers to the observation wavelength and $\lambda_{irr}$ to the irradiation wavelength. Please note that the equation in this form assumes that the photoproduct is not absorbing light at the wavelength of irradiation, and the reagent does not absorb light where the photoproduct is being measured. $I_0$ is the light emitted by the irradiation lamp and must be previously determined using an actinometer,[55] like ferrioxalate.[56]

The quantum yield of formation of $\mathbf{AH}^+$ is pH dependent, and in the case of compounds lacking the *cis-trans* isomerisation barrier it can be given by Equation I.15:[57]

$$\Phi = \Phi_{Ct\rightarrow Cc}\frac{k_{-h}[H^+]}{k_{-h}[H^+]+k_i K_t} = \Phi_{Ct\rightarrow Cc}\frac{[H^+]}{[H^+]+\dfrac{k_i K_t}{k_{-h}}} \qquad \textbf{Equation I-15}$$

Where Φ represents the observed quantum yield measured at each pH by the method of the initial slope which can be given by the product of the intrinsic quantum yield of the reaction by the efficiency of formation of $\mathbf{AH}^+$.

Pina and Maestri introduced the use of flash photolysis to study the network of flavylium compounds in 1997.[46] It is a powerful technique that provides kinetic information in the second's timescale complementary to the data obtained by pH-jumps technique. An easy experimental set up can be used with a common spectrophotometer.[58]

In Figure I.4 are depicted flash photolysis traces of 4',7-dihydroxyflavylium followed at 460 nm (flavylium cation/quinoidal base absorption) and 360 nm (**Ct** absorption) at different pH's.

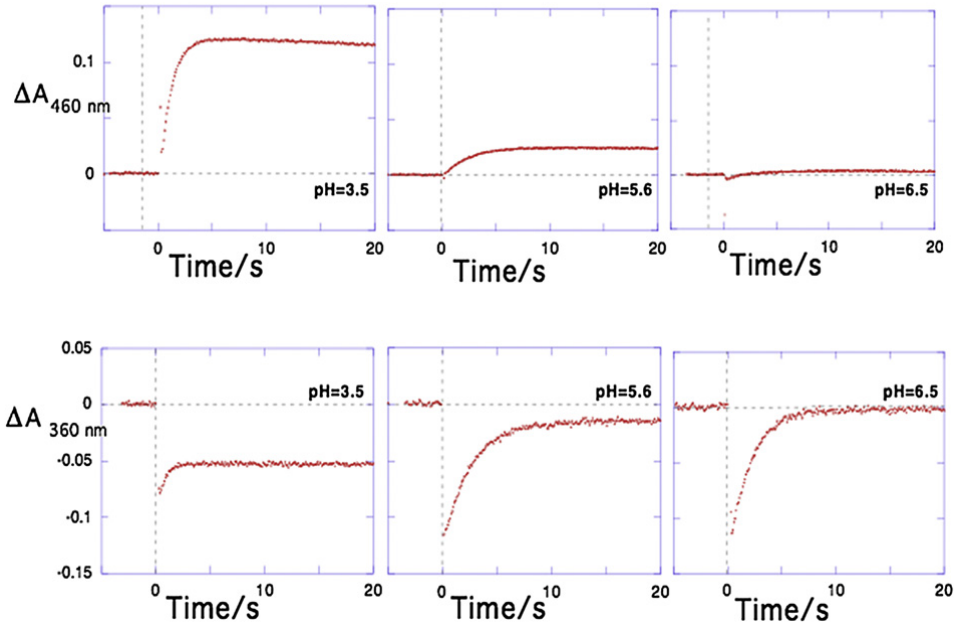


**Figure I.4** – Traces of 4',7-dihydroxyflavylium obtained by flash photolysis monitored at 460 nm (flavylium cation/quinoidal base) and 360 nm Ct.[29,47]

Immediately after the flash the bleaching of the **Ct** absorption is observed indicating that this species is consumed to give **Cc**, which generally possesses a lower molar absorption coefficient at this wavelength.[47] At 460 nm it is also clear the $\mathbf{AH}^+$ formation. This process is pH dependent and follows a first order kinetic process or higher depending on the compound. With the increase of pH the bleaching of **Ct** decreases therefore the $\mathbf{AH}^+$ formed also decreases.

In compounds with *cis-trans* isomerisation barrier like in the 4',7-dihydroxyflavylium, bleaching of **Ct**/formation of $\mathbf{AH}^+$ have coincident rate constants. The global kinetics is compatible with Equation I.16, in which the first term accounts for the recovery of **Ct** and the second term for the formation of $\mathbf{AH}^+$, once again assuming **B** and **Cc** in fast equilibrium.

$$k_{flash} = k_i \frac{K_t}{1+K_t} + k_{-h} \frac{[H^+]}{1+K_t} \qquad \textbf{Equation I-16}$$

Equation I.16 presupposes that both hydration and *cis-trans* isomerisation are much slower process than tautomerization and so are the rates determining steps and in this case a linear relation of the rate constant as a function of the proton concentration should be observed.

## I.3. Flavylium as a multi-state system

Flavylium salts are examples of systems having different states (corresponding to different colours), which can be reversibly affected by thermal impulses, pH, light, and even electrical.

As previously mentioned, molecular or supramolecular systems capable of existing in different forms (multistate) interconverted by different external stimuli (multi-functional) is the main requirement for building optical memories, compounds liable to suffer successive changes with different properties by action of external stimuli.

Along these lines, flavylium salts have been proposed as models for optical memories devices in the sense of horizontal supramolecular chemistry.[10]

The first scientist who carried out systematic investigations on photochromic compounds as optical memories was Hirshberg.[59] The design and construction of molecular devices is directly related to the chemistry of signal generation, transfer, conversion, storage and detection, a subject entitled as *semiochemistry* by Lehn.[6]

As previously mentioned the best known molecules applicable for these devices are photochromic compounds, bi-stable molecules that can be reversibly interconverted, where at least one of the reactions is induced by light.[1,13] In the following years, there has been a strong development of research on photochromic molecular memories, with a great number of patents granted, particularly in Japan.[13]

Its importance is very clear by looking to the potential information storage in chemical systems such as DNA that has an estimated capacity of $10^{21}$ bits/cm$^3$. A CD-ROM contains approximately $10^8$ bits/cm$^2$ while a photochromic material can offer increased capacity to $10^{21}$ bits/cm$^2$.[13]

Synthetic flavylium compounds have been proposed as multistate/multifunctional compounds as model systems *write-read-unlock-erase* (dual-mode systems) constituting the basis for an optical memory system with multiple storage and non-destructive readout capacity.[1,13] The 12 years know-how of our group on photochromic flavylium systems helps to predict the substitution pattern required for the flavylium system to have a kinetic barrier between the *cis* and *trans* chalcone (which is necessary to serve model systems for write-read-erase).[45,60,61,62,63,64] Depending on the nature of the substituents in the 4, 7 and 4' position several of the other forms described in Scheme I.3 may be involved. As referred the flavylium cation ($\mathbf{AH^+}$) is the thermodynamically more stable specie in strongly acid solution, and intensely coloured, at neutral or slightly acidic pH's the dominant species is the *trans* chalcone (**Ct**, faint staining), which by the action of light can be converted in **Cc**, $\mathbf{B_2}$ or even $\mathbf{AH^+}$.

## I.3.1. *Write-lock-read-unlock-erase cycles*

The challenging problem is to find the best system with multiple storage and non-destructive readout but only when necessary. The 4'-hydroxyflavylium[65], 4'-methoxyflavylium[66] and 4'-methylflavylium[67] are examples of such systems. Scheme I.13 describes the behaviour of 4'-methoxyflavylium which refers to a solution at pH = 3.0, where **Ct**, **Cc**, and $\mathbf{AH^+}$ play the role of the generic species **X**, **Y**, and **Z** respectively.[1,13]

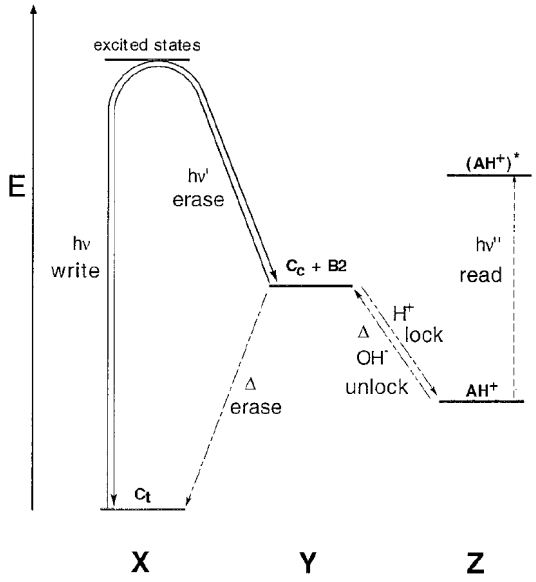


**Scheme I.13 -** Schematic energy level diagram for the species involved in the *write-lock-read-unlock-erase* system of 4'-methoxyflavilium, pH = 3.[66]

**1)** the stable form **Ct** can be photochemically converted by irradiation with 365 nm light (*write*) into a form **Cc** that can be reconverted back either thermally or on optical reading;

**2)** by a second stimulus, addition of acid, **Cc** can be converted into a kinetically inert form $\mathbf{AH^+}$ (*lock*). The acid can also be present from the beginning without perturbing the behaviour of the system (*autolocking*).

**3)** the $\mathbf{AH^+}$ species exhibits a spectrum clearly distinct from that of **Ct** and is photochemically inactive, so that it can be optically detected (*read*) without being erased;

**4)** by addition of base, $\mathbf{AH^+}$ can be reconverted into **Cc** (*unlock*);

**5)** **Cc** can be thermally or photochemically reconverted into the initial **Ct**, form (*erase*).

It should be noted that the locking time of the written information bit is not indefinite (at 25 °C and pH=3.0, the half-life of the back reaction from $\mathbf{AH^+}$ to **Ct** is *ca.* 8 days).

A similar behaviour is observed for 4'-hydroxyflavylium[65] and 4'-methylflavylium. Among the 4'-substituted flavylium ions, this last compound exhibits the lowest energy barrier for the *cis–trans* isomerisation reaction. Lowering the activation energy of the *cis–trans*

isomerisation reaction favours auto-erasing, discouraging its use for an optical memory system.[67] The 4'-hydroxy-3-methylflavylium compound can also be used to operate a *write-lock-read-unlock-erase* cycle.[60]

Due to its high isomerisation barrier, also 4'-hydroxy-6-nitroflavylium can be efficiently used in *write-lock-read-unlock-erase* cycles.[68] This compound performs like an optical memory by means of a slightly different cyclic process that involves the following steps: *write/lock-read-unlock-enable/erase-erase*, in which the information is enabled-erased by a second light stimulus.[68]

The 3',4'-(methylenedioxy)flavylium offers two pairs of chalcones enabling two coupled photochromic systems in acid and basic media. In the pH range 1 to 6, a cycle capable of *write–read–erase* can be designed. The starting point is the metastable **Ct** species at pH 1.0: **1**) using near-UV light, **Ct** is converted into **AH+** (*write* and *auto-lock*); **2**) once again **AH+** can be easily *readout*. **3**) The system can be *erased* by a pH jump to pH 6.0 in order produce **Cc** (in equilibrium with **B**), which is thermally reconverted into **Ct**. **4**) To prepare the system for a new cycle (*enable*), a second pH jump to 1 should be performed, scheme I.14.[49]

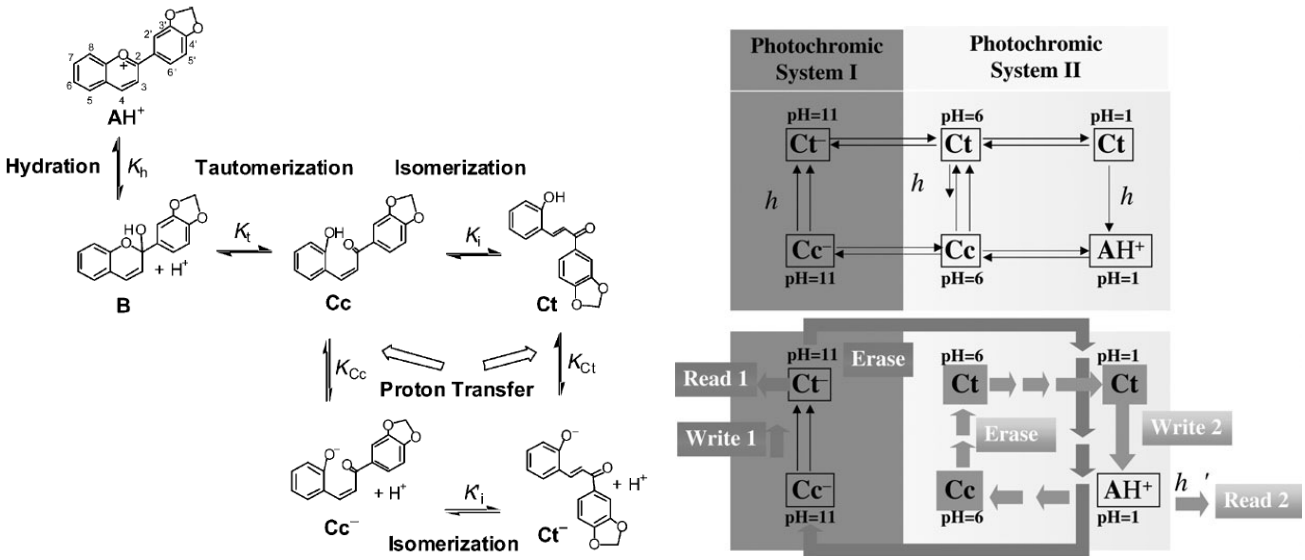


**Scheme I.14 -** The network of thermal and photochemical reactions of the compound 3',4'-methylenedioxy)flavylium allows two write–read–erase cycles to be defined.[49]

The other photochromic system is even more interesting because there is the possibility of two consecutive writing steps. **1**) Starting for example with $\mathbf{Cc}^-$ at pH 11, the first *write* step consists of the irradiation of this species that totally converts into $\mathbf{Ct}^-$; **2**) $\mathbf{Ct}^-$ can be examined by UV-Vis absorption spectroscopy (*read*). **3**) The system can be *erased* through a pH jump to 1 leading to the metastable **Ct** species. **4**) At this point a second *writing* step (the same as the previous cycle) is possible, converting the system into **AH+**. This last reaction can also be

carried out thermally. **5**) Finally, the system should be submitted to a second pH jump to the starting pH value, so that **Cc-** species is recovered, scheme I.17.[49]

For the 4'-dimethylamino compound, it is also possible to perform a *write-lock-read-unlock-erase* cycle, operating however in a slightly different way, starting from a **Ct** protonated species (at the amino group), Scheme I.15.[69]

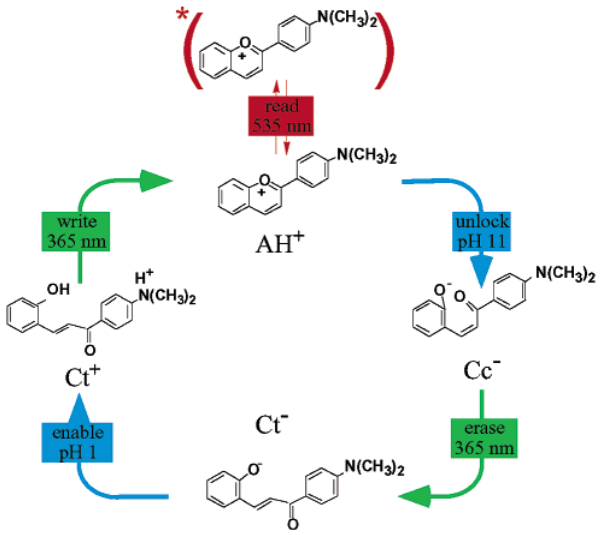


**Scheme I.15 –** Example of the write-lock-read-unlock-erase cycle based on the 4'-dimethylaminoflavylium compound.[69]

All of the above systems have the starting point at **Ct**. This can be a problem since **Ct** is photoreactive, making impossible to read without overwriting. It was demonstrated with the 4'-hydroxyflavylium ion that this difficulty can be overcome by starting at **AH**$^+$ which is the thermodynamically stable form at pH = 1.[65]

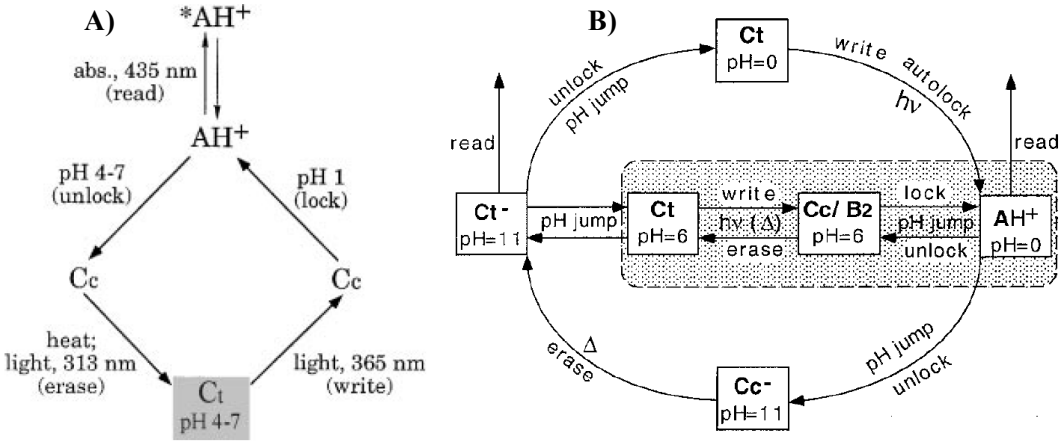


**Scheme I.16 –** Write-lock-read-unlock-erase cycles: **A**) from the **Ct** of the 4'-hydroxyflavylium; **B**) for unsubstituted flavylium

Since **AH**$^+$ is not photosensitive, it can be *read* by light excitation (i. e., by recording its absorption spectrum) without *writing*. Then it can be *unlocked* by a pH jump to 12, which yields

the metastable $\mathbf{Cc}^{2-}$ form. At this stage, one can *write* the optical information obtaining the stable (*locked*) $\mathbf{Ct}^{2-}$ form that can then be *read*. If necessary, the stored information into $\mathbf{Ct}^{2-}$ can be *unlocked* by a pH jump yielding **Ct** witch then be erased by light excitation, Scheme I.16A. The same optimized performance can be obtained starting from $\mathbf{Ct}^{2-}$.

For unsubstituted flavylium cation the previous cycle can be used to describe the system. But another possibility is to perform a cycle based on the anionic species presented in the basic media, Scheme I.16B.

## I.3.2. *Micelle Effect on the Write-lock-read-unlock-erase cycle*

The addition of micelles to the flavylium system can bring a new dimension to the flavylium complex network, enabling the switching between states with this third stimulus. Depending on the system and the type of the micelles added a different outcome should be expected. One example is the previous referred 4'-hydroxyflavylium which in the presence of negatively charged SDS micelles the $\mathbf{AH}^{+}$ form is stabilized, whereas with the addition of positively charged CTAB or neutral Triton X-100 micelles stabilize the uncharged forms.[70] The molar fraction distribution of the various species is altered as well as their interconversion rates.

An alternative cycle can be designed starting for instance at pH = 5.5 with a **Ct** solution based on the addition of SDS micelles changing the autolock of the system, see Scheme I.17.

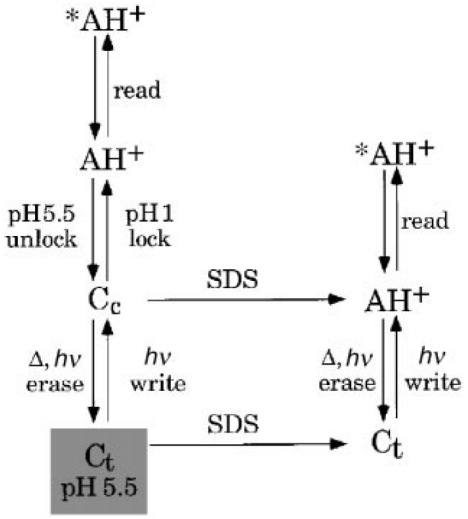


**Scheme I.17 -** Write–lock–read–unlock–erase cycles starting from the Ct form at pH 5.5. Left-hand side: light and pH jump inputs in the absence of micelles. Right-hand side: light input at the autolocking pH in the presence of SDS micelles.[70]

## I.3.3. *Permanent and Temporary Memories*

The human brain contains shallow and deep memory forms. The network of processes interconverting the various species 4'-hydroxyflavylium allows the presence of different levels of memory. Once the permanent (deep) $\mathbf{AH^+}$ form of memory has been obtained (Scheme I.18), a jump to pH 12 leads to the formation of a temporary (shallow) memory state, $\mathbf{Cc^{2-}}$, whose spontaneous slow *erasure* to give the deep $\mathbf{Ct^{2-}}$ memory can be accelerated by light. Reset can then be accomplished by a back pH jump to pH 4.[65]

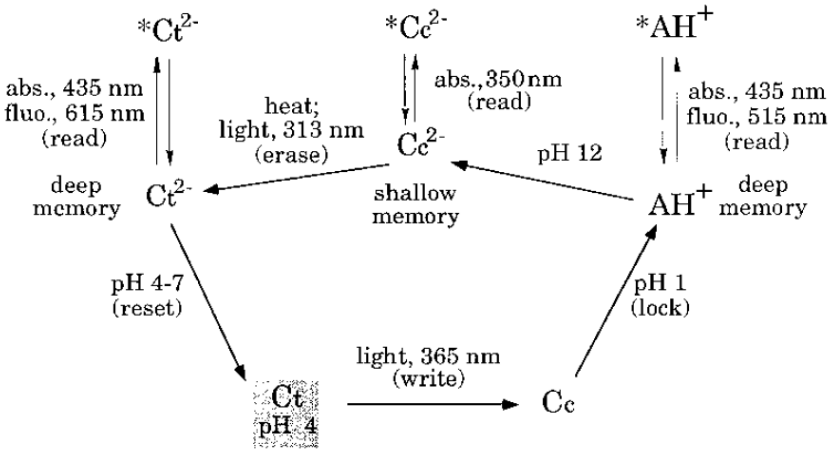


**Scheme I.18 -** A write–lock–read–unlock–erase cycle with two memory levels.[65]

## I.3.4. *Logic Operations*

A simple analogy with modern computer language is to consider light as an input and colour as the output signal.[11] A. P. de Silva[71,72,73] proposed this simple idea for the construction of logic gates.

Simple (bistable) photochromic systems perform YES/NO logic operations. Multistate/multifunctional molecular-level systems can be taken as bases for more complex logic operations.[71,74] Chemical systems capable to perform AND, OR, XOR, and XNOR logic operations and integration of logic functions and sequential operation of gates at the molecular scale have been reported.[13]

For flavylium compounds, light excitation and pH jumps can be taken as inputs and absorbance or fluorescence as outputs. Taking again 4'-hydroxyflavylium compound as an example and starting from the non emitting **Ct** species and taking the emission of $\mathbf{AH^+}$ at 515 nm as output signal, jump to pH = 1 alone or light excitation alone are not able to generate the output, whereas when these two inputs are applied in series, the output is obtained (AND logic function, Table I.1).

**Table I.1 -** Truth Table for the AND logic behaviour of the 4'-hydroxyflavylium compound starting from Ct at pH = 5.5[13]

| Input 1[a] | Input 2[b] | Output[c] |
|---|---|---|
| 0 | 0 | 0 |
| 1 | 0 | 0 |
| 0 | 1 | 0 |
| 1 | 1 | 1 |

In the presence of micelles the OR function is enable by the presence of the third input, starting from Ct at pH = 5.5 and taking the formation of $AH^+$ as an output, Table I.2.[70]

**Table I.2 -** Truth Table for the enable OR logic behaviour of the 4'-hydroxyflavylium compound starting from Ct at pH = 5.5[13]

| Input 1[d] | Input 2[e] | Input 3[f] | Output[g] |
|---|---|---|---|
| 1 | 0 | 0 | 0 |
| 0 | 1 | 0 | 0 |
| 1 | 1 | 0 | 0 |
| 0 | 0 | 0 | 0 |
| 1 | 0 | 1 | 1 |
| 0 | 1 | 1 | 1 |
| 1 | 1 | 1 | 1 |
| 0 | 0 | 1 | 0 |

An interesting system, based on the 4'-methoxyflavylium ion, capable of behaving according to an XOR (eXclusive OR) logic has been reported.[75] The system consists of an aqueous solution containing the **Ct** form of the 4'-methoxyflavylium ion and the $[Co(CN)_6]_3^-$ complex ion. When a solution of **Ct**, which is the thermodynamically stable form in the pH range 3-7, is excited by 365 nm light *trans-cis* photoisomerisation reaction occurs ($\Phi = 0.04$). If the solution is sufficiently acid (pH < 4), the **Cc** isomer is rapidly protonated with conversion to $\mathbf{AH^+}$, which is kinetically stable under such pH conditions and exhibits an intense absorption band with maximum at 434 nm. At higher pH values, however, protonation does not occur and

[a] pH jump to pH 1
[b] Light excitation at 365 nm
[c] Absorbance at 435 nm or emission at 515 nm of the $AH^+$ form
[d] pH jump to pH 1
[e] SDS micelle
[f] Light excitation at 365 nm
[g] Absorbance at 435 nm or emission at 515 nm of the $AH^+$ form

the photoproduct **Cc** goes back to **Ct**. excitation of $[Co(CN)_6]_3^-$ by 254 or 365 nm light in acid or neutral aqueous solution leads to the dissociation of a $CN^-$ ligand from the metal coordination sphere (quantum yield = 0.31), with a consequent increase in pH.[75] When an acid solution (pH = 3.6) containing $2.5x10^{-5}$ M **Ct** and $2.0x10^{-2}$ M $[Co(CN)_6]_3^-$ is irradiated at 365 nm, most of the incident light is absorbed by **Ct**, which undergoes photoisomerisation to **Cc**. Since the pH of the solution is sufficiently acid, **Cc** is rapidly protonated, with the consequent appearance of the absorption band with maximum at 434 nm characteristics of the $\mathbf{AH^+}$ species. On continuing irradiation, it can be observed that the absorption band increase in intensity, reach a maximum value, and then decrease up to complete disappearance. The reason for this behaviour under continuous light excitation is that as **Ct** is consumed with formation of $\mathbf{AH^+}$**,** an increasing fraction of the incident light is absorbed by $[Co(CN)_6]_3^-$, which undergoes dissociation, causing an increase in the pH of the solution. This not only prevents further formation of $\mathbf{AH^+}$, which would imply protonation of the **Cc** molecules that continue to be formed by light excitation of **Ct**, but also causes the back reaction to **Cc** (and then to **Ct**) of the previously formed $\mathbf{AH^+}$ molecules. Clearly, the examined solution performs like a threshold device as far as the input (light) / output (spectroscopic properties of $\mathbf{AH^+}$) relationship is concerned. Instead of a continuous light source, pulse flash irradiation can be used. Under the input of only one flash, a strong change in absorbance at 434 nm is observed, due to the formation of $\mathbf{AH^+}$. After 2 flashes, however, the change in absorbance practically disappears. In other words, an output (434 nm absorption) can be obtained only when *either* input 1 (flash I) *or* input 2 (flash II) are used, whereas there is no output under the action of *none* or *both* inputs. This shows that the described system behaves according to an XOR (eXclusive OR) logic, under control of an intrinsic threshold mechanism, Table I.3. It is noteworthy that the input and output signals have the same nature (light).[75]

**Table I.3 -** Truth Table for the XOR (eXclusive OR) logic behaviour of the 4'-methoxyflavylium compound starting from Ct at pH = 5.5[75]

| Input 1[a] | Input 2[a] | Output[b] |
|---|---|---|
| 0 | 0 | 0 |
| 1 | 0 | 1 |
| 0 | 1 | 1 |
| 1 | 1 | 0 |

[a] The two inputs are identical and consist of the amount of photons necessary to achieve the maximum response

[b] Variation of the absorbance at 434 nm or emission at 515 nm of the $AH^+$ species.

In the reaction networks of flavylium compounds a single molecule gives rise to several species reversibly interconverted by action of an external stimuli where complexity is built at the molecular level horizontally.[1]

Currently much research is being developed in the search of flavylium with new functionalities. Introduction of a conjugated double bond in the basic skeleton between the system and the phenyl benzopyrylium shifting the maximum absorption for greater wavelengths also allowing the existence of two possible *cis-trans* isomerisation of the neutral **Ct**.[76,77] Higher complexity was also achieved through the chemical transformation of one flavylium into another.[63,78] The substitution at position 6 of a hydroxyl group which allows the introduction of an electrical stimulus allows to obtain quasi-reversible cyclic voltammetry waves[79] or even by covalently binding the flavylium system to redox units that will be presented later.[80] Another great example was the employ of the flavylium salts as sensitizers for dye-sensitized solar cells.[81]

Several new multistate/multifunction systems can be designed, and new routes can be envisaged for these artificial systems can be applicable in real applications.

In this work it is intended to synthesize and study novel compounds capable of undergoing *cis-trans* photoisomerisation, i.e. photochromic compounds capable of functioning as optical memories[4,29,59] and reversible redox compounds units, in particular the synthesis and characterization of dyads and triads where the flavylium cation is covalently linked to redox units or to complexion units is envisaged.

# CHAPTER II. New Stimuli to Flavylium Networks

Publications associated with this chapter:

Sandra Gago, Vesselin Petrov, Ana M. Diniz, A Jorge Parola, Luís Cunha-Silva, Fernando Pina, "Unidirectional Switching between Two Flavylium Reaction Networks by the Action of Alternate Stimuli of Acid and Base" *J. Phys Chem A*, **2012**, 11(1): 372-380

Artur Moro, Ana M. Diniz, Vesselin Petrov, Fernando Pina, "Chemistry of 7,8-dihydroxy-2-(4-dimethylaminostryryl)-1-benzopyrylium. A photochemistry system switching from yellow to green", *J. Photochem. Photobiol. A: Chemistry*, **2013**, 263, 17-23.

# II. New Stimuli to Flavylium Networks

Synthetic flavylium salts constitute a versatile family of compounds possessing the same basic structure of anthocyanins, the ubiquitous compounds responsible for most of the red and blue colours of flowers and fruits.[1,17,37,41,82] Their physical-chemical properties are greatly dependent of the nature and position of the functional groups attached to the 2-phenyl-1-benzopyrylium skeleton.[1] As pointed out in the Introduction, in aqueous solution, synthetic flavylium salts give rise to a network of different chemical species interconvertible by pH and light modifications, being paradigmatic examples of multistate compounds.[13] Besides their role as biological dyes, the flavylium chromophores have acquired importance in materials science applications being also viewed as models for optical memories capable of *read-write-erase* processes.[60,61,62,63,83]

In this chapter the introduction of two stimuli to the flavylium system is presented. In the first part of the chapter an Acid/Base alternate stimuli is added to 2-(4-carboxyphenyl)-7-diethylamino-1-benzopyrilium allowing the conversion of one flavylium system into another. In the second part complexation stimuli is added to 7,8-dihydroxy-2-(4-dimethylaminostyryl)-1-benzopyrylium. The thermodynamics, kinetics and photochemistry of these new systems are characterized.

## II.1. 2-(4-carboxyphenyl)-7-diethylamino-1-benzopyrilium

As previously referred, flavylium compounds have been exploited as models for optical memories, as *write-lock-read-unlock-erase* systems.[84] Until now, the major developments regarding these systems and flavylium chemistry have been achieved at the level of the substituent's and how the correct choice of the latter allows a better lock of the system.[1] These studies focus mainly on the flavylium system at neutral pH.

In this particular case the new stimuli is added at acidic pH with the interconversion of the flavylium ion from an acid to an ester flavylium, a completely reversible system.

### II.1.1. *The reaction network*

As previously mentioned, in the absence of a hydroxyl substituent there is no formation of quinoidal base **A** and usually the formation of **B4** is verified.[41,83,85] The network of chemical reactions exhibited by the 2-(4-carboxyphenyl)-7-diethylamino-1-benzopyrilium is described by Scheme II.1 and the system can be treated by means of the chemical equilibria described in Schemes I.6 – I.9.

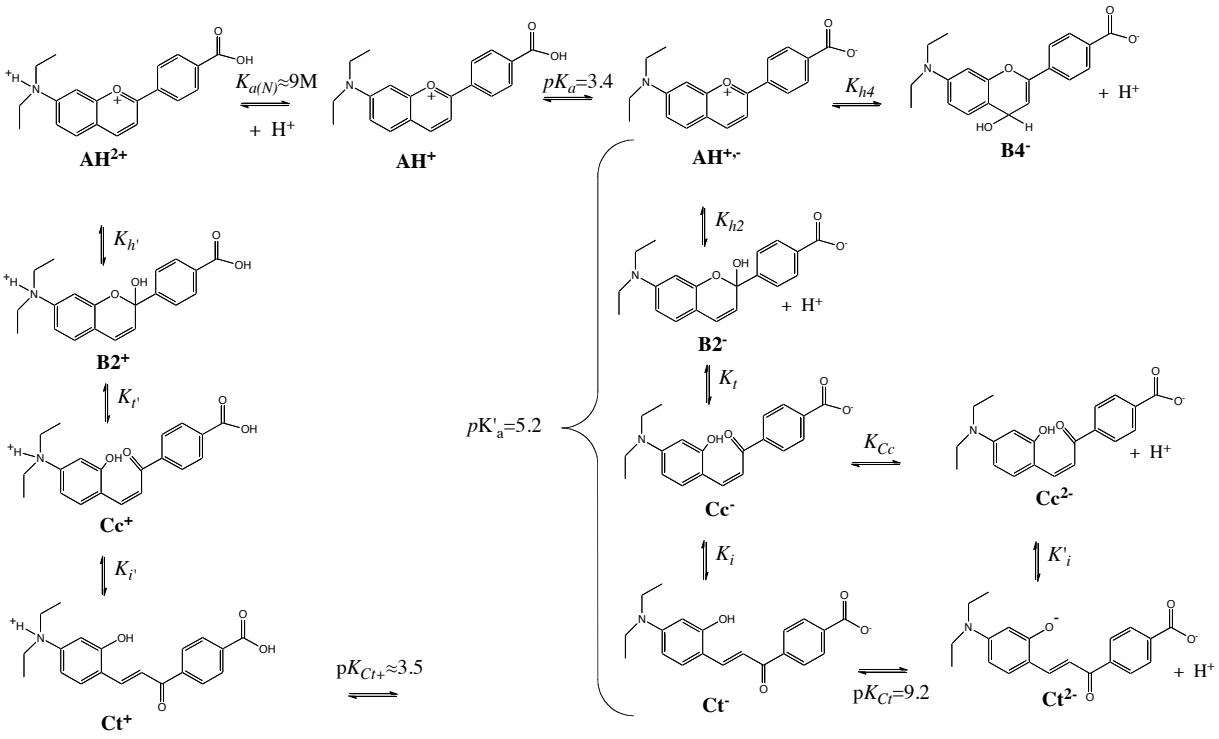


**Scheme II.1 –** Network of chemical reactions of 2-(4-carboxyphenyl)-7-diethylamino-1-benzopyrylium

All the studies were performed in 20 % ethanol. The spectral variations of equilibrated solution as a function of pH are depicted in Figure II.1 and are consistent with a sequence of reactions showed in Scheme II.1. The protonation of the amine group at extremely acid pH's with a p$K_a \approx$ -0.95, Figure II.1A. The first small inflexion between 2 < pH < 7 (Figure II.1B) is fitted with p$K$=3.4 and is due to the deprotonation of the carboxylic group which is better detected by fluorescence, Figure II.1D (open circles), as previously reported for the analogous compound 4-(2-carboxyphenyl)-7-diethylamino-4'-dimethylamino-1-benzopyrylium.[86] The higher acidity of the carboxylic substituent, p$K_a$=3.4, in comparison with benzoic acid p$K_a$=4.2, is expected from the influence of the positive charge of the flavylium cation. The remaining spectral changes obtained in Figure II.1B are due to the network of chemical reactions that lead to the *trans*-chalcone with p$K$'$_a$=5.2.

It is worth noting at this point that the *trans*-chalcone (**Ct**) is not a neutral species. Due to the deprotonation of the carboxylic group at lower pH values forming a zwitterionic species **AH**$^{+-}$, all the remaining species of the system should be deprotonated leading to the formation of **Ct**$^-$ instead of the common neutral **Ct**. This was also confirmed by $^1$H NMR data, see page 38, Figure II.7.

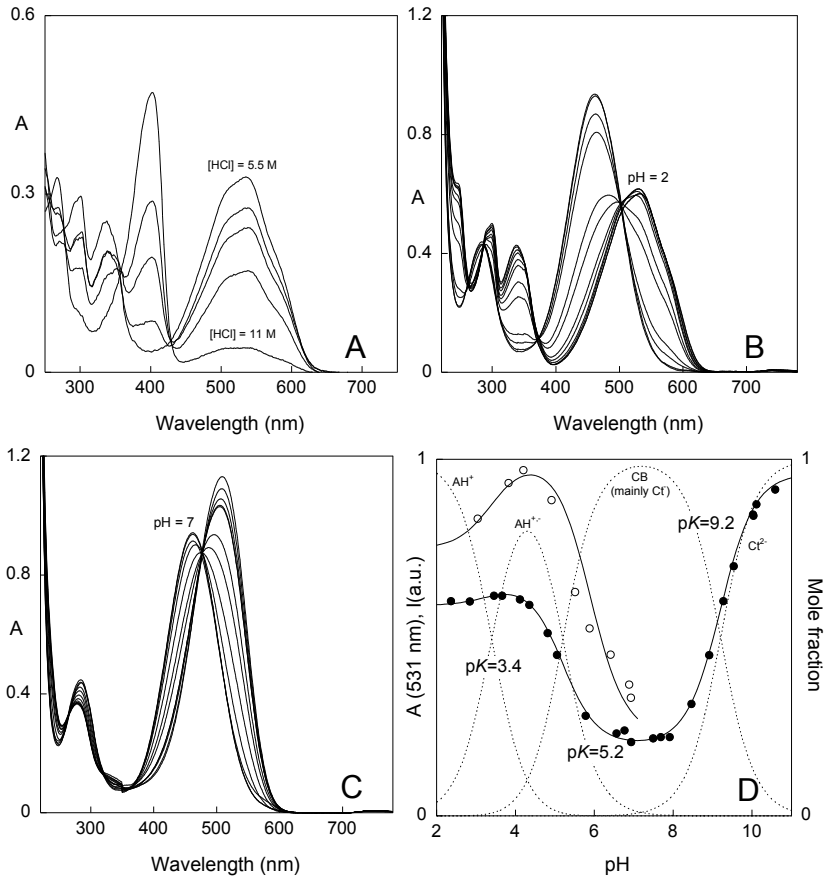


**Figure II.1-** Spectral variations of the compound 2-(4-carboxyphenyl)-7-diethylamino-1-benzopyrylium , 3.43x10$^{-5}$ M, in aqueous solutions (20% ethanol) upon equilibration in the dark (3 h) as a function of pH: **A**- spectra at extremely acidic solutions; **B**- 2<pH<7; **C**- 7<pH<11.5; **D**- simultaneous fitting of the absorption at 531 nm (•) and emission at $\lambda_{exc}$=500 nm, $\lambda_{em}$=630 nm (○).

Figure II.1C depicts a titration of $\mathbf{Ct^{2-}}$ to $\mathbf{Ct^{-}}$ with a p$K_{Ct-}$ = 9.2. The formation of (ionized) *trans*-chalcone ($\mathbf{Ct^{2-}}$) at pH=12 was also confirmed by $^1$H NMR on the basis of the large coupling constant between $H_3$ and $H_4$, Fig.II.7.

From the data of Fig. II.1B, Equation II.1 can be written:

$$K'_a = K_{h4} + K_{h2} + K_{h2}K_t + K_{h2}K_tK_i = \mathbf{10^{-5.2}} \qquad \textbf{Equation II-1}$$

In order to characterize the kinetics of the network of chemical reactions, a series of pH jumps from equilibrated solutions at pH=1.1 to higher pH values was performed, Fig. II.2. If the pH jump is carried out to pH=7.9, Fig. II.2A, the flavylium cation (ionized on the carboxylic group, $\mathbf{AH^{+,\cdot}}$) is the species observed immediately after the jump and the system evolves to the *trans*-chalcone (also ionized in the carboxylic group, $\mathbf{Ct^{-}}$). At pH=8.9, Fig. II.2B, it is possible to see the evolution over time from the flavylium cation to the ionized *trans*-chalcone. This transformation has three kinetic processes, the first two cannot be seen in the minutes to hours time scale of this experiment but through stopped flow experiments it is possible to identify them, see explanation on page 34 and 35. In the case of the same experiment to pH=12.2, Fig.

II.2C, the species formed after the jump is not the flavylium cation, but instead a new species with an absorption band centred at 509 nm appears immediately after the jump. Since the flavylium band is no longer recorded and that we are at a high pH value (pH=12.2) it can be assumed that in this case the hydration of the flavylium cation takes place before the time needed to record an absorption spectrum in our spectrophotometer (*ca.* 1 min). The new specie formed is $\mathbf{Cc^{2-}}$ and the observed process is due to the *cis-trans* isomerization, $\mathbf{Cc^{2-}}$ that originates $\mathbf{Ct^{2-}}$. This process will be discussed again on the basis of the stopped flow experiments, page 34.

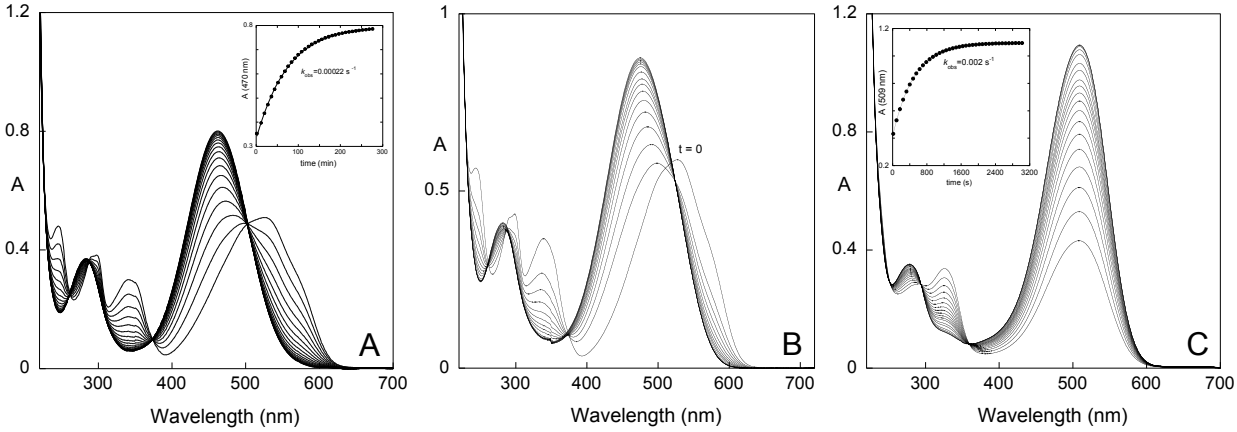


**Figure II.2 – A-**Spectral variations of the compound 2-(4-carboxyphenyl)-7-diethylamino-1-benzopyrylium 3.4x10-$^5$ M, upon a pH jump from 1.1 to 7.9; **B**- the same for pH=8.9. **C**- the same for 12.2.

The observed rate constants (slowest process) as a function of pH can be accounted for by considering two different processes controlling depending on the pH, see Figure II.3. At lower pH values the hydration is the controlling step and a U shaped curve is obtained, which is given by Equation I-10 (page 13, $k_{hydration}$). The fitting follows Equation II-2, from which $K_{h2}$ can be determined, see later the details for the calculation of the [$OH^-$] coefficient. At higher pH values the hydroxyl attacks the flavylium cation and hydration becomes faster than the isomerisation rendering this last process as the rate-determining step, which is given by Equation I-11 (page 14, $k_{isomerization}$). Recalling that the *trans*-chalcone is ionized, and that the isomerization refers to $\mathbf{Cc^{2-}}$ to $\mathbf{Ct^{2-}}$ (pH higher than p$K_{Ct-}$ = 9.2), the curve can be fitted by means of Equation II.3.

The plateau at higher pH values is reached when the ionized $\mathbf{Cc^{2-}}$ reaches the pseudo equilibrium, i.e., equilibrium of all the basic species before significant formation of the $\mathbf{Ct^{2-}}$. The fitting achieved by means of Equation II.3 reflects the fraction of $\mathbf{Cc^{2-}}$ existent at the pseudo equilibrium.

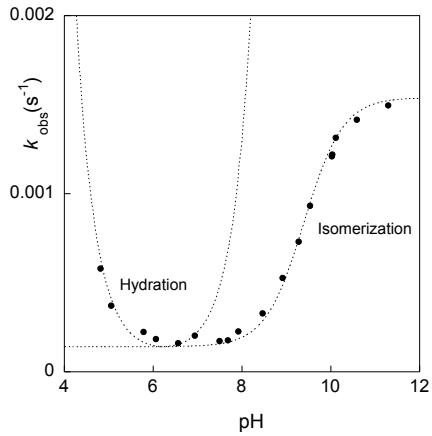


**Figure II.3 -** Representation of the rate constants of the direct pH jumps versus pH. Fitting was achieved according to Eq. II.2 (hydration) and Eq. II.3 (isomerisation).

$$k_{hydration}(s^{-1}) = 1.4\text{x}10^{-4} + 35[\text{H}^+] + 1.2\text{x}10^{3}[\text{OH}^-] \qquad K_{h2}=4\text{x}10^{-6}\ \text{M}^{-1} \qquad \textbf{Equation II-2}$$

$$k_{isomerization}(s^{-1}) = \frac{10^{-9.4}}{[\text{H}^+]+10^{-9.4}} 0.0014 + 1.4x10^{-4} \qquad \textbf{Equation II-3}$$

The concept of pseudo-equilibrium was described in Schemes I.8 and I.9 for flavylium with OH substituents, being in this case (without OH) presented in Equation II.4:

$$\text{AH}^+ + \text{H}_2\text{O} \rightleftharpoons \text{CB}^\wedge + \text{H}_3\text{O}^+ \qquad K^\wedge_a$$

$$K^\wedge_a = K_{h2} + K_{h4} + K_{h2}K_t \qquad \textbf{Equation II-4}$$

Being [CB^]=[B4]+[B2]+[Cc], and considering that in Equation II.4 the species are ionized at the carboxylic substituent, Equation II.5 can be obtained.

$$\text{AH}^{+,-} + \text{H}_2\text{O} \rightleftharpoons \text{CB}^\wedge + \text{H}_3\text{O}^+ \qquad K^\wedge_a$$

$$[\text{CB}^\wedge] = [\text{B4}^-] + [\text{B2}^-] + [\text{Cc}^-] \qquad \textbf{Equation II-5}$$

$$\text{Cc}^- \rightleftharpoons \text{Cc}^{2-} + \text{H}^+ \qquad K_{Cc^-/Cc^{2-}}$$

Equation II.6 gives the mole fraction of $Cc^{2-}$

$$\chi_{Cc^{2-}} = \frac{K_{h2}K_tK_{Cc^-/Cc^{2-}}}{[\text{H}^+]^2 + K^\wedge_a[\text{H}^+] + K_{h2}K_tK_{Cc^-/Cc^{2-}}} \qquad \textbf{Equation II-6}$$

According to the fitting of Equation II.3, $\frac{K_{h2}K_tK_{Cc^-/Cc^{2-}}}{K^\wedge_a} = 10^{-9.4}$ and the intrinsic value of the isomerisation is $k_i^{'}$=0.0014 $s^{-1}$. Considering that the experimental evidence points out to

[CB$^{\wedge}$] ≈ [Cc$^{-}$] and $K_a^{\wedge} \approx K_{h2}K_t$ it can be concluded that $K_{Cc^-/Cc^{2-}} \approx 10^{-9.4}$. This value is close to $K_{Ct^-/Ct^{2-}} = 10^{-9.2}$, Fig. II.1D, as expected from the usually observed similarity between the acidity constants of the *cis* and *trans* chalcones.[51]

In order to characterize the pseudo-equilibrium, a series of pH jumps from pH=1.0 to pH higher than 9 were performed and monitored by stopped flow, Fig. II.4. The stopped flow data confirms the slow process of Figure II.2C attributed to the *cis-trans* isomerisation (time scale of hours) but also reveals two other fast processes. At pH = 12 a first process with $k_{obs}$ = 21.9 $s^{-1}$ is due to the hydration process which is very fast at this pH. The second fast process with $k_{obs}$ = 0.20 $s^{-1}$ accompanied with an increase in absorption at 527 nm can be accountable for the formation of the flavylium cation from B4$^{-}$(hydration). This can be explained if during the first step B4$^{-}$, B2$^{-}$ and Cc$^{2-}$ are formed and in a second step the kinetic product B4$^{-}$ gives rise to the final pseudo-equilibrium involving essentially Cc$^{2-}$ through flavylium.

This implies the existence of a very fast tautomeric equilibrium (between B2$^{-}$ and Cc$^{2-}$), which is due to the catalytic effect of the hydroxyl ion in the ring-opening closure previously described.[42] The faster observed process is related with hydration and its rate is directly proportional to the concentration of the hydroxyl ion, Fig. II.4C, with an observed rate constant 1.2x10$^{3}$ $s^{-1}$ and can be attributed to the sum of the rate constants $k_{B2}^{OH} + k_{B4}^{OH}$, responsible for the hydroxyl ion attack to the flavylium cation in position 2 and 4 respectively. The final equilibrium is achieved throughout *cis- trans* isomerisation.

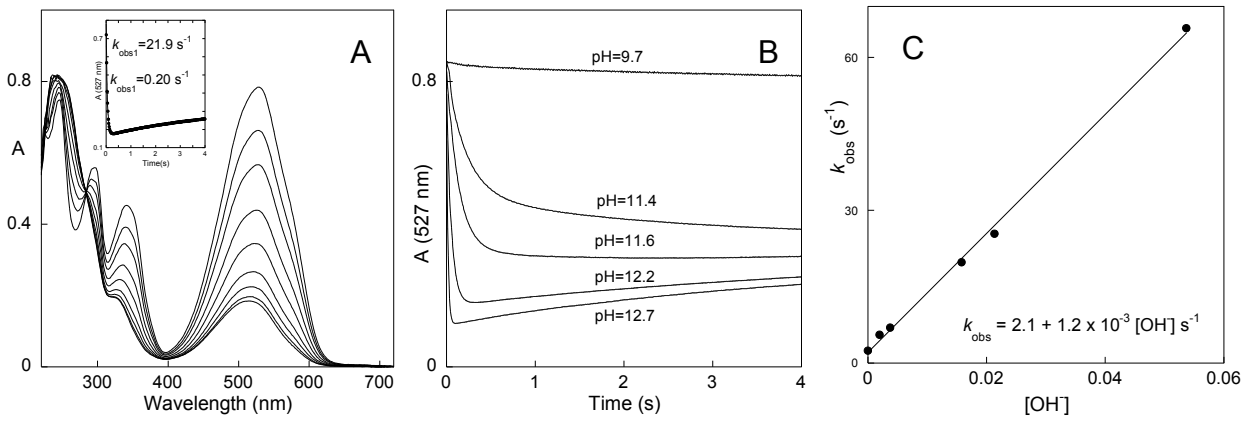


**Figure II.4** A- Spectral variations of the compound 2-(4-carboxyphenyl)-7-diethylamino-1-benzopyrylium 4.3x10$^{-5}$ M, after a pH jump from 1.1 to 12.2 followed by stopped flow; B-stopped flow traces after a pH jump from 1.1 to the basic region; C- rate constants as a function of the hydroxyl concentration.

A sequence of pH jumps from non-equilibrated solutions at pH=13 and back again to pH=1 were also performed, the absorption being monitored in the last step, Fig.II.5A. Protonation is faster than the mixing time of the stopped flow and by consequence all the

species present at pH=13 are immediately frozen in the respective protonated species. In other words, all $B2^-$, $B4^-$ and $Cc^{2-}$ existent at pH=13 upon the initial pH jump become B2, B4 and Cc, the observed kinetic processes regard these species. The bi-exponential trace in the inset of Fig.II.5B is in accordance to a faster kinetics that converts B2 and B4 into flavylium cation (2.4 $s^{-1}$), followed by a slower one leading to more flavylium cation from Cc via $B_2$. A reverse pH jump from an equilibrated solution at pH=13 to pH=1 was also performed. In this case, the conversion of Ct to flavylium cation is much slower as shown in Fig. II.5B. The ratio of the amplitudes in Fig. II.5A, is 0.38 meaning that the pseudo equilibrium at pH=13 is constituted by 38% $B2^-$ and $B4^-$ and 62 % of $Cc^{2-}$ (at pH=13).

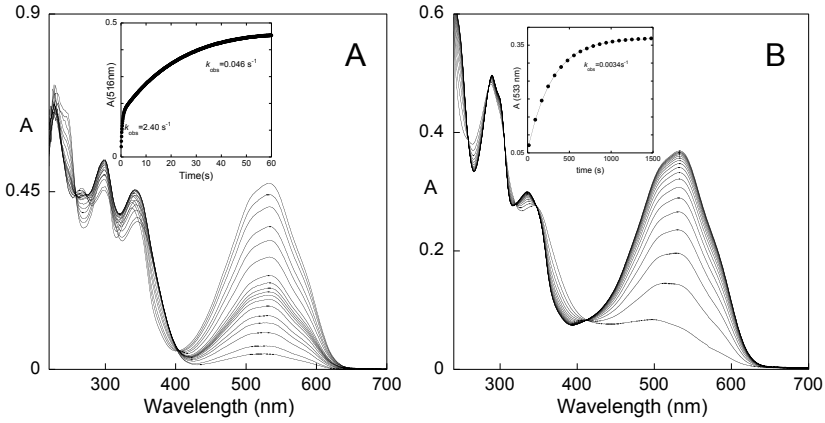


**Figure II.5** -**A**-Spectral modifications of the compound 2-(4-carboxyphenyl)-7-diethylamino-1-benzopyrylium $4.3x10^{-5}$M in water: ethanol (20%) upon a reverse pH jump from solutions at pH=13 (non-equilibrated) followed by stopped flow; **B** -The same upon equilibration followed by a normal spectrophotometer.

## II.2. *7-diethylamino-2-(4-(methoxycarbonyl)phenyl)-1-benzopyrylium hydrogensulfate*

Solutions of the compound 2-(4-carboxyphenyl)-7-diethylamino-1-benzopyrylium in methanol are converted into the methyl ester derivative 7-diethylamino-2-(4-(methoxycarbonyl)phenyl)-1-benzopyrylium upon addition of hydrochloric acid. This fact allows conceiving a unidirectional cycle (Scheme II.2) where the flavylium ester derivative is converted into the free carboxylic acid through the respective *trans*-chalcone upon alternating acid-base inputs. While the base catalysed hydrolysis of esters is a well-known reaction, the esterification of a carboxylic acid at room temperature is less usual. In the case of the present compound the positive charge of the benzopyrylium unit facilitates the attack of methanol to the carboxylic acid group on the *para* position.

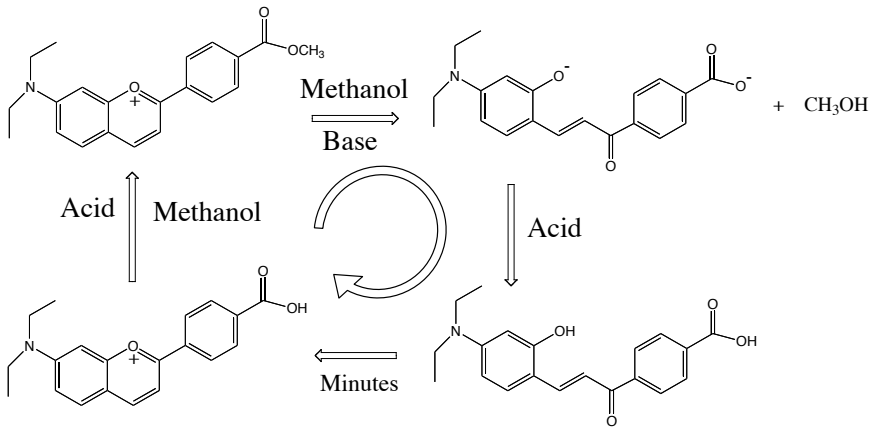


**Scheme II.2**

Besides recrystallization from 2-(4-carboxyphenyl)-7-diethylamino-1-benzopyrylium in a mixture of methanol/acid, 7-diethylamino-2-(4-(methoxycarbonyl)phenyl)-1-benzopyrylium can also be obtained according to the synthetic procedure described in the experimental part, see below. For this reason the following experiments have been carried out in water containing 20% of ethanol. In this case the solutions are stable, unless differently is mentioned.

## II.2.1. *Crystal structure of the trans-chalcone*

Crystalline material of *trans*-chalcone of 7-diethylamino-2-(4-(methoxycarbonyl)phenyl)-1-benzopyrylium suitable for single-crystal X-ray diffraction analysis was obtained by recrystallization in ethanol of the precipitate obtained in a mixture water: ethanol, and the unveiled structure confirms undoubtedly the formation of the chalcone species in the configuration *trans* (Figure II.6a). Systematic searches in the literature and in the Cambridge Structure Database (CSD, Version 5.32 of 2011)[87,88] confirm that this compound was not reported previously. The crystal structure was determined in the triclinic system and in the centrosymmetric space group *P*-1 (more details related with the crystallographic data collection and structure refinement can be found in experimental section and Table 1). The asymmetric unit cell (asu) consists of two crystallographic independent Ct molecules, each one rotated 180º in the horizontal plane relatively to the other. Furthermore, the two molecules display distortion conformational considerably distinct. In molecule 1 (that contains the N1 atom) the dihedral angle between the average planes of the two aromatic rings is c.a. 35.16º, while the correspondent angle in the molecule 2 (that contains the N2 atom) is c.a. 31.87º. Adjacent Ct molecules interact through strong O−H···O intermolecular hydrogen bonds (orange dashed lines in figure II.6b) involving one hydroxyl group and oxygen atom of the carbonyl group (C=O) in the neighbouring molecule leading to the formation of one-dimensional supramolecular arrangement: O4−H1···O7 with $d_{(H1\cdots O7)}$ = 1.858(19) Å and $\text{angle}_{(O4\text{-}H1\text{-}O7)}$ = 171(4)º, and O2−H2···O3 with $d_{(H2\cdots O3)}$ = 1.814(19) Å and $\text{angle}_{(O8\text{-}H2\text{-}O3)}$ = 177(3)º; symmetry

transformations used to generate equivalent atoms, (i) *x*, *y−1*, *z*. This supramolecular arrangement is further reinforced by the cooperative effect of various intermolecular C−H···O weak interactions (green dashed lines in figure 6b): C14−H14···O6, C16−H16···O7, C18−H18A···O6, C35−H35···O2, C37−H37···O3, C39−H39B···O2 , with H···O distances in the range between 2.558(3) and 2.716(3) Å and the C-H-O angles ranging from 131.3(2) and 177,6(2)º.

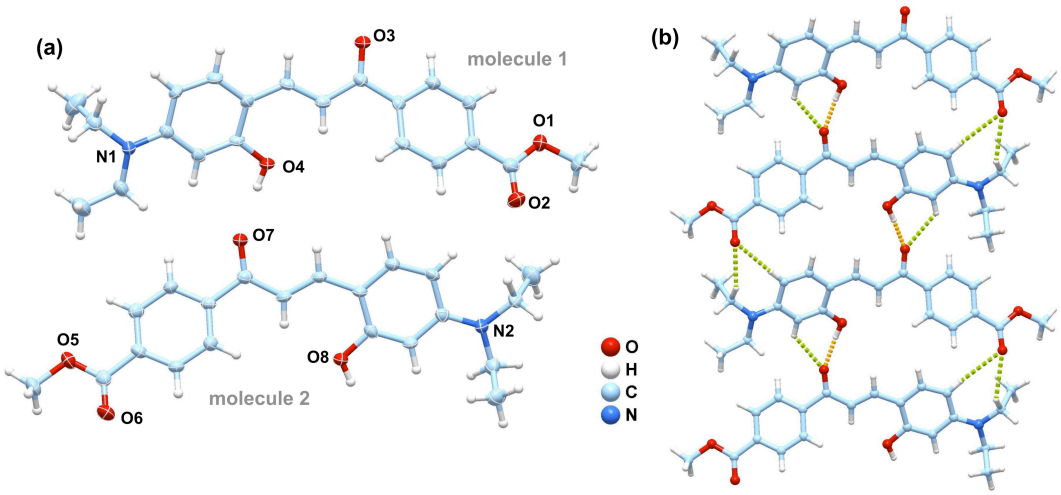


**Figure II.6 (a)** Asymmetric unit cell of the crystalline structure of the *trans*-chalcone of 7-diethylamino-2-(4-(methoxycarbonyl)phenyl)-1-benzopyrylium showing the labelling scheme for the oxygen and nitrogen atoms; All atoms are represented as thermal ellipsoids drawn at the 50% probability level, excluding the hydrogen atoms which are drawn as spheres with arbitrary radii. (b) Strong O−H···O (orange dashed lines) and weak C−H···O (green dashed lines) hydrogen bounds between adjacent molecules.

## II.2.2. *De-esterification of 7-diethylamino-2-(4-(methoxycarbonyl)phenyl)-1-benzopyrylium*

When aqueous solutions of the compound 7-diethylamino-2-(4-(methoxycarbonyl)phenyl)-1-benzopyrylium in *d*-methanol are basified, the $^{1}$H NMR spectrum taken immediately after shows unequivocally the disappearance of the singlet of the methoxy group and the appearance at 3.34 ppm of a singlet that is characteristic of (non-deuterated) methanol. Acidification of this solution shows the appearance of the protonated *trans*-chalcone that evolves to 2-(4-carboxyphenyl)-7-diethylamino-1-benzopyrylium, Figure II.7.

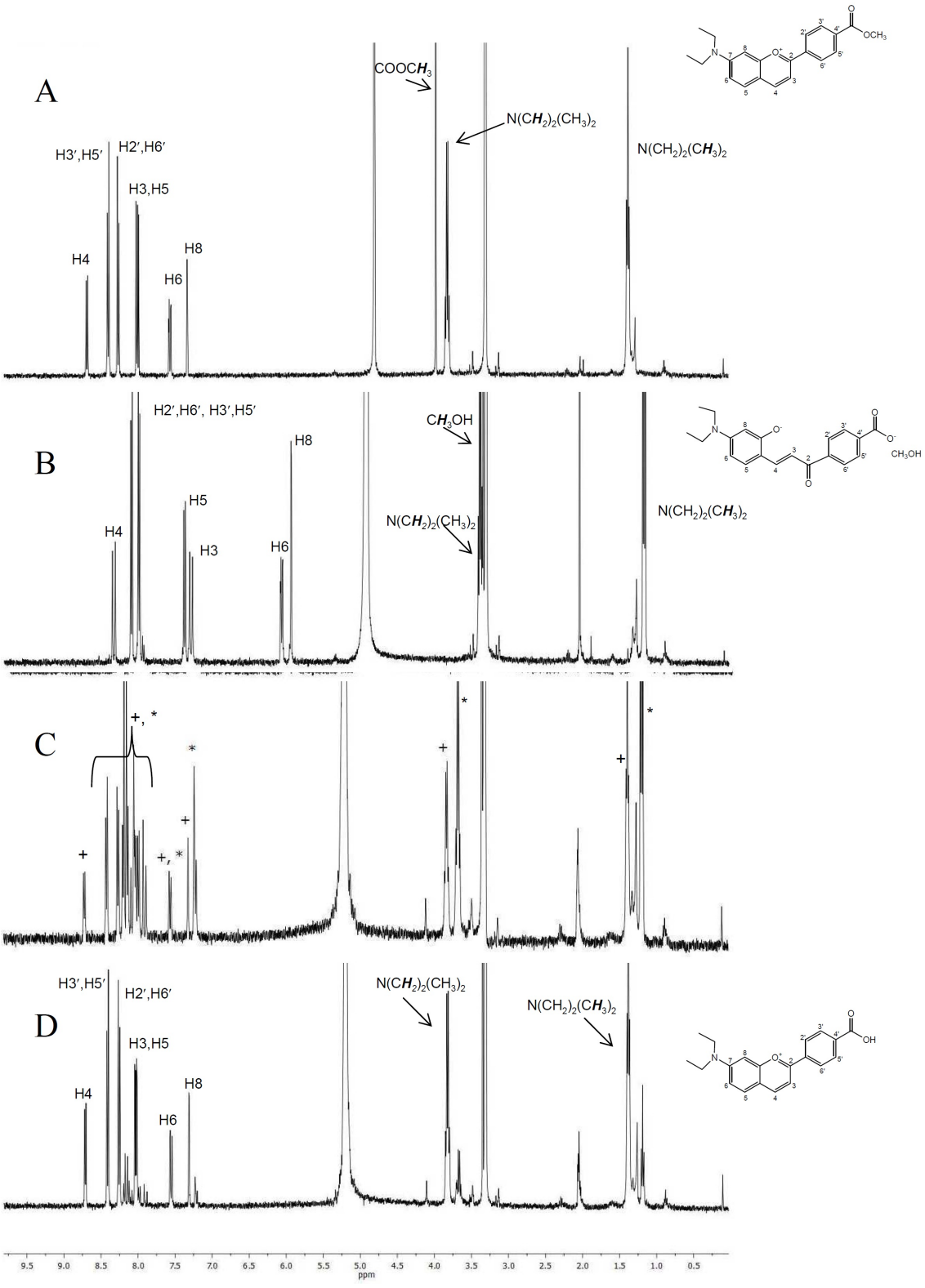


**Figure II.7** - $^{1}$H NMR spectra at room temperature in $CD_3OD$ of: **A** - 7-diethylamino-2-(4-(methoxycarbonyl)phenyl)-1-benzopyrylium; **B**- the same compound after addition of NaOD ($Ct^{2-}$ form); **C** and **D**- evolution of the system after addition of DCl to the previous solution (+) denotes the presence of the flavylium cation and * the presence of the Ct form).

## II.2.3. *The reaction network*

Once understood the switching between the acid group and ester group, the study of the chemical network of reactions was done similarly as previously. In order to avoid ester hydrolysis the study was restricted to acid to neutral pH's. Once again the protonation of the amino group is only obtained at very acid pH values and a similar p$K_a$ ≈ - 0.95 was verified, Figure II.8A. The value is easy to understand since the difference between acid and ester group is in ring **B** and has small influence on the ring **A**. In Figure II.8B is depicted the absorption spectra of equilibrated solutions where is possible to verify the equilibrium between the flavylium and the *trans*-chalcone. Also noteworthy to point out that this chalcone is a neutral one. The fitting of the data at 470 and 530 nm renders a p$K_a$' = 4.95. This value is comparable with the previously obtained for the acid analogues (p$K_a$' = 5.2). However in the acid, the deprotonation of the carboxylic group (p$K$ = 3.4) can stabilize at a certain extent the flavylium cation and difficult hydration, resulting on a p$K_a$' slightly higher.

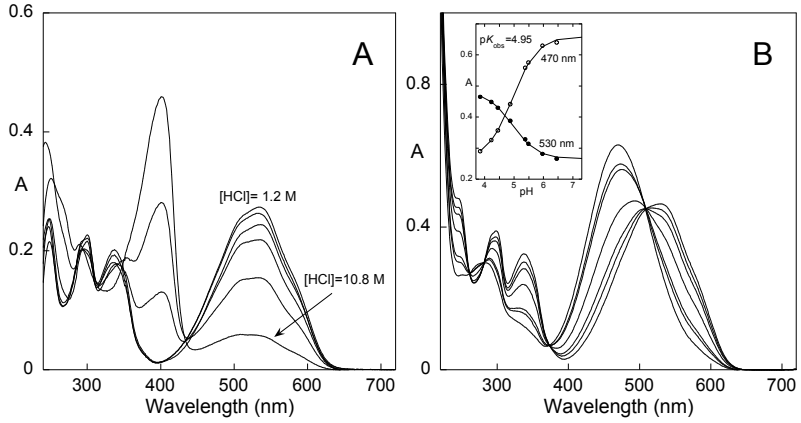


**Figure II.8 -** Absorption spectra of the compound 7-diethylamino-2-(4-(methoxycarbonyl)phenyl)-1-benzopyrylium, 2.7x10$^{-5}$M in water: ethanol (80:20) upon equilibration: **A**-at extremely acidic medium (1.1x10$^{-5}$M, in water), inflection point occurs for [HCl] ≈9M; **B** - 3.9<pH<7.9, fitting was achieved for p$K$'$_a$= 4.95.

Regarding the kinetics of the system pH jumps from pH=1.0 to higher pH values were carried and the UV-Vis absorption modifications monitored, Figure II.9.

In Figure II.9A it is depicted one example to pH =7.5 and it is clear the evolution from $\mathbf{AH^+}$ to **Ct**, an identical pattern being observed in the pH range between 3 and 8. This behaviour indicates a process controlled by the hydration reaction similarly to the carboxyl derivative. Fitting was achieved for $k_{h2}$=0.00026 s$^{-1}$ and $k_{-h2}$=15 M$^{-1}$s$^{-1}$, p$K_h$=4.8, that compares with 5.4 for the carboxylic derivative confirming again that the ester compound is more easily hydrated, Figure II.9B.

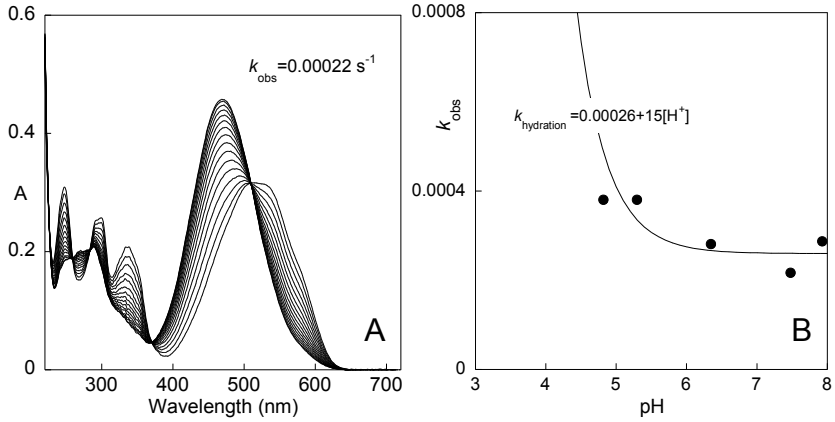


**Figure II.9 A-** Spectral variations after a pH jump from an equilibrated solution of the compound 7-diethylamino-2-(4-(methoxycarbonyl)phenyl)-1-benzopyrylium in water: ethanol (80:20) at pH=1 to pH=7.5 ($1.8x10^{-5}$M); **B**-Observed rate constants of the direct pH jumps as a function of pH jumps.

## II.3. 7,8-dihydroxy-2-(4-dimethylaminostyryl)-1-benzopyrylium

Styrylflavylium salts are analogues of anthocyanins distinguished by the introduction of a conjugated double bond in the basic skeleton, between benzopyrylium system and the phenyl group, Figure II.10.

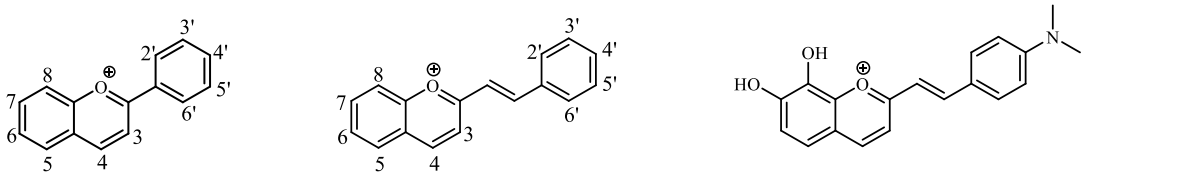


**Figure II.10-** Struture of flavylium (2-phenyl-1-benzopyrylium), 2-stryryl-1-benzopyrylium and the 7,8-dihydroxy-2-(4-dimethylaminostyryl)-1-benzopyrylium

The advantage of introducing the styryl group instead of the phenyl group is to extend the conjugation, originating a significant bathochromic shift of the maximum absorption and often resulting in more intense shades when compared to common flavylium systems.

Unlike synthetic flavylium, the existing literature on this type of compounds is greatly reduced.[26,89,90] Studies by Amic *et al*. showed a p$K_a$ increase with the introduction of the double bond, delaying the loss of colour for higher pH values by increasing their stability at acidic pH's. [83,89]

Another important factor in this type of compounds is the existence of two possible *cis-trans* isomerisation pathways of the chalcone at neutral or basic pH's, unveiling another state in the models for write-read-erase at the molecular level. Depending on the stability and behaviour

of the two connections (λ max absorption, thermal stability, energy needed for isomerization), it will be able to *write-lock-read-unlock-erase* diverse information in a single molecular component.

In addition to the lack of studies on this family of compounds, their possible application in the food industry as a colouring[26] or the construction of molecular devices makes their study and characterization important nowadays.

With these concepts in mind, our motivation was to take full profit of the aforementioned advantages, which led us to synthesize 7,8-dihydroxy-2-(4-dimethylaminostyryl)-1-benzopyrylium. Another particularity of this compound is the presence of the catechol group which allows complexation with metals. The formation of flavylium metal complexes namely with $Al^{3+}$, induces an anthocyanin-like behaviour, particularly regarding their colour.[91]

The styrylflavylium compounds follow the same network of chemical reactions as anthocyanins[42,92] and related compounds and consequently it is possible to characterize their reactivity by the same thermodynamic and kinetic approach.[10,76,77,93]

## II.3.1. *The reaction network*

Previous studies showed that the amino groups in position 7 or 4' of the flavylium cation are protonated only at extremely acidic solutions.[51,52,94] This is due to the donor capacity of these ligands to transfer charge for the conjugate π system of the flavylium cation, rendering the nitrogen less available to accept the protons. The spectral variations reported in Fig. II.11A shows that this is also the case of styrylflavylium, 7,8-dihydroxy-2-(4-dimethylaminostyryl)-1-benzopyrylium. Protonation of the amine renders its lone pair not to be available to the extended conjugation of the molecule resulting in a blue shift of the absorption band as previously observed for amino substituted flavylium cations.[32,62,95]

Due to some precipitations problems, the majority of the studies were performed in a mixture of water/methanol (1:1 v/v). Always assume these conditions unless noted otherwise. The absorption spectra acquired 1 min after a pH jump from pH=1 to higher pH values followed by a common spectrophotometer is represented in Fig. II.11B. Identical spectral variations are obtained if the pH jumps are followed by stopped flow 20 ms after the jump. The pH dependence of the spectra is compatible with the existence of a fast equilibrium involving the styryl flavylium cation and the respective quinoidal base, with acidity constant, $pK_a$= 5.3. The spectral variations for the thermal equilibrated solutions in the range 2<pH<7 are shown in Fig. II.11C, with an acidity constant equal to $pK'_a$=4.3, leading to $K_a+K_h(1+K_t)+K_hK_tK_i=10^{-4.3}$. In the equilibrium only 10% of **A** remains.

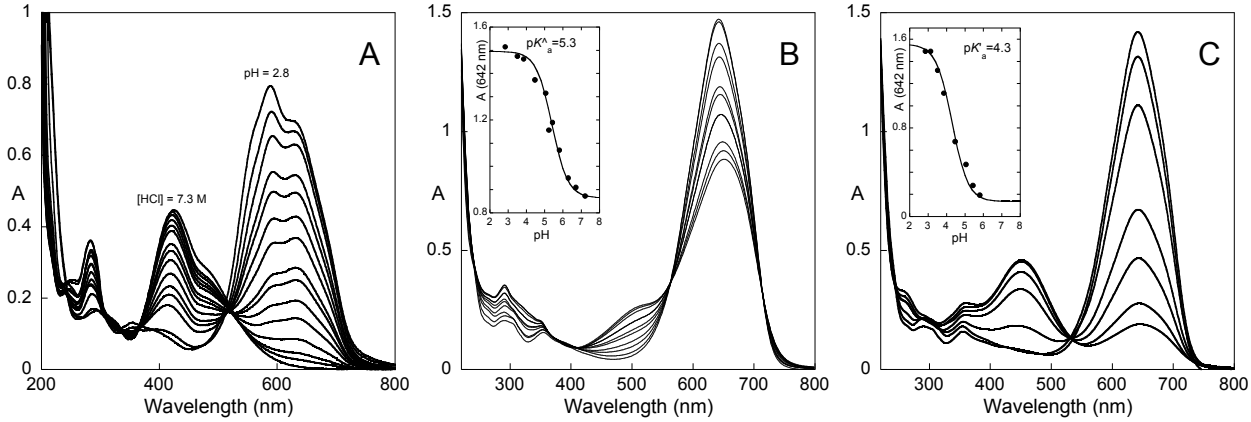


**Figure II.11** - Spectral variations of 7,8-dihydroxy-2-(4-dimethylaminostyryl)-1-benzopyrylium $3.0x10^{-5}$ M in water at extremely acidic pH values (**A**). Absorption spectra of the same $3.3x10^{-5}$M in a mixture of water/methanol (50:50 v/v) circa 1 min after a pH jump from pH=1.0 to higher pH values (**B**) and the same for solutions after thermal equilibrated as a function of pH, p$K$'$_a$=4.3 (**C**).

The flavylium $\mathbf{AH}^+$ and the chalcones can be interconverted through pH changes. Fig II.12A shows the spectral variations upon a pH jump from an equilibrated solution at pH =1 to pH = 5.8 where the disappearance of a mixture of $\mathbf{AH}^+$/**A** follows a mono-exponential decay. As also reported in previous work with amino substituent flavyliums, it is common to occur the formation of $\mathbf{CtH}^+$ that also originates $\mathbf{AH}^+$ as the thermodynamic product at relatively acid pH values. If that were the case a curve characteristic of the flavylium salts would be expected to describe the kinetic behaviour.[32,52,61] However, no such graph was obtained for this styrylflavylium system.

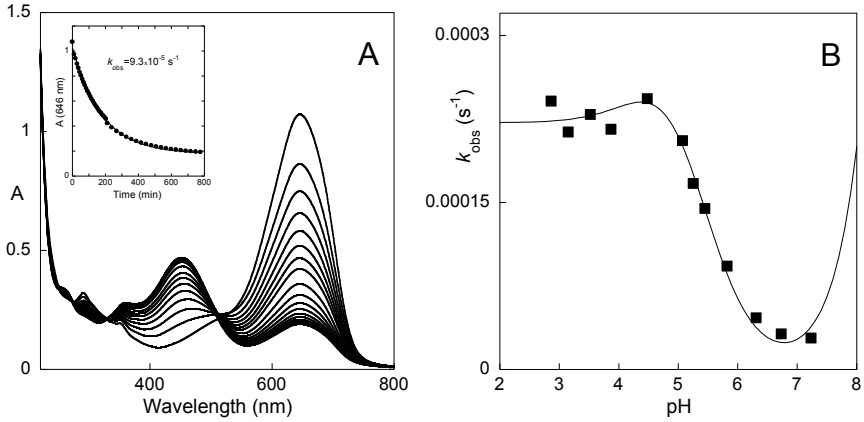


**Figure II.12 - A.** Spectral variations of the compound 7,8-dihydroxy-2-(4-dimethylaminostyryl)-1-benzopyrylium upon a pH jump from pH=1.0 to 5.8; **B.** Rate constant of the slowest process as a function of pH: fitting was achieved for $K_hK_tk_i$=1.04x10$^{-8}$ M$^{-1}$ s$^{-1}$, K$_t$$k_i$/$k_{-h}$=3.6x10$^{-5}$ M; $k_{-i}$= 2.3x10$^{-4}$ s$^{-1}$.The hydroxylation of the base taking place in basic medium was also considered, $K_h^{OH}$=200M$^{-1}$.

By plotting the observed rate constants *versus* pH of several pH jumps carried, Figure II.12B, a different case was observed. Fitting of the curve was achieved for $K_hK_tk_i$=1.04x10$^{-8}$ M$^{-1}$s$^{-1}$, $K_tk_i/k_{-h}$=3.6x10$^{-5}$ M and $k_{-i}$= 2.3x10$^{-4}$ s$^{-1}$ and p$K$a=5.3. The ratio of the

constants $K_tK_hk_i/K_tk_i/k_{-h}$ leads to $k_h$= 2.9x10$^{-4}$ s$^{-1}$. This value compares with those of anthocyanins and related compounds, which are of the order of magnitude 10$^{-1}$-10$^{-2}$ s$^{-1}$.

The different bell shaped obtained is due to the extremely low value of the hydration constant when compared with flavylium derivatives.[42] In Table II.1 and Table II.2 the solution of the global fitting is presented. This is not the only solution of the system, but it is the only that follows some restrictions which reflect accurately the experimental data, namely predicting at the equilibrium 88% of Ct, 10% of A and 2% of B and Cc, in agreement with the absorption spectra of Fig. II.11C.

**Table II.1 -** Equilibrium constants of the compound 7,8-dihydroxy-2-(4-dimethylaminostyryl)-1-benzopyrylium

| p$K'_a$ | p$K_a$ | $K_h$ (M$^{-1}$) | $K_t$ | $K_i$ |
|---|---|---|---|---|
| 4.3 | 5.3 | 6.2x10$^{-7}$ M$^{-1}$ | 0.9 | 87 |

**Table II.2 -** Rate constants of the compound 7,8-dihydroxy-2-(4-dimethylaminostyryl)-1-benzopyrylium

| $k_h$ (s$^{-1}$) | $k_{-h}$(s$^{-1}$) | $k_t$(s$^{-1}$) | $k_{-t}$(M$^{-1}$s$^{-1}$) | $k_i$(s$^{-1}$) | $k_{-i}$(s$^{-1}$) |
|---|---|---|---|---|---|
| 2.9x10$^{-4}$ | 500 | 0.78 | 0.86 | 0.02 | 2.3x10$^{-4}$ |

Inspection of Table II.1 and II.2 indicates that the values of the rate and equilibrium constants of the hydration and isomerization processes are much smaller than the tautomerization, justifying the use of Equation I.13. In Fig. II.13 are represented the individual rates of the three processes based on the data of Table II.1 and II.2 confirming that for pH>3 the tautomerization is by far the fastest process of the network justifying once again the use of Equation I.13.

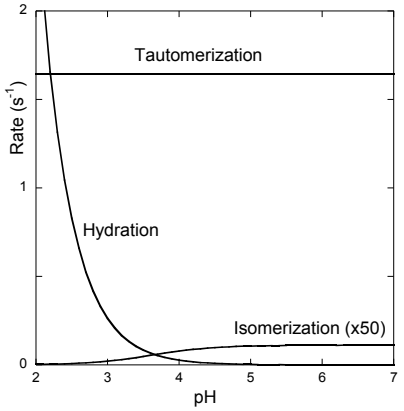


**Figure II.13 –** Representation of the individual rate constants of the hydration, tautomerization and isomerization

At lower pH values the rate-controlling step is the isomerization reaction. The respective rate is the product of $k_i$ (0.02 $s^{-1}$) by the mole fraction distribution of the cis-chalcone, which is expected to be 0.01 at the plateau, with an overall rate constant of 0.0002 $s^{-1}$ in good agreement with the value reported in Fig. II.12B. At higher pH values the control is essentially given by the hydration constant, which inflects according to the p$K_a$ value.

Studies concerning basic pH's were performed but degradation products of catechol were verified.

## II.3.2. *Photochemistry*

As previously verified for other styrylflavylium systems no photochemistry was found in aqueous solution. However, as in the case of other amino styrylflavylium ions, an efficient photochromic system could be obtained in CTAB micelles.[52]

Surfactant or surfactants, are molecules that contain a polar head (hydrophilic) and nonpolar tail (hydrophobic). When placed in aqueous solution they tend to associate themselves, leaving the polar part in contact with water, and removing the hydrophobic tail thereof. When in high concentration (greater than the critical micelle concentration or CMC), surfactant molecules are organized in the form of micelles, spherical aggregates with the hydrophobic tails on the inside the micellar core, and the hydrophilic heads outside in contact with water. Different effects between micelles and flavylium have been reported, both in the stabilization of some species and alteration of its chemical equilibria,[96] as well as in terms of their effects on the flavylium photochromic properties.[97]

CTAB or cetyltrimethylammonium bromide is a cationic surfactant with a CMC in water of $1 \times 10^{-3}$ M.[98] In an aqueous solution in the presence of CTAB micelles, **Ct** is stabilized within the micelle to more acidic pH values, without $\mathbf{AH}^+$ in the medium. Irradiation of such solutions leads to the formation of $\mathbf{AH}^+$ and its consequent release out of the micelle and into the aqueous medium, which results in the respective colour change to the corresponding flavylium form.[97,99]

By irradiating a solution of **Ct** of 7,8-dihydroxy-2-(4-dimethylaminostyryl)-1-benzopyrylium in the presence of CTAB micelles ([CTAB] = 0.013 M) at pH = 1.9 a significant change is verified from yellow to green, Figure II.14. The green colour is a mixture of the blue flavylium cation and some remaining *trans*-chalcone. As reported previously[52] the p$K'_a$ of the flavylium network is shifted towards low values due to effect of the positive charge of the CTAB micelles that destabilize the flavylium cation and stabilize the *trans*-chalcone. In these conditions the photochemistry could be carried out at lower pH values, which is an advantage since the flavylium is known to be chemically more stable at lower pH values. The mechanism of the photochemistry of flavylium compounds in CTAB micelles was previously described.[51]

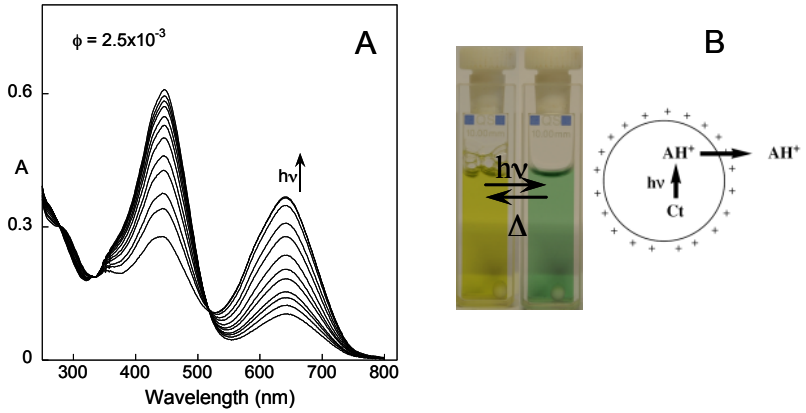


**Figure II.14** - Irradiation at 436 nm of the compound 7,8-dihydroxy-2-(4-dimethylaminostyryl)-1-benzopyrylium 3.3 x$10^{-5}$ M in the presence of CTAB 0.013 pH=1.9; Φ= 2.5x$10^{-3}$; $I_0$ = 1.08x$10^{-6}$ Einstein $min^{-1}$ (**A**) Corresponding colour change from the irradiation of the **Ct** (yellow) to a mixture of $\mathbf{AH^+}$/**A** and **Ct** forms (green) at t = 0 and t = 75 min (**B**).

The *trans*-chalcone interacts strongly with the micelle and is eventually located near to the respective surface. Irradiation of the *trans*-chalcone leads to the flavylium cation formation, which is injected to the bulk solution by the repulsive interaction with the positively charged micelle surface. The system goes back to the initial state by thermal re-equilibration, with a rate constant equals to 4.9x$10^{-4}$ $s^{-1}$.

## II.3.3. *Complexation with $Al^{3+}$*

As already mentioned, anthocyanins are known to be responsible for many of the colors from red to blue in flowers and fruits. They are found in nature within the vacuoles at moderately acidic to neutral pH. Knowing that the most stable colored form is the flavylium (blue) and that the quinoidal base (blueish) is merely a transient species, nature managed to find several ways to endure these beautiful colors. One of these strategies involves the complexation with metals.[91]

In an attempt to mimic nature the interaction with flavyliums, its properties in the presence of $Al^{3+}$ was studied. In fact, it is known from previous studies that the quinoidal base of the catechol is capable of binding to $Al^{3+}$ forming stable complexes.[91]

In Figure II.15 is depicted the absorption spectra's of stable solutions at acidic and moderately acidic conditions in the presence and absence of $Al^{3+}$. While at pH = 1 there is no change in the absorption spectra and thus no interaction with the addition of $Al^{3+}$, at pH = 3.2 a significant difference is verified. In the absence of $Al^{3+}$ the majority species is the $\mathbf{AH^+}$ which is in agreement with the p$K_a$', but when $Al^{3+}$ is present, a slight red shift in the absorption maximum is observed, indicating the formation of the quinoidal base and thus, its complexation with $Al^{3+}$.

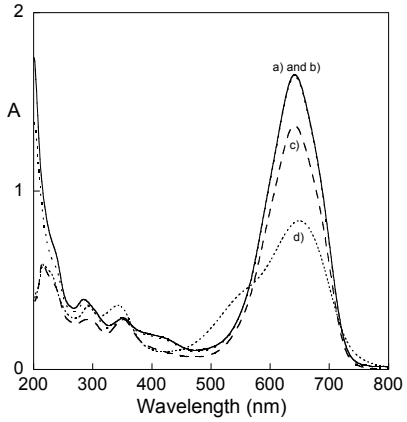


**Figure II.15 -** Absorption spectra of the compound 7,8-dihydroxy-2-(4-dimethylaminostyryl)-1-benzopyrylium $5x10^{-5}$M, water: methanol (1:1): a) and b) pH=1.0 in the absence and presence of $Al^{3+}$, 0.005 M, respectively; c) and d) the same at pH=3.2.

## II.3.4. *Photochemistry in the presence of $Al^{3+}$*

In order to check the influence of the interaction of $Al^{3+}$ with the quinoidal base in the photochemistry of the compound, a solution of **Ct** of 7,8-dihydroxy-2-(4-dimethylaminostyryl)-1-benzopyrylium was irradiated and carried out under the same conditions of Figure II.14, but in the presence of $Al^{3+}$ 0.033 M, see Figure II.16.

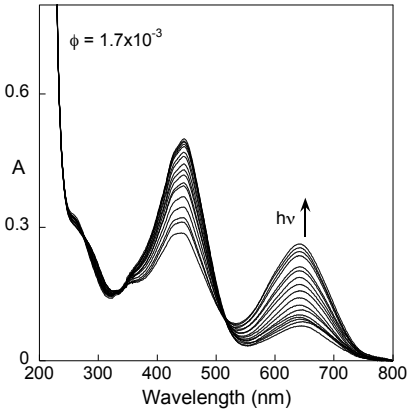


**Figure II.16 -** Irradiation at 436 nm of the compound 7,8-dihydroxy-2-(4-dimethylaminostyryl)-1-benzopyrylium $3.3x10^{-5}$M, in the presence of CTAB 0.013 M and $[Al^{3+}]$=0.033 M pH=1.9, $\phi$= $1.7x10^{-3}$; $I_0$ = $1.08x10^{-6}$ Einstein.$min^{-1}$

Qualitatively the spectral variations are similar in the absence and presence of $Al^{3+}$, Figs. II.14 and II.16. However, in the presence of the metal the extension of the flavylium formation is slightly smaller, which is reflected on the quantum yields, $2.5x10^{-3}$ and $1.7x10^{-3}$ respectively in the absence and presence of the metal. Taking into account the positive charge of the surface micelle, the metal should be located in the bulk water solution; consequently the styrylflavylium ($\mathbf{AH^+}$) that is ejected from the micelle upon irradiation should be electrostatically destabilized because no flavylium complexation with cations was observed in solution at this pH. The reverse back reaction is slightly slower in the presence of the metal, probably through the metal

interaction with the *trans*-chalcone that remains in bulk solution. The effect is very small because the mole fraction of the *trans*-chalcone at pH=1.9 in the bulk solution is expected to be *circa* 0.4%.

## II.4. Conclusions

New stimuli were successfully introduced in the flavylium network allowing, on one hand, the interconversion between flavylium coumpounds and, on the other hand, the complexation with $Al^{3+}$ cation and the extension of the colour palette.

## II.5. Experimental Part

*General:* All reagents and solvents were of analytical grade. $^{1}H$ and $^{13}C$ NMR spectra were recorded at 400 MHz and 100 MHz respectively with a Bruker AMX400 in $CDCl_3$ referenced to the solvent for both proton and carbon spectra. Elemental analyses (EA) were performed in a Thermofinnigan Flash EA 112 series. Mass spectra were run on an Applied Biosystems Voyager-DE™ PRO.

*Absorption measurements:* All spectroscopic measurements were performed using Mili-Q water, Methanol and Ethanol HPLC-grade. Spectroscopic experiments were carried out in buffered solutions (Universal Buffer of Theorell and Stenhagen[100]) pH values were measured with a MeterLab pHM240 pH meter from Radiometer Copenhagen or in a pH-meter Basic 20+ (Crison Instruments). For solutions with HCl concentration above 0.1 M, pH was calculated from –log [HCl]. UV/Vis absorption spectra were recorded with a Varian-Cary 5000 Spectrophotometer, a Varian-Cary 100 Bio spectrophotometer or in a Shimadzu VC2501-PC.

All irradiations were performed in a 200W Mercury arc-lamp at 436nm. Ferrioxalate actinometer [56] (0,006M) was irradiated under the same conditions for the determination of $I_0$.

*Stopped-Flow experiments:* Stopped-flow data were acquired in an Applied Photophysics SX20 stopped flow spectrometer equipped with a PDA.1/UV photodiode array detector with a minimum scan time of 1.3 ms and a wavelength range of 200–785 nm.

### II.5.1. Synthesis of 7-diethylamino-2-(4-(methoxycarbonyl)phenyl)-1-benzopyrylium hydrogensulfate

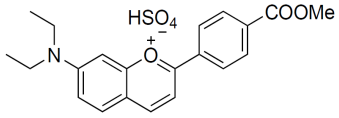


The compound was prepared from condensation of 4-diethylamino-2-hydroxybenzaldehyde (0.31 g; 1.6 mmol) with 4-acetylbenzoic acid (0.26 g; 3 mmol).[101] The reagents were dissolved in 6 ml of acetic acid, 2 ml of $H_2SO_4$ and 2 ml of $CH_3OH$. The reaction mixture was stirred overnight. By the following day ethyl acetate was added and a purple solid precipitated, was filtered off and carefully washed with diethyl ether and dried

yielding 0.58 g of 7-diethylamino-2-(4-(methoxycarbonyl)phenyl)-1-benzopyrylium hydrogensulfate (1.4 mmol, 85%): **$^1$H NMR** ($CD_3OD$, 300 K, 400.13 MHz) δ (ppm): 8.69 (1H, H4, d, $^3J$ = 7.8 Hz), 8.40 (2H, d, $H_{3'}$, $H_{5'}$, $^3J$ = 8.8 Hz); 8.27 (2H, d, $H_{2'}$, $H_{6'}$, $^3J$ = 8.7 Hz); 8.01 (2H, dd, $H_3$, $H_5$, $^3J$ = 8.7 Hz, $^4J$ = 5.9 Hz); 7.57 (1H, dd, $H_6$, $^3J$ = 9.5 Hz, $^4J$ = 2.4 Hz); 7.34 (1H, d, H8, $^4J$ = 1.7 Hz); 3.98 (3H, s, COO-$CH_3$); 3.83 (4H, q, N-$CH_2$), 1.39 (6H, t, $CH_3$). **MALDI-TOF/MS**: *m/z* (%): calcd for $C_{21}H_{22}NO_3^+$: 336.16; found: 336.16 [$M^+$] (100%); elemental analysis (%) calcd for $C_{21}H_{22}NO_3HSO_4$ ($M_r$ = 433.47): C 58.19, H 5.35, N 3.23; found: C 57.88, H 5.60, N 3.05.

***Results for 7-diethylamino-2-(4-(methoxycarbonyl)phenyl)-1-benzopyrylium chloride obtained from recrystallization of 2-(4-carboxyphenyl)-7-diethylamino-1-benzopyrylium hydrogensulfate in acidic (HCl) metanol:***

**MALDI-TOF/MS**: *m/z* (%): calcd for $C_{21}H_{22}NO_3^+$: 336.16; found: 336.2 [$M^+$] (100%); elemental analysis (%) calcd for $C_{21}H_{22}NO_3Cl.3H_2O$ ($M_r$ = 418.70): C 59.22, H 6.53, N 3.29; found: C 59.91, H 6.46, N 3.35.

## II.5.2. Synthesis of 2-(4-carboxyphenyl)-7-diethylamino-1-benzopyrylium hydrogensulfate

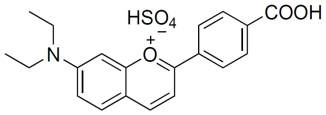


This compound was prepared from condensation of 4-diethylamino-2-hydroxybenzaldehyde (0.58 g; 3 mmol) and 4-acetylbenzoic acid (0.49 g; 3 mmol). The reagents were dissolved in 9 ml of acetic acid and 3 ml of $H_2SO_4$. The reaction mixture was stirred overnight. By the following day diethyl ether was added and a purple solid precipitated, was filtered off and carefully washed with diethyl ether and dried yielding 1.22 g of 2-(4-carboxyphenyl)-7-diethylamino-1-benzopyrylium hydrogensulfate (2.9 mmol, 96%). **$^1$H-NMR** ($CD_3OD$/DCl, pD≈1.0, 400.13 MHz) δ (ppm): 8.7 (1H, $H_4$, d, $^3J_{H4\text{-}H3}$ = 7.8 Hz), 8.39 (2H, d, $H_{3'}$, $H_{5'}$, $^3J_{H3',H5'\text{-}H2',H6'}$= 8.4 Hz); 8.22 (2H, d, $H_{2'}$, $H_{6'}$, $^3J_{H2',H6'\text{-}H3',H5'}$= 8.4 Hz); 8.02 (2H, t, $H_3$, $H_5$, $^3J_{H3\text{-}H4}$ = 7.8 Hz, $^3J_{H5\text{-}H6}$ = 9.5 Hz); 7.55 (1H, dd, $H_6$, $^3J_{H6\text{-}H5}$ = 9.5 Hz, $^4J_{H6\text{-}H8}$ = 1.9 Hz); 7.33 (1H, d, $H_8$, $^4J_{H8\text{-}H6}$ = 1.5 Hz); 3.81 (4H, m, N-$CH_2$), 1.37 (6H, s, $CH_3$); **MALDI-TOF/MS**: *m/z* (%): calcd for $C_{20}H_{20}NO_3^+$: 322.14; found: 322.2 [$M^+$] (100%); **EA** (%) calcd for $0.9(C_{20}H_{20}NHO_3{\cdot}2HSO_4)+0.1(C_{20}H_{20}NO_3{\cdot}HSO_4)$[102]: C 47.31, H 4.53, N 2.76; found: C 47.54, H 4.43, N 2.88;

***Isolation of the trans-chalcone of 7-diethylamino-2-(4-(methoxycarbonyl)phenyl)-1-benzopyrylium: (E)-1-(4-acetylphenyl)-3-(4-diethylamino)-2-hydroxyphenyl)prop-2-en-1-one:***

The pH of 10 ml of ethanol/water (1:1) solution of 7-diethylamino-2-(4-(methoxycarbonyl)phenyl)-1-benzopyrylium hydrogensulfate was adjusted to 7.0 with addition

of 1 M NaOH dropwise. This mixture was warmed to reflux for 1h and allowed to cool overnight. The solvent was decanted and the precipitated solid washed with ether several times and vacuum dried to give a brown solid (25 mg, 18%). **$^1$H-NMR** (400.13 MHz, $CD_3OD$, r.t., 400.13 MHz): δ(ppm) 8.13 (2H, d, $H_2$,$H_6$, or $H_3$,$H_5$, $^3J$ = 8.1 Hz), 8.08 (d, 1H, $H_4$, $^3J$ = 15.0 Hz), 8.03 (2H, d, $H_2$,$H_6$, or $H_3$,$H_5$, $^3J$ = 8.3 Hz), 7.49 (1H, d, $H_5$, $^3J$ = 9.6 Hz), 7.48 (1H, d, $H_3$, $^3J$ = 15.0 Hz), 6.31 (1H, dd, $H_6$, $^3J$ = 8.9 Hz, $^4J$ = 1.5 Hz), 6.14 (1H, d, $H_8$, $^4J$ = 2.0 Hz), 3.93 (3H, s, COO-$CH_3$), 3.41 (4H, q, N-$CH_2$), 1.19 ppm (6H, t, $CH_3$). **MS** (EI): *m/z* (%): calcd for MS (EI): *m/z* (%): calcd for $C_{21}H_{23}NO_4^+$: 353.16; found: 353.2 [$M^{+\cdot}$] (56%); 338.14 (100%) [M-$CH_3^{+\cdot}$]; elemental analysis (%) calcd for $C_{21}H_{23}NO_4.1.5H_2O$ ($M_r$ = 380.43): C 66.30, H 6.89, N 3.68; found: C 66.23, H 6.95, N 3.68.

***Ionized trans-chalcone of 2-(4-carboxyphenyl)-7-diethylamino-1-benzopyrylium hydrogensulfate ($Ct^{2-}$)***

**$^1$H-NMR** (400.13 MHz, $CD_3OD$/NaOD, r.t., 400.13 MHz): δ= 8.33 (1H, d, H4, $^3J$ = 14.9 Hz), 8.09 (2H, d, $H_2$, $H_6$, or $H_3$, $H_5$, $^3J$ = 8.4 Hz), 7.99 (2H, d, $H_2$, $H_6$, or $H_3$, $H_5$, $^3J$ = 8.4 Hz), 7.38 (1H, d, $H_5$, $^3J$ = 9.0 Hz), 7.29 (1H, d, $H_3$, $^3J$ = 14.9 Hz), 6.07 (1H, dd, $H_6$, $^3J$ = 9.0 Hz, $^4J$ = 2.5 Hz), 5.94 (1H, d, $H_8$, $^4J$ = 2.5 Hz), 3.54 (4H, q, N-$CH_2$), 3.35 (3H, s, C$H_3$OH, product of the ester hydrolysis), 1.18 ppm (6H, t, $CH_3$).

## II.5.3. Single-crystal X-ray diffraction

Single-crystals of the *trans*-chalcone, $C_{21}H_{23}NO_4$, of 7-diethylamino-2-(4-(methoxycarbonyl)phenyl)-1-benzopyrylium were harvested from the crystallization vial and immersed in highly viscous FOMBLIN Y perfluoropolyether vacuum oil (LVAC 140/13). A suitable crystal was selected and mounted on a Hampton Research CryoLoop with the assistance of a Stemi 2000 stereomicroscope.[103] Data were collected on a Bruker X8 Kappa APEX II charge-coupled device (CCD) area-detector diffractometer (Mo $K_\alpha$ graphite-monochromated radiation, λ = 0.71073 Å) controlled by the APEX2 software package,[104] and equipped with an Oxford Cryosystems Series 700 cryostream monitored remotely using the software interface Cryopad.[105] Images were processed using the software package SAINT+,[106] and data were corrected for absorption by the multi-scan semi-empirical method implemented in SADABS.[107] The structure was solved by direct methods implemented in SHELXS-97,[108,109] and refined from successive full-matrix least-squares cycles on F2 using SHELXL-97.[108,110] All non-hydrogen atoms were successfully refined using anisotropic displacement parameters.

Hydrogen atoms associated with the hydroxyl (O–H) groups were markedly visible in difference Fourier maps and were included in the structure with the O–H distances restrained to 0.90(2) Å, and Uiso fixed at 1.5 × Ueq of the parent oxygen atom. H-atoms bound to carbon

were located at their idealized positions using appropriate HFIX instructions in SHELXL: 43 for the aromatic, 23 for the –CH2 carbons and 137 for the terminal $–CH_3$ methyl groups. All these atoms were included in subsequent refinement cycles in riding-motion approximation with isotropic thermal displacements parameters ($U_{iso}$) fixed at 1.2 or 1.5 × $U_{eq}$ of the carbon atom to which they are attached.

Information concerning the crystallographic data collection and structure refinement is summarized in Table II.3.

**Table II.3** Crystal and structure refinement data for compound *trans*-chalcone, **Ct**

| Formula | $C_{21}H_{23}NO_4$ |
|---|---|
| *Mr* | 353.40 |
| Crystal description | Orange plates |
| Crystal size /mm | 0.20 × 0.09 × 0.01 |
| Temperature / K | 150(2) |
| Crystal system | Triclinic |
| Space group | *P*-1 |
| *a* /Å | 12.039(2) |
| *b* /Å | 13.110(2) |
| *c* /Å | 13.346(2) |
| $\alpha$ /° | 85.202(8) |
| $\beta$ /° | 67.787(7) |
| $\gamma$ /° | 68.725(8) |
| Volume /Å$^3$ | 1813.7(5) |
| *Z* | 4 |
| $\rho_{calculated}$ /g cm$^{-3}$ | 1.294 |
| *F*(000) | 752 |
| $\mu$ /mm$^{-1}$ | 0.089 |
| $\theta$ range /° | 3.61 – 23.11 |
| Index ranges | -12 ≤ h ≤ 13<br>-14 ≤ k ≤ 14<br>-14 ≤ l ≤ 14 |
| Reflections collected | 19454 |
| Independent reflections | 4692 ($R_{int}$ = 0.0829) |
| Final *R* indices [I>2σ(I)] | $R_1$ = 0.0506<br>w$R_2$ = 0.0978 |
| Final *R* indices (all data) | $R_1$ = 0.1261<br>w$R_2$ = 0.1307 |
| Largest diff. peak and hole /e Å$^3$ | 0.206 and −0.212 |

Crystallographic data (excluding structure factors) for the structure in this paper have been deposited with the Cambridge Crystallographic Data Centre as supplementary publication nº. CCDC-838069. Copies of the data can be obtained, free of charge, on application to CCDC, 12 Union Road, Cambridge CB2 1EZ, UK, (fax: +44-(0)1223-336033 or e-mail: deposit@ccdc.cam.ac.uk)

## II.5.4. 7,8-dihydroxy-2-(4-dimethylaminostyryl)-1-benzopyrylium hydrogensulfate

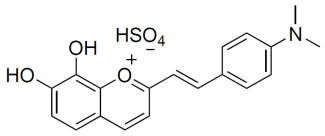


The compound was prepared from condensation of 2,3,4-trihydroxybenzaldehyde (3 mmol, 0.46 g) with p-dimethylaminostyrylmethylketone[77] (3 mmol, 0.57 g). The reagents were dissolved in 8 ml of acetic acid and 2 ml of $H_2SO_4$. The reaction mixture was stirred overnight. By the following day ethyl acetate was added and a dark solid precipitated, was filtered off and carefully washed with ethyl acetate and dried yielding 1.12 g of 7,8-dihydroxy-2-(4-dimethylaminostyryl)-1-benzopyrylium hydrogensulfate (2.75 mmol, 91.6 %). **$^1$H-NMR** (DCl /$CD_3OD$, pD≈1.0, 400.13 MHz) δ (ppm): 8.84 (1H, d, $H_4$, $^3J_{H4\text{-}H3}$= 8.6 Hz); 8.55 (1H, d, $H_\beta$, $^3J_{H\beta\text{-}H\alpha}$= 15.6 Hz); 7.99 (2H, d, $H_{2'}$, $H_{6'}$, $^3J_{H2',H6'\text{-}H3',H5'}$= 8.9 Hz); 7.79 (1H, d, $H_3$, $^3J_{H3\text{-}H4}$= 8.6 Hz); 7.63 (1H, d, $H_5$, $^3J_{H5\text{-}H6}$= 8.8 Hz); 7.52 (1H, d, $H_\alpha$, $^3J_{H\alpha\text{-}H\beta}$= 15.6 Hz); 7.48 (2H, d, $H_{3'}$, $H_{5'}$, $^3J_{H3',H5'\text{-}H2',H6'}$= 8.9 Hz); 7.38 (1H, d, $H_6$, $^3J_{H6\text{-}H5}$= 8.8 Hz); 3.29 (6H, s, $N(CH_3)_2$. **$^{13}$C-NMR** (DCl /$CD_3OD$, pD≈1.0, 400.13 MHz) δ (ppm): 171.89; 157.75; 153.16 ($C_4$); 151.07; 150.66; 149.71 ($C_\beta$); 147.48; 134.41; 134.02 ($C_{2'}$, $C_{6'}$); 124.02 ($C_5$); 120.86; 120.60 ($C_6$); 119.5 ($C_{3'}$, $C_{5'}$); 116.86 ($C_3$); 44.53 ($C_{CH3}$). **MS-MALDI/TOF+**: calcd for $C_{16}H_{13}O_2^+$: 308.13 (100%); found: 308.07 $[M]^+$ (100%).

# CHAPTER III. Redox-active Moieties

Publications associated with this chapter:

Ana M. Diniz, Carlos Pinheiro, Vessilin Petrov, A. Jorge Parola, Fernando Pina, "Synthesis and Characterization of a Symmetric Bis(7-hydroxyflavylium) Containing a Methyl Viologen Bridge" *Chem. Eur. J.*, **2011**, 17, 6359−6368.

# III. Redox-active Moieties

With the purpose of enhancing the numbers of available states and extend the chemistry of flavylium salts, supramolecular systems containing flavylium units and reversible redox-active moieties were designed and synthesized. In this particular case viologen was chosen for his known reversible electrochemistry.[111] Several compounds were synthesised, a dyad composed by a 7-hydroxyflavylium unit linked by a methylene bridge to a viologen unit in position 4' (*viologen-flavylium dyad*); a symmetrical triad where two identical 7-hydroxyflavylium units are linked to methylviologen through positions 4' (*flavylium-viologen-flavylium triad*) and the model compound 7-hydroxy-4'-methylflavylium. The thermodynamics and kinetics of the network of chemical reactions involving the flavylium moieties as well as the model compound were completely characterized and also the redox behaviour of the viologen unit.

## III.1. Introduction

4,4'-Bipyridyl (bpy) belongs to the family of the 4,4'-bis quaternary compounds better known as viologens. Its electrochemical behaviour has been extensively reviewed as they have one of the lowest reduction potentials among organic systems and high reversibility.[111] Once discovered their properties as redox indicators have proved useful for biological studies.[112] They differ from other indicators on two main aspects: the colour is exhibited by the reduced form, whereas usually the oxidized form is the coloured one and also the oxidation-reduction potential is pH independent.[113,114] Once the form radical cation has a strong absorption band in the visible, are also good candidates for the investigation of photo-electrochemical processes.[111] Currently they have different applications, such as electronic transfer in solar energy systems, herbicides and electrochemical films.[112]

Being one of the most studied redox systems in both academy and industry (where they are commercialized as electrochromic materials), it was selected due to its well-characterized reversible redox behaviour that would allow to enlarge the possible number of available states and to respond to electric stimuli. It is reduced at potentials below those usually observed for flavylium cations allowing to run electrochromic cycling with the chalcone moiety while at the stable uncoloured oxidised form of methylviologen, the flavylium/chalcone pH coupled photochromism can operate.

## III.2. Synthesis and characterization

The synthesis of flavylium compounds is usually achieved through the acid catalysed condensation of acetophenones with benzaldehydes, following a method early introduced by Robinson[115] and slightly modified by Katritzky *et al.*[116] The synthetic pathway to obtain de desired methylviologen-flavylium is described in Scheme 1. In order to avoid by-products, the synthetic pathway proposed involved the coupling of the acetophenone to the redox unit – viologen, and the final step; the condensation with benzaldehydes which originates the flavylium salt.

Bromination of 4'-methylacetophenone yielded 4'-bromomethylacetophenone **1** that was reacted with 4,4'-bipyridine to give *bis*-acetophenone **3** in 83 % yield. The synthesis of **3** was adapted from a procedure previously described by *Porter et al.*[117] to prepare extended viologens. Initially, only the symmetric compound was synthesized but by mono-alkylation of 4,4'-bypiridine, compound **2**, unsymmetrical moieties were easily obtained. The final step was achieved by condensation with 2,4-dihydroxybenzaldehyde under strongly acidic conditions[115,116] to give the desired viologen-bridged compounds **4** and **5** with **95** and **60%** yield respectively.

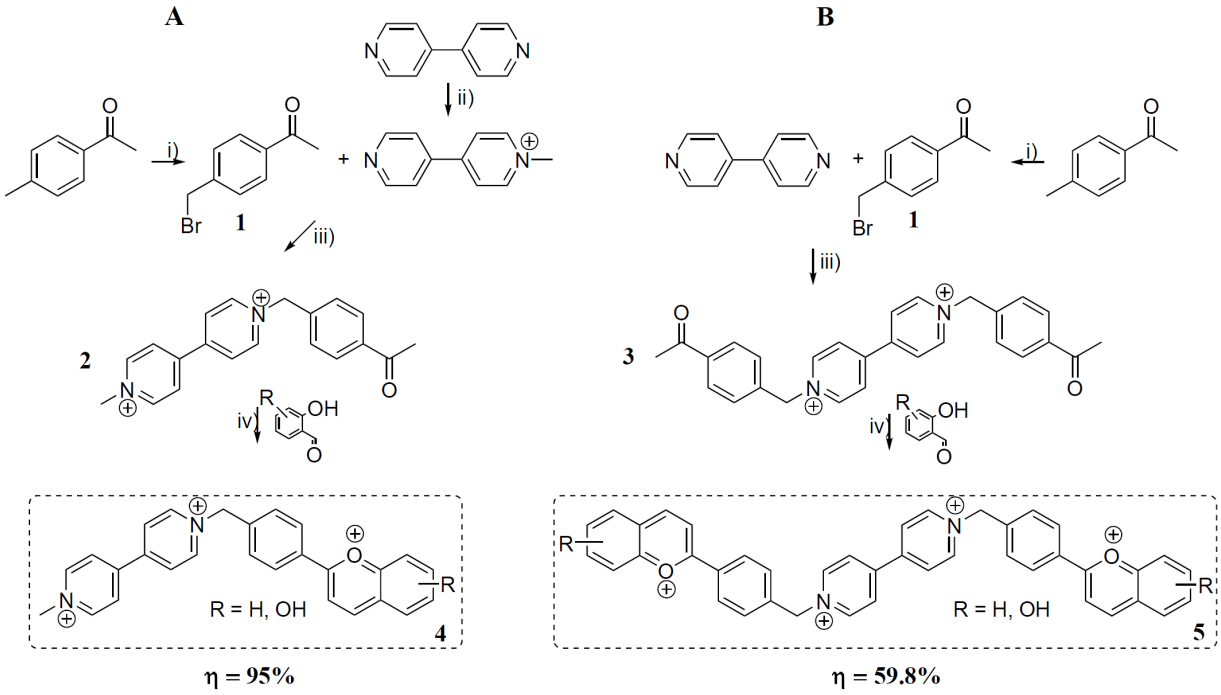


**Scheme III.1**- Synthetic paths of attaching flavylium compounds to viologen: Left side A and right side B. Conditions: i) NBS/AIBN/$CCl_4$ ii) Trifluoromethanesulfonic acid methyl ester /Ethyl ether dry iii) DMF/reflux iv) $CH_3COOH/H_2SO_4$

The desired compounds were obtained, both equally important once they allow the coupling of acid/base compounds and / or photochromic to electrochromic compounds. The existence of the mono substituted pathway shows possible the synthesis of an unsymmetrical *bis* flavylium that can lead to a different and wide variety of colours and behaviours.

For comparative studies, the model compound 7-hydroxy-4'-methylflavylium tetrafluoroborate (**6**) salt was prepared by condensation of 2,4-dihydroxybenzaldehyde with 4'-methylacetophenone in the presence of acetic anhydride and tetrafluoroboric acid with a yield of 27%. All the detailed synthesis can be found further ahead.

## III.3. Model compound: 7-hydroxy-4'-methylflavylium tetrafluoroborate

### III.3.1. *The reaction network in water*

The network of chemical reactions of model compound **6** was characterized following the same strategy as in the previously chapter. The strategy consists on the study of the pH dependent thermodynamic equilibria as well as of the kinetics that results from a perturbation of the system by pH jumps and by light. The changes in absorption spectra upon direct pH jumps from stock solutions of model compound **6** at pH=1.0 ($\mathbf{A}H^+$) to higher pH values are shown in Figs. III.1A and III.1B.

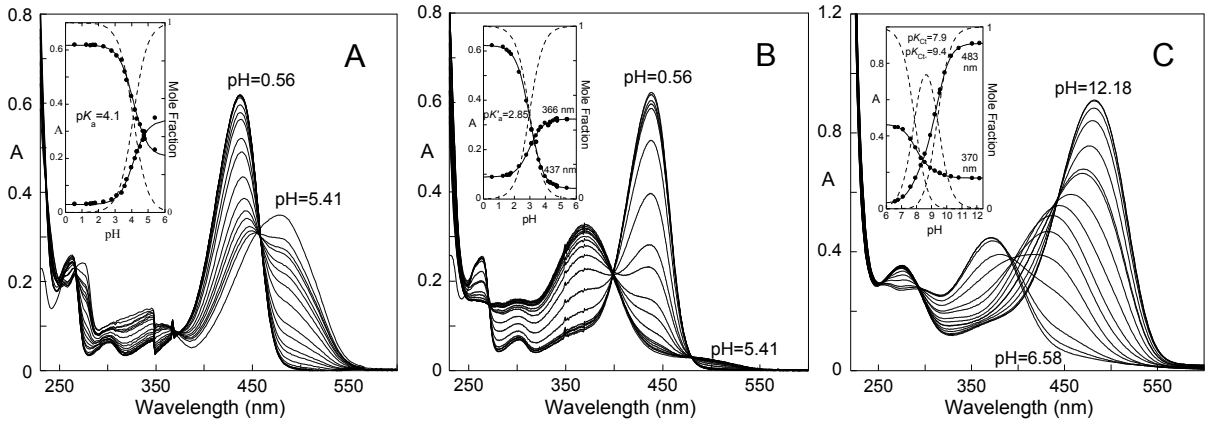


**Figure III.1 –** UV-Vis spectral variations occurring upon a pH jump from a stock solution of the model compound 6 at pH = 1 ($6.4 \times 10^{-5}$ M) to higher pH values: spectra recorded immediately after the pH jump (<1 min after adding base) (**A**) and upon thermodynamic equilibrium being reached (~24 h) (**B**). Spectral variations upon reverse pH jumps of a solution at pH =12 ($Ct^{2-}$) to less basic pH values leading to the protonation of the *trans*-chalcones are shown in (**C**). Insets: fittings (full lines) of the absorbance values (•) at the specified wavelengths superposed to the mole fraction distribution of species (trace lines).

In Figure III.1A the absorption spectra were taken *circa* 30 seconds after the pH jump. The shape and position of the bands clearly indicate the formation of the quinoidal base allowing to calculate p$K_a$=4.1, Scheme I.5. Fig. III.1B shows the pH dependent absorption of the equilibrated solutions after 1 day in the dark, leading to p$K'_a$=2.85. These values compare with p$K_a$=3.55 and p$K'_a$=2.70 for 7-hydroxyflavylium.[118] The slightly lower acidity and higher p$K'_a$ of **6** relatively to 7-hydroxyflavylium are consequences of the electron donor properties of the methyl substituent at position 4' when compared with the proton. On the other hand, pH jumps to high pH values (pH > 12) lead to the formation of the ionized *trans*-chalcone $\mathbf{Ct}^{2-}$, as observed for similar flavylium compounds.[119] This species can be titrated back to acidic pH, forming $\mathbf{Ct}^{-}$ and **Ct** with p$K_a$'s of 9.4 and 7.9, as shown in Fig. III.1C. If the titration continues to more acidic pH values (not shown) formation of flavylium takes place because it is the stable species in acidic medium, as seen in Fig. III.1B.

From the data of Fig. III.1, Equations can be written:

$$K_a = 10^{-4.1} \qquad \textbf{Equation III-1}$$

$$K'_a = K_a + K_h + K_h K_t + K_h K_t K_i = 10^{-2.85} \qquad \textbf{Equation III-2}$$

Kinetic information about the network of chemical reactions can be obtained by displacing the system from equilibrium by means of a pH jump. pH jumps can be performed in both directions, starting from equilibrated solutions at pH 1.0 to high pH values, or vice versa. Figure III.2A refers to a pH jump experiment from an equilibrated solution at pH 1.0 to pH 3.2. The results obtained show the conversion of $\mathbf{AH}^{+}$ into the *trans*-chalcone (**Ct**).

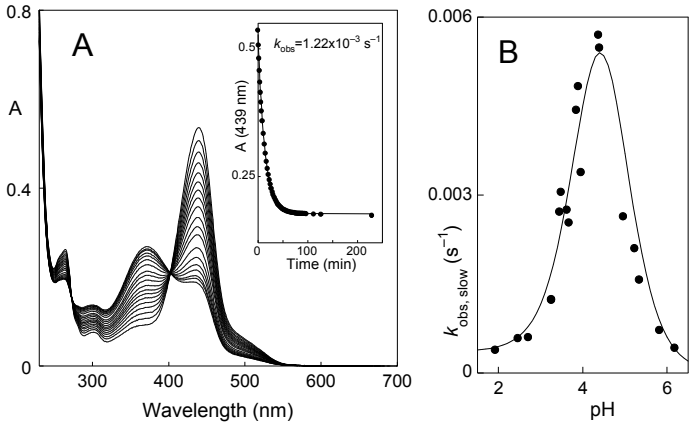


**Figure III.2 –** Time evolution of UV-Vis spectra upon a pH jump from a stock solution of compound **6** at pH = 1 to pH = 3.2 ($6.4 \times 10^{-5}$ M) (**A**); inset: fitting of the absorbance at 439 nm with a single exponential allows to calculate $k_{obs}$ at pH = 3.2. $k_{obs}$ rate constants plotted against pH lead to bell-shaped curve (**B**).

Representation of the rates of the direct pH jumps as a function of pH leads to the previously described[99] bell-shaped curve characteristic of the compounds lacking a high thermal *cis-trans* isomerisation barrier, Fig. III.2B. This kinetics can be accounted by Equation I.13.[97] Fitting of the data was achieved for $K_hK_ik_i$ = 8.1 × $10^{-7}$ M $s^{-1}$, $k_{-i}$ = 5.0 × $10^{-4}$ $s^{-1}$ and $k_iK_i/k_{-h}$ = 3.7 × $10^{-5}$ M.

## III.3.2. *Photochemistry in water*

*Continuous irradiation*

In agreement with similar compounds[118,120] it was found that **Ct** is photoactive. Photochemical behaviour of **Ct** under continuous irradiation are reported in Fig III.3A (pH = 4.3) and Fig III.3B (pH = 5.3). In both cases it is clear the disappearance of the **Ct** to give a mixture of $\mathbf{AH}^+$ and **A** in Fig. III.3A and practically only **A** in Fig. III.3B. This dependence of the specie formed by the pH is easily explained by means of Scheme I.5, and the data reported in Fig. III.1A, (p$K_a$= 4.1) As showed, at more acidic values, the formation of the flavylium cation is favoured, while on going to higher pH values, the formation of the quinoidal base is verified via flavylium cation, since we are already at higher pH values that the p$K_a$ determined. The maximum value for the observed quantum yield is obtained for pH ≤ 3, Fig III.3C. It should be noted that the decrease observed for low pH values is due to the decrease in the molar fraction of the **Ct** in the equilibrium as the pH becomes lower than 2. The important point is that the observed quantum yield decreases sharply at high pH values where the molar fraction of *trans*-chalcone reaches its maximum value. This result is due to the fact that at high pH values the transformation of **Ct** to $\mathbf{A}/\mathbf{AH}^+$ is prevented, favouring the reversion of **Cc** into **Ct**.

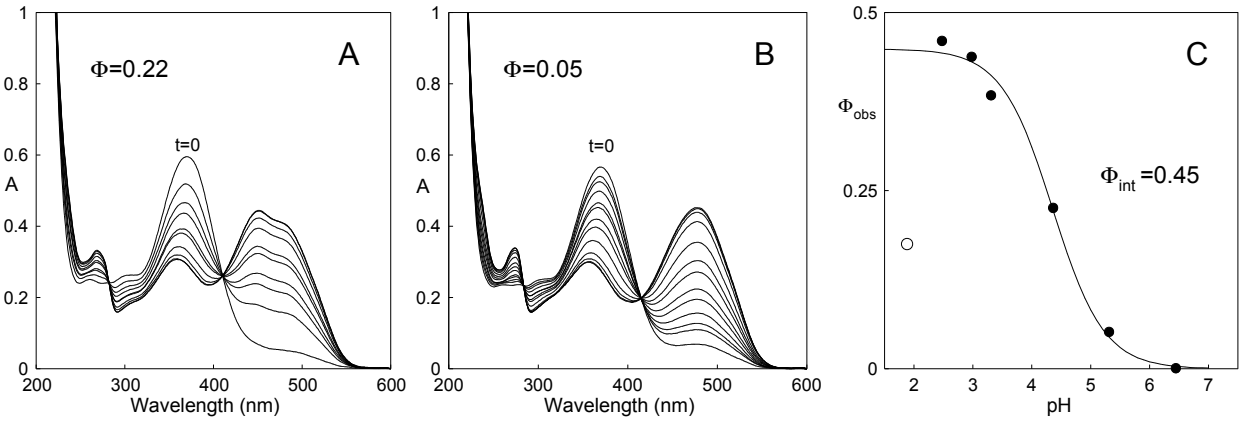


**Figure III.3** – Spectral variations observed upon continuous irradiation (365 nm) of dark equilibrated solutions of Ct 4.17 × $10^{-5}$ M as a function of time at pH = 4.3 (**A**) and 5.3 (**B**). The quantum yields of formation of quinoidal base A and flavylium cation $AH^+$ were calculated on the basis of the total light absorbed by the system and plotted as a function of the pH of the irradiated solution (**C**).

The quantum yield is pH dependent and can be approximately given by Equation III.1[99]

$$\Phi = \Phi_{int} \frac{\frac{k_{-h}[H^+]}{1+K_t}}{\frac{k_{-h}[H^+]}{1+K_t} + \frac{k_i K_t}{1+K_t}} = \Phi_{int} \frac{[H^+]}{[H^+] + \frac{k_i K_t}{k_{-h}}} \qquad \textbf{Equation III-3}$$

In Equation III.3 it is assumed that hemiketal **B2** and *cis*-chalcone **Cc** are in fast equilibrium. Formation of the coloured species ($\mathbf{A}H^+$ or **A**) upon irradiation of **Ct** to give **Cc** is the product of the intrinsic quantum yield of the photoisomerization reaction, $\Phi_{int}$, by the efficiency of formation of $\mathbf{A}H^+$ from **Cc** (ratio between the rate at which $\mathbf{A}H^+$ or **A** is formed from **Cc** and the rates of all processes contributing for the disappearance of **Cc**). Fitting was achieved for $\Phi_{int} = 0.45$ and $k_i K_t / k_{-h} = 4.1\times10^{-5}$ M, this last value in good agreement with the fitting obtained with Equation I.13 ($3.7\times10^{-5}$ M, Fig. III.2B).

*Pulsed irradiation*

Pulsed radiation is a powerful complementary technique to study the flavylium reaction network since it does not need any pH modification and is a source of kinetic information as shown in Fig. III.4, where equilibrated solutions containing **Ct** were irradiated. After the flash, the system can be monitored at a wavelength where **Ct** absorbs (Fig. III.4A) as well as at the flavylium or quinoidal base absorptions, depending on pH (Fig. III.4B). In Fig. III.4A, a bleaching is observed immediately after the flash that corresponds to the disappearance of **Ct** to give **Cc** (which is known to possess a lower absorption coefficient compared to **Ct**). The second process corresponds to the recovery of some **Ct** absorption as a result of the thermal back reaction from **Cc** to **Ct** in competition with flavylium/quinoidal base formation observed in Fig. III.4B. These two processes are parallel reactions and the observed rate constant, $k_{obs}$, is the sum of both. In other words, the rate constant measured at 365 nm (**Ct**) and 436 nm ($\mathbf{A}H^+$/**A**) is the same, within experimental error, as expected. The $[H^+]$ dependence of this process is represented in Fig. III.4C.

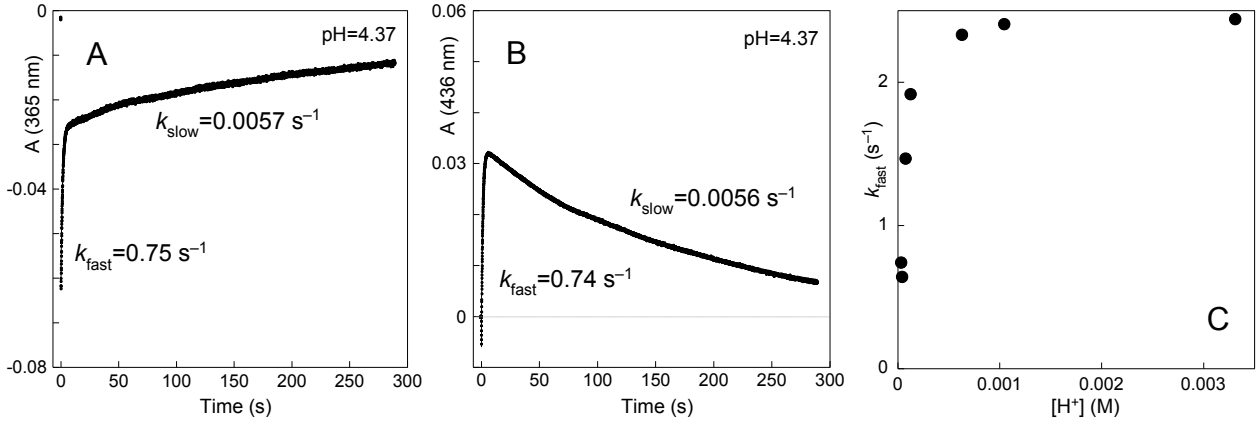


**Figure III.4** – Time evolution of the absorbances at 365 nm (Ct absorption, **A**) and 436 nm ($AH^+$/A absorption, **B**) upon flash irradiation of a solution of model compound 4 at pH = 4.37. The rate constant for the fast process, $k_{fast}$, as a function of proton concentration is plotted in (**C**).

At high proton concentrations, the hydration/dehydration reaction (Scheme I.7) is faster than the tautomerization (Scheme I.8) due to its direct dependence on $[H^+]$ and the rate-determining step of the process is the tautomerization. As soon as **B2** is formed from **Cc** it immediately dehydrates to give $\mathbf{A}H^+$, and the rate is controlled by the value of $k_{-t}$, Equation III.4. At lower proton concentrations, the rate-determining step is the hydration/dehydration and the proton dependence should be given by Equation III.5.

$$k_{obs,fast\ (plateau)} = k_{-t} = 2.5\ s^{-1} \qquad \textbf{Equation III-4}$$

$$k_{obs,fast} = k_h + \frac{K_t k_i}{1+K_t} + \frac{k_{-h}\left[H^+\right]}{1+K_t} = 0.25 + 2.2\times10^3\left[H^+\right] \qquad \textbf{Equation III-5}$$

The slower process reported in Figs. III.4A and III.4B is the complete recovery of **Ct** and disappearance of $\mathbf{A}H^+$ to reach the initial equilibrium condition. It is the same kinetic process of the pH jumps and both follow Equation I.13.

A global fitting of the data including, time-resolved acid-base titrations in Fig. III.1 (Equations III.1 and III.2), pH jump experiments yielding the bell-shaped curve in Fig. 2B (Equation I.13), quantum yields in Fig. III.3C (Equation III.3) and flash photolysis experiments in Fig. III.4C (Equation III.4 and III.5) allows calculating all the equilibrium and rate constants of the system; see in page 67 the Tables III.2 and III.3.

# III.4. Viologen-flavylium dyad: 1-methyl-1'-[(7-hydroxyflavylium-4'-il) methyl]-4,4'- bipyridinium hexafluorofosfate

The purpose of this new family of compounds is the introduction of new stimulus in the well-established chemical network reactions of the flavylium salts. For the study of this new system, pH and light dependent chemical network reactions were studied and characterized and finally the study of the electrochemistry of the system. With the introduction of redox stimuli it should be possible to obtained *trans* chalcone **Ct** in the oxidized and reduced form, allowing new available states, Scheme III.2.

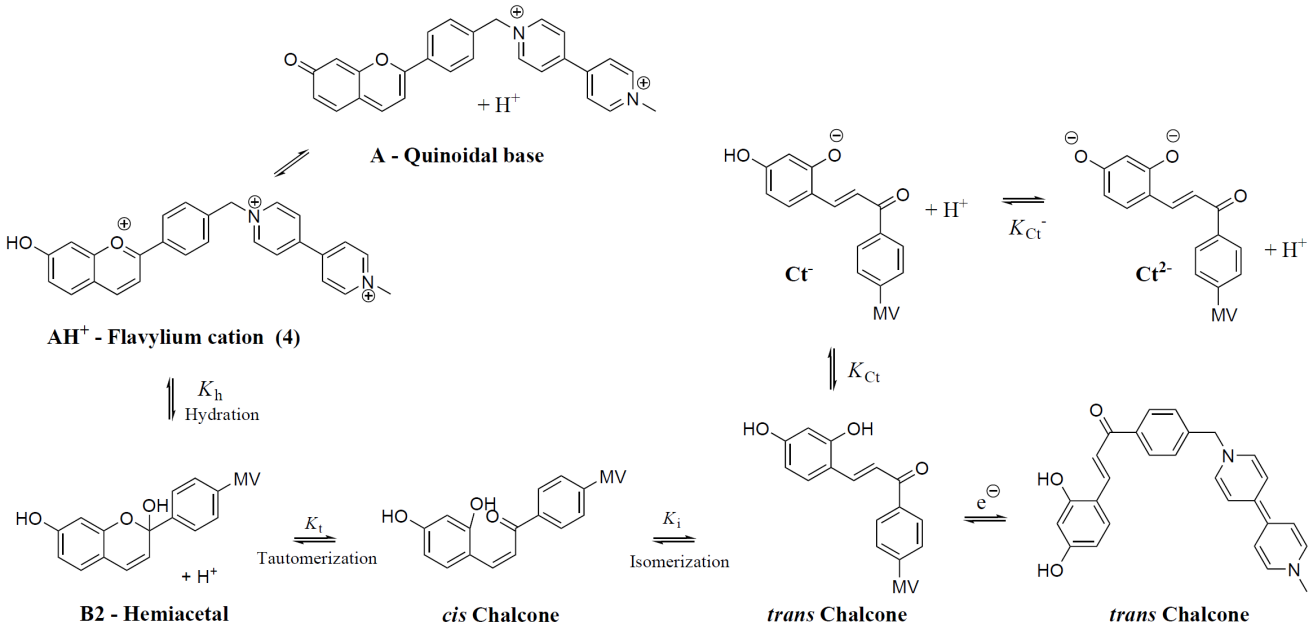


**Scheme III.2 -**Network of chemical reactions of viologen-flavylium dyad **4.**

## III.4.1. *The reaction network in water*

Once the model compound is studied, a more extensive characterization was performed for the dyad and triad previously synthesized. The same pH and light dependent network of chemical reactions characteristic of the synthetic flavylium were found.

The changes in absorption spectra taken in a common UV/Vis spectrophotometer upon direct pH jumps from stock solutions of the viologen-flavylium dyad at pH 1.0 ($\mathbf{AH^+}$) to higher pH values (Fig III.5A) reveals the fast formation of the *trans*-chalcone **Ct** leading to erroneous determination of the p$K_a$. With the aid of a stopped-flow equipped with a diode array spectrophotometer it was possible to determine accurately the p$K_a$ value for the formation of the

quinoidal base of 4.65 (Fig. III.5B) instead of the initially measured value of 2.7 monitored at 425 and 475 nm after 5 ms. Fig. 5C shows the pH dependent absorption of the equilibrated solutions after 1 day in the dark, leading to p$K'_a$=1.68.

Like previously referred and as in acidic pH values, the behaviour for more basic pH values is similar to other flavylium compounds. At higher pH's (pH > 12) the formation of the ionized *trans*-chalcone (**Ct**$^-$ at pH > 7.5, **Ct** $^{2-}$ at pH > 9), can be obtained by deprotonation of the hydroxyl groups, and observed in the equilibrium; fittings at 376 and 489 nm, with p$k_a$'s of 7.52 and 8.9, Fig III.5A.

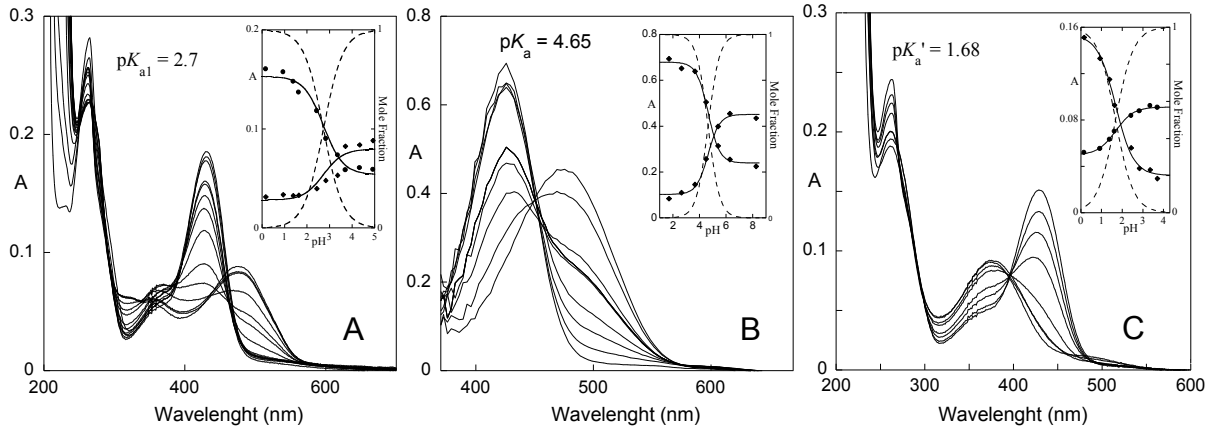


**Figure III.5. –** UV-Vis spectral variations occurring upon a pH jump from a stock solution of the mono flavylium at pH = 0 ($5.2 \times 10^{-5}$ M) to higher pH values: spectra recorded immediately after the pH jump (<1 min after adding base) (**A**) the same after 5 ms ($1.21 \times 10^{-4}$ M) (**B**) and upon thermodynamic equilibrium being reached (~24h) (**C**). Insets: fittings (full lines) of the absorbance values (•) at the specified wavelengths superposed to the mole fraction distribution of species (trace lines).

Comparison of the global p$K'_a$ of *flavylium-viologen dyad* **4** (p$K_a$ = 1.68) with that of the model compound **6** (p$K_a$ = 2.85) reflects the effect of the positive charge of the viologen bridge in the acid/base behaviour making *flavylium-viologen dyad* **4** to be more acidic. See all the equilibrium and rate constants of these systems in Table III.2 and III.3, page 67.

Information about the kinetic behaviour of the system can be obtained through a series of pH jumps from thermal equilibrated solution at pH = 0 to higher pH values, see for example the spectral variations that follow a pH jump from an equilibrated solution at pH = 0 to pH = 4.7, Fig. III.6B.

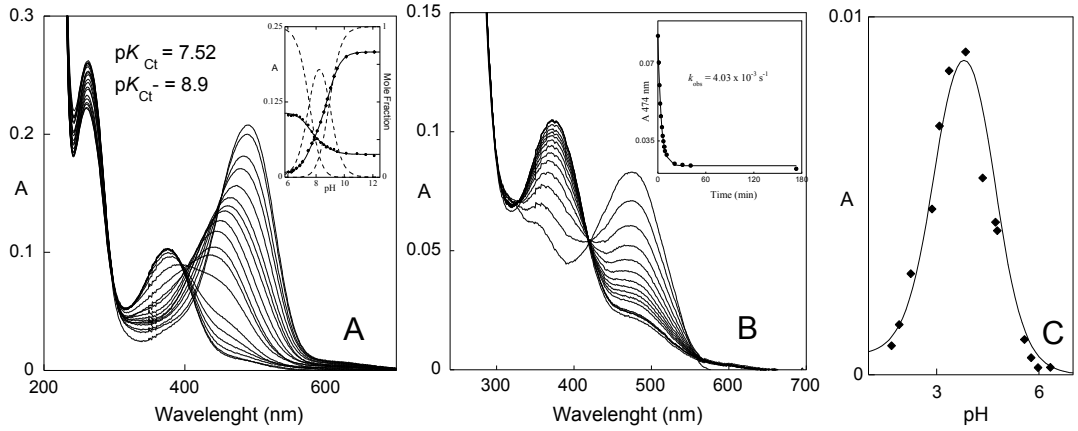


**Figure III.6**. Spectral variations upon reverse pH jumps of a solution at pH =12 ($Ct^{2-}$) to less basic pH values leading to the protonation of the *trans*-chalcones are shown in (A). Inset: fittings (full lines) of the absorbance values (•) at the specified wavelengths superposed to the mole fraction distribution of species (trace lines).Time evolution of UV-Vis spectra upon a pH jump from a stock solution of compound **4** at pH = 0 to pH = 4.7 ($5.2 \times 10^{-5}$ M); inset: fitting of the absorbance at 474 nm with a single exponential allows to calculate $k_{obs}$ at pH = 4.7 (**B**). The $k_{obs}$ as a function of pH. (**C**)

The process follows first-order kinetics and clearly shows the immediate formation of the quinoidal base **A** that is transformed into **Ct**. The equilibrium is reached with a remaining percentage of **A** of ~0.1%. By plotting the $k_{obs}$ values determine upon a series of pH jumps versus pH we obtain once again the bell shape[99] curve characteristic of the compounds lacking a high thermal *cis-trans* isomerisation barrier, Fig III.6C. This kinetics can be accounted for by Equation I.13.[97] Fitting of the data was achieved for $K_hK_tk_i = 1.19 \times 10^{-5}$ M $s^{-1}$, $k_{-i} = 5.70 \times 10^{-4}$ $s^{-1}$ and $k_iK_t/k_{-h} = 1.03 \times 10^{-3}$ M.

## III.4.2. *Photochemistry in water*

Like in the model compound, continuous irradiations were performed but no photochemistry was found in the viologen-flavylium dyad, see below pulsed irradiations.

*Pulsed irradiation*

Several aqueous solutions of **Ct** at different pH's between pH 3.0 and 5.4 were irradiated and monitored at 372 (**Ct**) 426 ($\mathbf{AH^+}$) and 472 nm (**A**). All the pH's showed a consumption of **Ct** (higher at lower pH values since is easier the formation of the flavylium cation) but with ΔA in the order of 0.001, showing also the lack of photochemistry of the system. Figure III.7A shows the formation of $\mathbf{AH^+}$ at pH = 3 which has an almost complete recovery after 60 seconds and at pH 4.4 (Fig III.7B) the consumption of **Ct** to give **Cc** and a second process with faster recovery of the thermal back recovery of **Ct.** Figure III.7C shows that at pH 5.4 already no quinoidal base is formed.

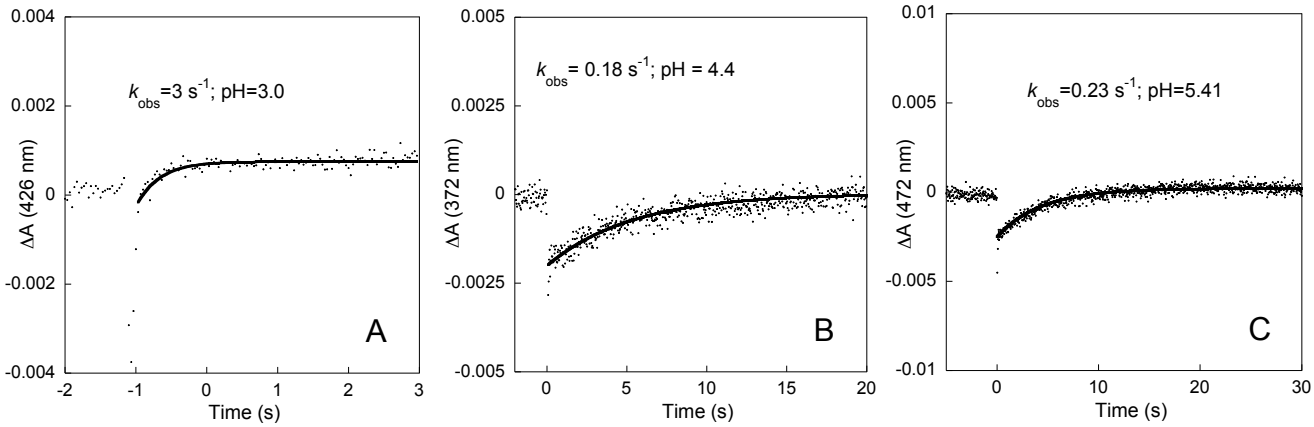


**Figure III.7 –** Time evolution of the absorbances upon flash irradiation of a stable solution of Ct. At 426 nm pH = 3.0 (**A**) at 372 nm pH = 4.4 (**B**) at 472 nm pH = 5.41 (**C**).

When compared to the model compound we obtain ΔA 30 times higher and with slower recovery processes making possible the existence of photochemistry.

## III.5. Flavylium-viologen-flavylium triad: 1,1'-di[(7-hydroxyflavylium-4'-il) methyl]-4,4'-bipyridinum perchlorate

### III.5.1. *The Reaction network*

Regarding the flavylium-viologen-flavylium triad synthesised, it was more difficult to carry out the studies due to problems of solubility and precipitation leading us to perform the studies in 20% of Acetonitrile. Once again, determination of the p$K_a$ had to be performed by stop flow apparatus due to the high rate of the hydration reaction leading to the presence of already some **B** and **Cc** when the spectra are run in a common UV-Vis spectrophotometer instead of the dyode array spectrophotometer used in the stopped-flow equipment. At this point it's important to recall that the compound under study possesses two flavylium units covalently linked by a viologen unit. Depending on how the two flavylium feel each other we could obtain a single pKa since is the same flavylium or two different pKa's in the case of the first deprotonation influences the second one.

When monitoring the formation of the quinoidal base monitored at $\lambda_{max}(AH^+)$ = 430 nm and $\lambda_{max}(A)$ = 480 nm (Fig. III.8A), it was not possible to distinguish two-separated pKa's. This does not mean that they are equal since it is difficult to distinguish by spectrophotometer two pKa's when they differ by less than one pH unit.[121] However, the experimental data presented in Fig. III.8A indicate that if the two pKa's are not equal they are at least very close and thus the influence of the deprotonation in one branch of the compound has only a small effect on the

other. For the global p$K'_a$ we obtained a value of 1.01 depicting the acidity of the compound, Fig III.8B.

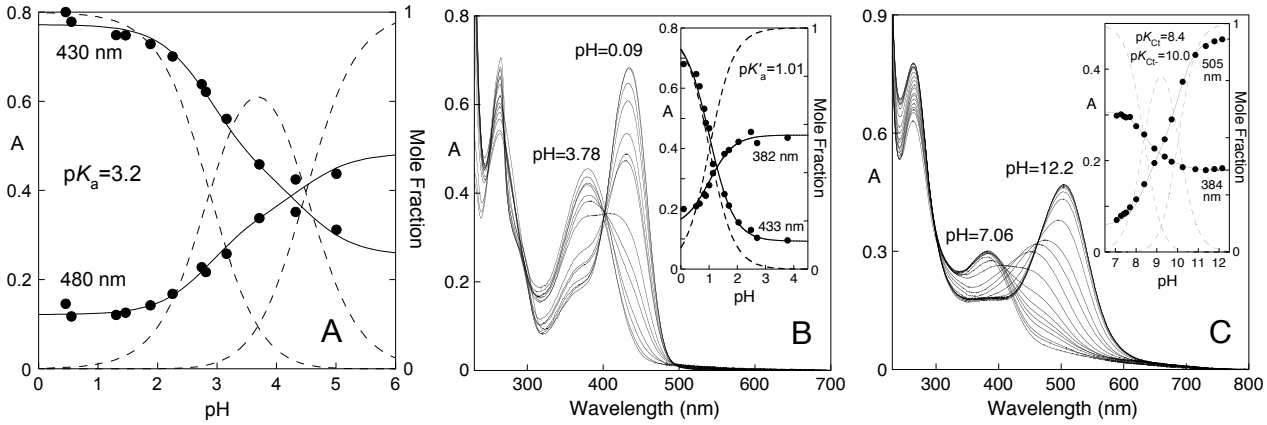


**Figure III.8** – Absorbance data and/or absorption spectra of *flavylium-viologen-flavylium triad* **5** immediately after a pH jump from a stock solution $7.1 \times 10^{-5}$ M at pH = 0 to higher pH values; B- the same at the equilibrium; C- spectral variations upon pH jumps of a solution at pH =12 ($Ct^{2-}$) to less basic pH values, leading to the protonation of the *trans*-chalcones; fittings at 384 and 505 nm, with p$K_a$'s of 8.4 and 10.0. Solutions in water containing 20% acetonitrile.

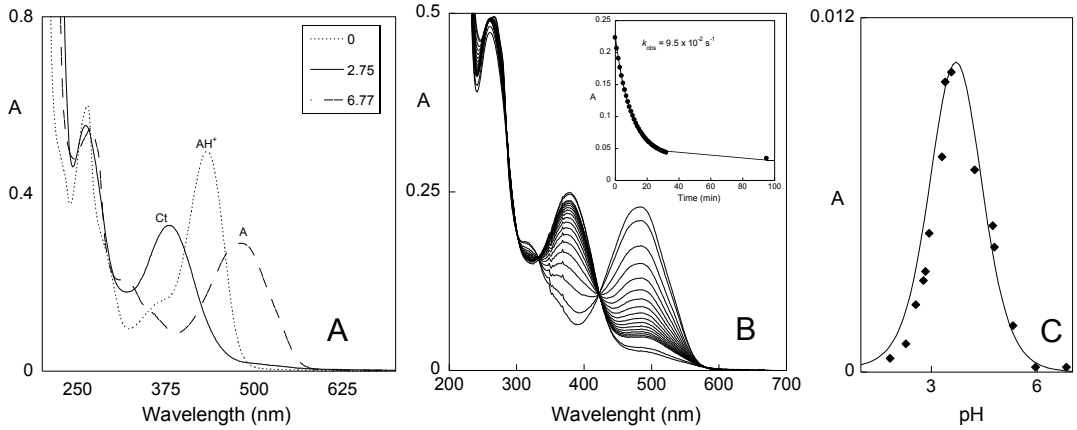


**Figure III.9 -** Absorption spectrum of compound **5** (pH=0) $AH^+$, (pH=6.7) A, (immediately after a pH jump from pH=0, and (pH=2.8) at the equilibrium (**A**). Time evolution of UV-Vis spectra upon a pH jump from a stock solution of compound 5 at pH = 0 to pH = 5.3 ($7.1 \times 10^{-5}$ M); inset: fitting of the absorbance at 480 nm with a single exponential allows to calculate $k_{obs}$ of $9.5 \times 10^{-2}$ $s^{-1}$ (**B**). The $k_{obs}$ as a function of pH (**C**)

Depicted in Fig III.9A are the absorption spectra of transient specie **A** and the species obtained in equilibrated solutions at acidic/neutral pH's. The kinetics of the formation of the equilibrium species from direct pH jumps is pH dependent corresponding to the disappearance of the quinoidal base in this case to form **Ct**; see for example the spectral variations that follow a pH jump from an equilibrated solution at pH = 0 to pH = 5.3, Fig III.9B. Representation of the rates constants calculated at different pH values is shown in Fig III.9C displaying once again the

bell-shaped curve previously described for flavylium compounds.[99] Fitting of the data was achieved for $K_hK_tk_i = 1.18 \times 10^{-5}$ M s$^{-1}$, $k_{-i} = 1.2 \times 10^{-4}$ s$^{-1}$ and $k_iK_t/k_{-h} = 4.5 \times 10^{-5}$ M.

Comparison of the p$K_a$ of *flavylium-viologen-flavylium triad* **5** (p$K_a$ = 3.2) with that of the model compound **6** (p$K_a$ = 4.1) reflects the effect of the positive charge of the viologen bridge on the 7-OH group making it more acidic. The same was observed for the global p$K'_a$, see all the equilibrium and rate constants of these systems in Table III.2 and III.3. The global acidity constant defined by Eq. I.1 is higher for *flavylium-viologen-flavylium triad* **5** (p$K'_a$ = 1.0) than for the model compound **4** (p$K'_a$ = 2.85). The acidity constants of the chalcones in *flavylium-viologen-flavylium triad* **5**, p$K_{Ct}$ = 8.4 and p$K_{Ct^-}$ = 10.0, compare with the values of 7.9 and 9.4, respectively, in the model compound **6**. This is only explained if the acidic form is relatively more stabilized than the basic one, and we do not have any reliable explanation unless to consider that the ionized chalcones are less stable in the solvent mixture used due to its zwitterionic character.

**Table III.1 -** Equilibrium constants for model compound **6** (water), viologen-flavylium dyad **4** (water) and flavylium-viologen-flavylium triad **5** (water: acetonitrile 80:20 v/v) at 295 K.

| | $K_h$ (M) | $K_t$ | $K_i$ | p$K_a$ | p$K'_a$ |
|---|---|---|---|---|---|
| model compound **6** | $1.7\times10^{-6}$ | 4.8 | 200 | 4.1 (4.1)* | 2.78 (2.85)* |
| viologen-flavylium dyad **4** | $5.03\times10^{-6}$ | 15.3 | 272 | 4.65 (4.65)* | 1.68 (1.68)* |
| flavylium-viologen-flavylium triad **5** | $1.4\times10^{-5}$ | 0.86 | $8.2\text{x}10^{3}$ | 3.2 (3.2)* | 1.0 (1.01)* |

* Experimentally observed

**Table III.2** Equilibrium constants for model compound **6** (water), viologen-flavylium dyad **4** (water) and flavylium-viologen-flavylium triad **5** (water: acetonitrile 80:20 v/v) at 295 K.

| | $k_h$ (s$^{-1}$) | $k_{-h}$(M$^{-1}$s$^{-1}$) | $k_t$ (s$^{-1}$) | $k_{-t}$ (s$^{-1}$) | $k_i$(s$^{-1}$) | $k_{-i}$(s$^{-1}$) |
|---|---|---|---|---|---|---|
| model compound **6** | 0.02 | $1.3\times10^{4}$ | 12 | 2.5 | 0.11 | $5\times10^{-4}$ |
| viologen-flavylium dyad **4** | 0.012 | $2.3\text{x}10^{4}$ | 5 | 0.32 | 0.15 | $5.7\text{x}10^{-4}$ |
| flavylium-viologen-flavylium triad **5** | 0.26 | $1.9\times10^{4}$ | 1.25 | 1.45 | 1.0 | $1.2\times10^{-4}$ |

## III.5.2. *Photochemistry*

The photochemistry of the bis *trans*-chalcone is much less efficient than the one of the model compound **6**, but more efficient than the viologen-flavylium dyad.

*Continuous irradiation*

Equilibrated solutions of bis *trans*-chalcone at moderated acid pH's were irradiated at 365 nm. At pH = 1.83, Fig III.10A it is possible to verify the formation of more flavylium than at pH = 2.37, Fig III.10B. The consumption of **Ct** is rather insignificant as is the colour change. This is due to the high value of $k_i$ (from **Cc** to give **Ct**) when compared to the model compound.

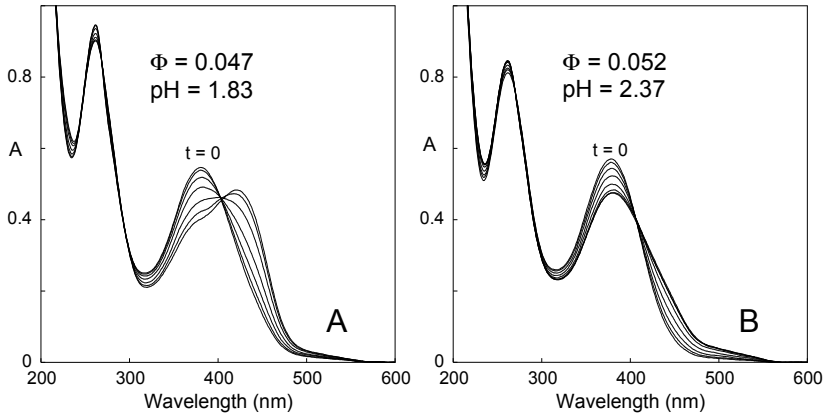


**Figure III.10 -** Spectral variations observed upon continuous irradiation at 365 nm of dark equilibrated solutions of the bis **Ct** $2.46 \times 10^{-5}$ M as a function of time in water: acetonitrile 80:20 v/v, at pH=1.83 (**A**) and pH=2.37 (**B**).

*Pulsed irradiation*

Once again, pulse irradiation studies were held to equilibrate solution of bis *trans*-chalcone. In Fig III.11 is depicted an irradiation performed at pH = 1.7 and monitored at the **Ct** wavelength consumption (377 nm, Fig III.11A) and at the $\mathbf{AH}^+$ formation (430 nm, Fig. III.11B). Both processes fit with the same $k_{obs}$ for the fast processes. The amplitude of the process is higher than in the case of the viologen-flavylium dyad, reason why some photochemistry can be observed in this case but even still, quite inferior when compared with the model compound.

As obtained in the model compound, the rate constant for the fast process at 377 nm is $[H^+]$ dependent and is represented in Fig III.11C. At high proton concentration the rate-determining step is the tautomerization controlled by $k_{-t}$ (Equation III.6) and at low proton concentration the rate-determining step is the hydration/dehydration given by Equation III.7.

$k_{\text{obs, fast (plateau)}} = k_{\text{-t}} = 3.7\ \text{s}^{-1}$ **Equation III-6**

$$k_{obs,fast} = k_h + \frac{K_t k_i}{1+K_t} + \frac{k_{-h}\left[\text{H}^+\right]}{1+K_t} = 0.72 + 1.0\times10^4\left[\text{H}^+\right]$$ **Equation III-7**

In this case the plateau obtained at 3.7 $s^{-1}$.

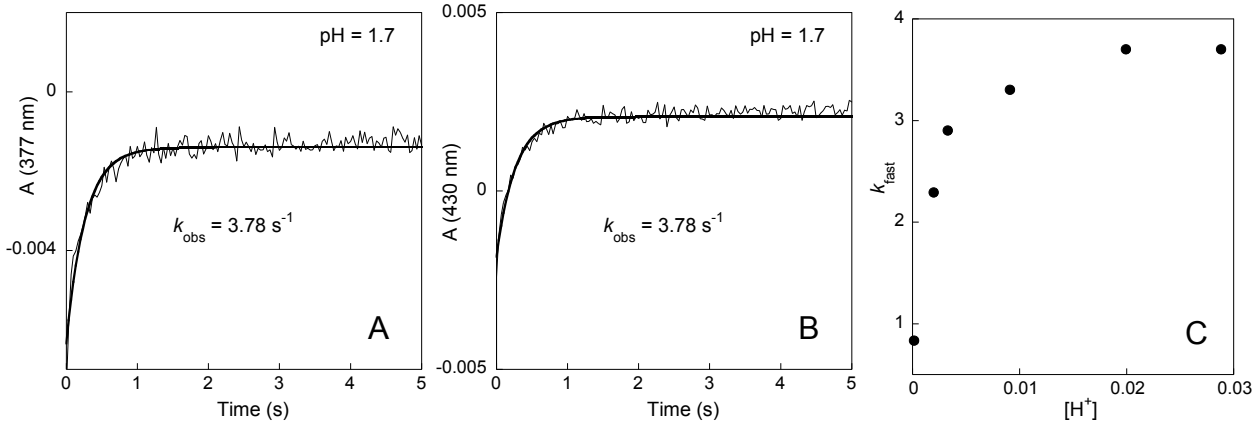


**Figure III.11 -** Time evolution of the absorbances at 377 nm (Ct absorption, **A**) and 430 nm ($AH^+$ absorption, **B**) upon flash irradiation of a solution of model compound 5 at pH = 1.7. The rate constant for the fast process, $k_{\text{fast}}$, as a function of proton concentration is plotted in (**C**).

## III.5.3. *Addition of SDS micelles*

Another objective of this work is to take profit from the two positive charges brought by the viologen substituent. Sodium dodecyl sulphate (SDS) micelles possessing a negative surface should in principle stabilize all the species of the flavylium network and influence not only the thermodynamic but also the kinetics of the flavylium network of chemical reactions, possibly increasing the photochemistry.

Direct pH jumps from stock acidic solutions of the flavylium-viologen-flavylium triad **5** in water and [SDS] = 0.1 M to higher pH values were monitored immediately after a pH by UV/Vis spectrophotometer, Fig III.12A. A fitting of the data was only possible with two p$K_a$ values. This is probably due to the stabilization of the flavylium cation with the SDS micelles making the deprotonation more difficult and the behaviour of the two flavylium different.

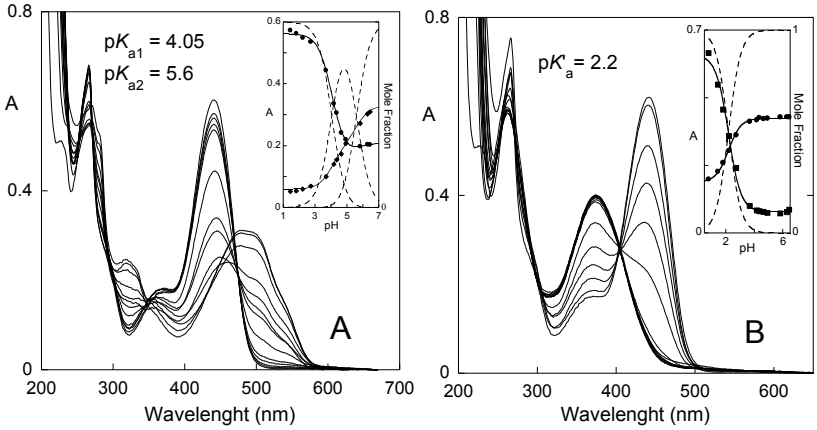


**Figure III.12 -** Absorption spectra of *flavylium-viologen-flavylium triad* **5** immediately after a pH jump from a stock solution $4.3 \times 10^{-5}$ M at pH = 0 to higher pH values; B- the same at the equilibrium. Solutions in water containing 0.1M of SDS.

When compared in the absence of SDS ($pK_a$ = 3.2) and in the presence of SDS the compound is less acidic, with $pK_{a1}$ = 4.05 and $pK_{a2}$ = 5.6. The same can be said for the global acidity constant $pK_a^{'}$ = 2.2 (Fig III.12B) when compared to $pK_a^{'}$ = 1.01 (Fig. III.8B).

In order to study the kinetic properties of the system, pH jumps from 1 to more basic pH values were performed and followed by UV–Vis absorption spectroscopy. In Fig. III.13A an example of a pH jump to 5.5 is presented. It is possible to see the disappearance of the flavylium cation converted into the *trans*-chalcone, **Ct**. Fig. III.13B reports the best fitting of the $k_{obs}$ values determined upon pH jumps *versus* pH with $K_hK_ik_i = 2.5 \times 10^{-7}$ M $s^{-1}$, $k_{-i} = 9.8 \times 10^{-6}$ $s^{-1}$ and $k_iK_i/k_{-h} = 8.9 \times 10^{-5}$ M.

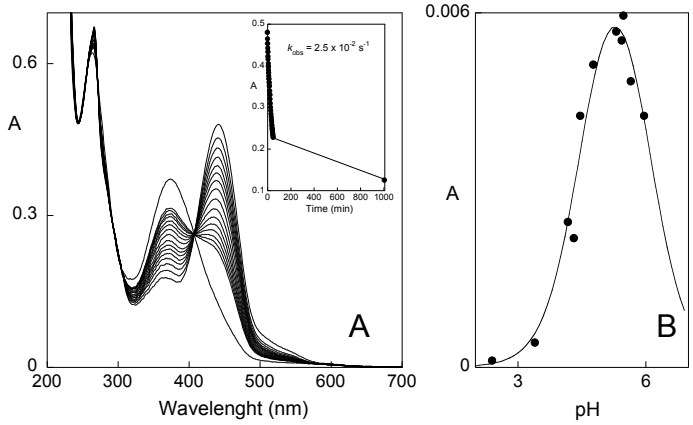


**Figure III.13 -** (**A**). Time evolution of UV-Vis spectra upon a pH jump from a stock solution of compound 5 at pH = 0 to pH = 5.5 ($4.3 \times 10^{-5}$ M); inset: fitting of the absorbance at 472 nm with a single exponential allow to calculate $k_{obs}$ of $5.9 \times 10^{-3}$ $s^{-1}$ (**B**). The $k_{obs}$ as a function of pH.

Since the purpose of joining the SDS was of more importance at the photochemical level and being the general behavior of the compound in the presence and absence of SDS micelles similiar, we proceeded to study the photochemistry of the system in the presence of SDS.

*Continuous irradiation*

Continuous irradiations of aqueous solutions of **Ct** at different pH values with 365 nm light causes spectral changes as shown in Fig III.14A (pH = 2.7) and Fig III.14B (pH = 3.7). In the first case, the disappearance of **Ct** to give only $\mathbf{AH}^+$ while in the second case a clear formation of a mixture of $\mathbf{AH}^+/\mathbf{A}$. This is easily explained considering that at pH = 3.7 we are near from the p$K_a$ determined (4.05) favouring the formation of the quinoidal base.

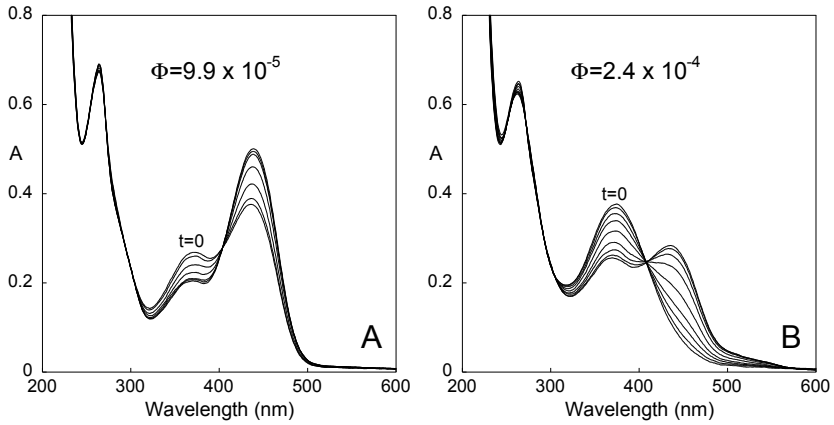


**Figure III.14** - Spectral variations observed upon continuous irradiation (365 nm) of dark equilibrated solutions of Ct $1.43 \times 10^{-5}$ M as a function of time at pH = 2.7 (**A**) and 3.7 (**B**).

## III.5.4. *NMR study*

In order to fully understand if the two flavylium reaction networks are independent from each other or in spite of the methylene viologen bridge separating them, the chemical changes taking place in one branch influence the other, NMR studies were performed. Solutions thermally equilibrated of *flavylium-viologen-flavylium triad* **5** were made less acidic by addition of base and the respective kinetic processes followed by $^1$H NMR. In Fig III.15 is depicted the NMR numeration attributed in case of the flavylium cation or the *trans*-chalcone and in Fig III.16 are shown $^1$H NMR spectrum from a pH jump performed from pH = 0 to pH =1.6 taken at different times.

After a careful analysis of the NMR spectra's the more accessible region to properly analyse are the non-aromatic peaks corresponding to methylene's groups. At the initial moment (t = 0) only one singlet is visible but over time a small percentage of a second singlet starts to appear. We know that each flavylium is involved in a fast equilibrium with its quinoidal base counterpart on one hand and that each hemiketal is in fast equilibrium with its *cis*-chalcone counterpart on the other. In other words, both hemiketal/*cis*-chalcone pairs are transient species not detected by $^1$H NMR, as verified experimentally. So the only

species with lifetimes that can be detected by $^1$H NMR and responsible for the singlet's of the methylene's groups are **AH$^+$** and **Ct**.

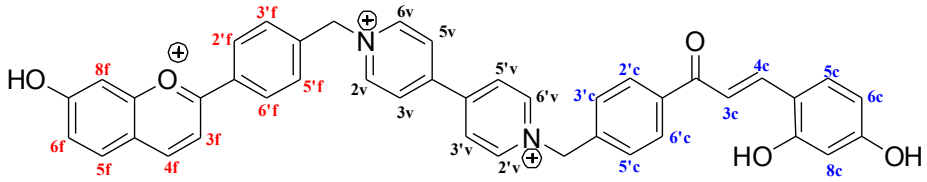


**AH$^+$ - Flavylium cation** **Ct - *trans* Chalcone**

**Figure III.15 –** NMR numeration for AH$^+$–MV–Ct species

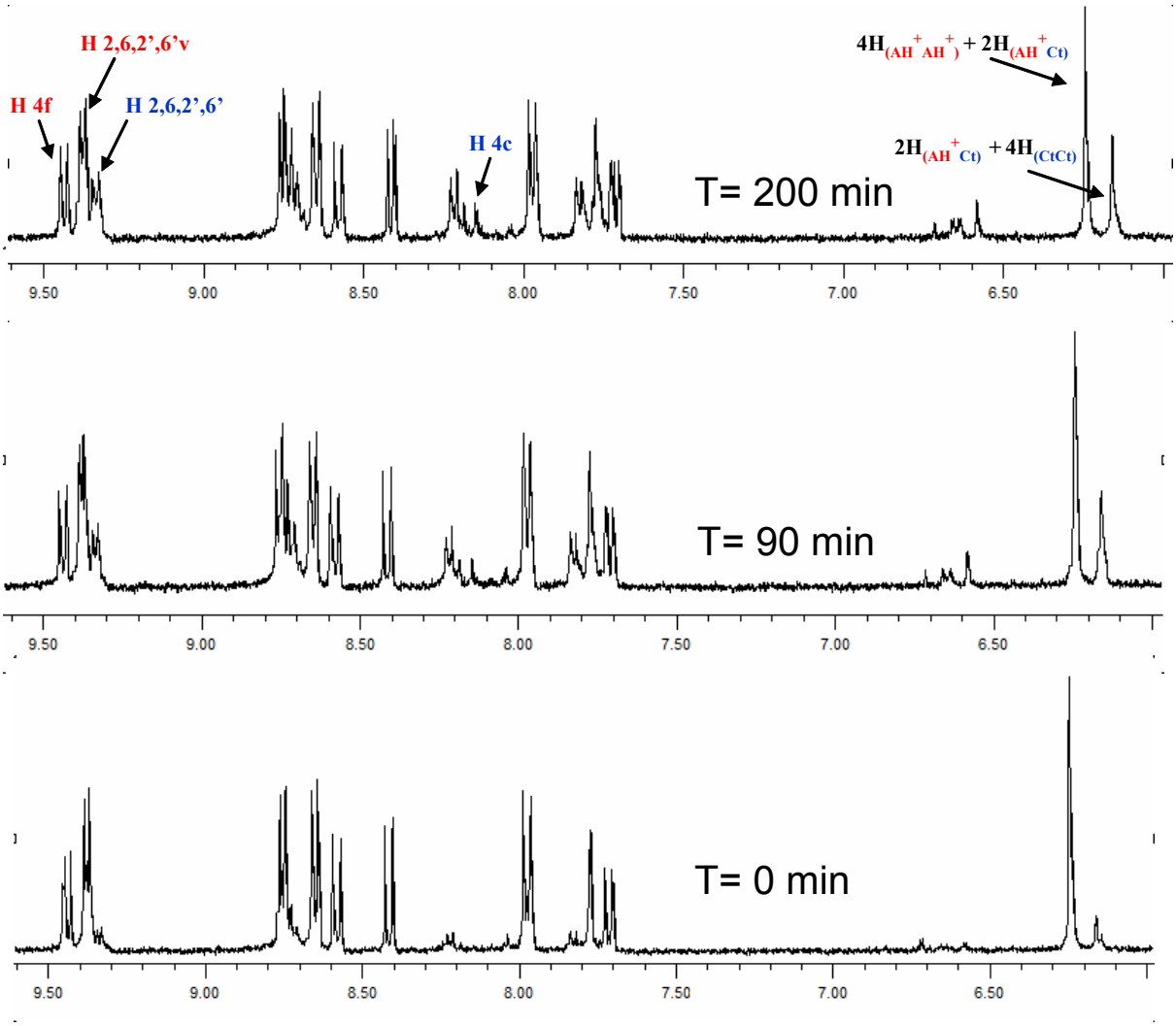


**Figure III.16 –** $^1$H-NMR spectra (400 MHz, $D_2O$:$CD_3CN$ 80:20 v/v, 25°C) of the pH jump carried out from pH≈0 to pH=1.6 at 0, 90 and 200 minutes.

Full assignment of the picks was also necessary to understand the complete system, Table III.1.

**Table III.3–** NMR assignment for $AH^+$–MV–Ct species.

| | Flavylium(ppm) | Chalcone (ppm) |
|---|---|---|
| $\mathbf{H_{3f}}$ | 8.34 (d, $J^3$ ($H_{3f}$-$H_{4f}$) = 8.4 Hz | 7.99 (d, $J^3$ ($H_{3f}$-$H_{4f}$) = 15.5 Hz |
| $\mathbf{H_{4f}}$ | 9.44 (d, $J^3$($H_{4f}$-$H_{3f}$) = 8.4 Hz)* | 7.57 (d, $J^3$($H_{4f}$-$H_{3f}$) = 15.5 Hz) |
| $\mathbf{H_{5f}}$ | 8.20 (dd, $J^3$ ($H_{5f}$-$H_{6f}$) = 9.2 Hz, $J^4$ ($H_{5f}$-$H_{4f}$) = 1.6 Hz) | 7.61 (d, $J^3$ ($H_{5f}$-$H_{6f}$) = 8.8 Hz) |
| $\mathbf{H_{6f}}$ | 7.50 (dd, $J^3$ ($H_{6f}$-$H_{5f}$) = 9.2 Hz, $J^4$ ($H_{6f}$-$H_{8f}$) = 2.0Hz) | 6.47 (dd, $J^3$ ($H_{6f}$-$H_{5f}$) = 8.8 Hz, $J^4$ ($H_{6f}$-$H_{8f}$) = 2.4Hz) |
| $\mathbf{H_{8f}}$ | 7.54 (s) | 6.42 (d, $J^4$ ($H_{8f}$-$H_{6f}$) = 2.4Hz) |
| $\mathbf{H_{2,6,2',6'}}$ | 9.18 (d, $J^3$ ($H_2$-$H_3$) = 6.8Hz | 9.14 (d, $J^3$ ($H_2$-$H_3$) = 6.8Hz |
| $\mathbf{H_{3,5,3',5'}}$ | 8.55 (d, $J^3$ ($H_3$-$H_2$) = 6.8Hz | 8.51 (d, $J^3$ ($H_3$-$H_2$) = 6.8Hz |
| $\mathbf{H_{2'f,6'f}}$ | 8.45 (d, $J^3$ ($H_{2'f}$-$H_{3'f}$) = 8.4Hz) | 7.63 (dd, $J^3$ ($H_{2'f}$-$H_{3'f}$) = 8.4Hz, $J^4$ ($H_{2'f}$-$H_{6'f}$) = 2.4 Hz) |
| $\mathbf{H_{3'f,5'f}}$ | 7.77 (dd, $J^3$ ($H_{3'f}$-$H_{2'f}$) = 8.4Hz, $J^4$ ($H_{3'f}$-$H_{5'f}$) = 1.6 Hz) | 8.05 (d, $J^3$ ($H_{3'f}$-$H_{2'f}$) = 8.4Hz |
| $\boldsymbol{CH_2}$ | 6.05 (s) | 5.97 (s) |

*Remove from the spectrum at pH=1.1

The question is if the two flavylium reaction networks have a stochastic behaviour, *i.e.* are they independent from each other? Each flavylium network can thus be viewed as an equilibrium involving **A**$H^+$**/A,** a transient intermediate **X** (**B2** in fast equilibrium with **Cc**) and **Ct** (**A**$H^+$**/A** ⇆ **X** ⇆ **Ct**), Scheme III.4.

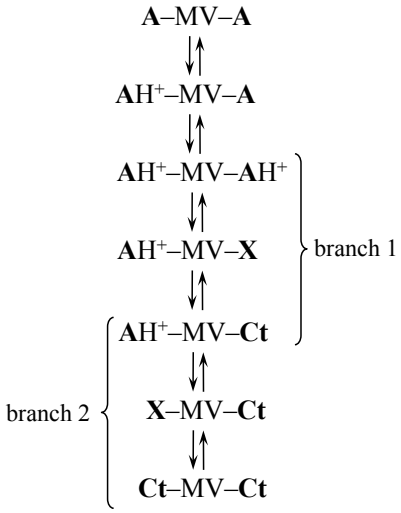


**Scheme III.3** – Simplified network of chemical reactions arising from *flavylium-viologen-flavylium triad* **5**.

In Fig. III.17, a $^1$H NMR spectrum run 32 min upon a pH jump to pH=1.6 is shown. This NMR data allows to discriminate between the species **A**$H^+$–MV–**A**$H^+$ (all-flavylium), **A**$H^+$–MV–

**Ct** and **Ct**–MV–**Ct** (all *trans*-chalcone). In particular, the methylene peaks of the MV spacer can be decomposed into the contributions from **A**H$^+$–MV–**A**H$^+$ (taken at low pH values or at the initial time of the pH jump), **Ct**–MV–**Ct** (at higher pH values after complete conversion of both **A**H$^+$ moieties into **Ct**) and from the intermediate **A**H$^+$–MV–**Ct** species. The decomposition was achieved by a global fitting of Lorentzian curves for different conversion times, as exemplified in Fig. III.17 for $t$ = 32 min. The normalized areas of the Lorentzian curves allow calculation of the mole fraction of each species over time from which a kinetic analysis can be carried out.

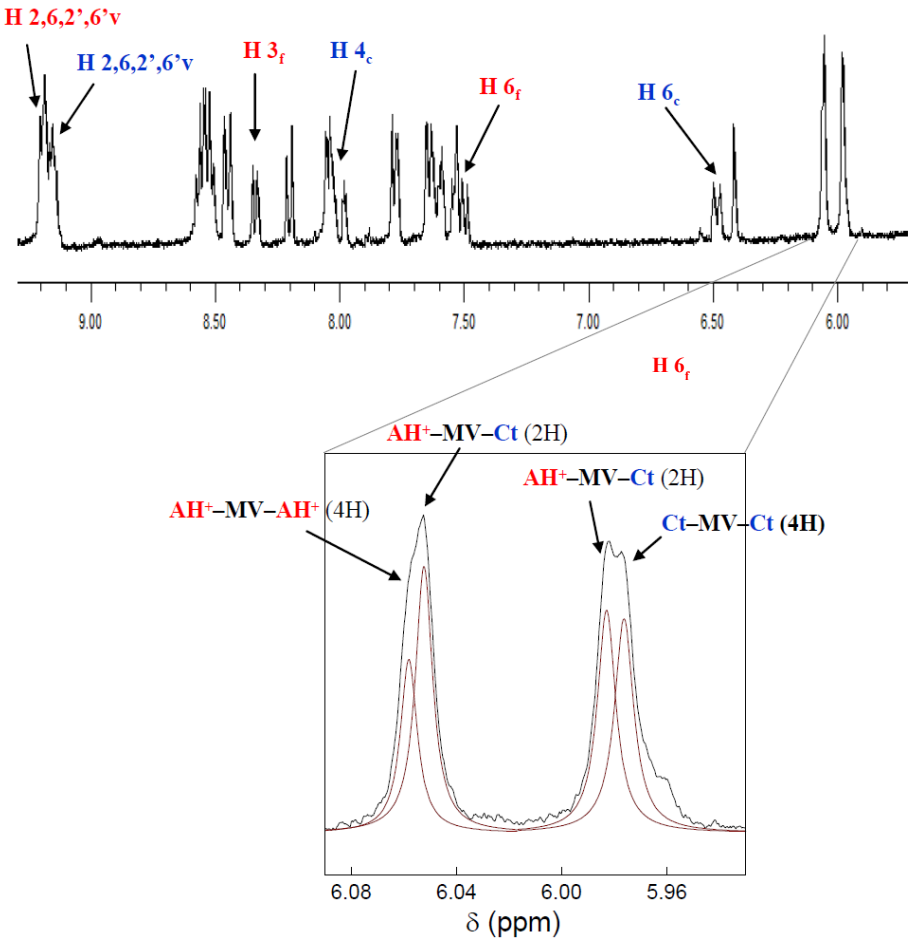


**Figure III.17** – $^1$H NMR spectrum of *flavylium-viologen-flavylium triad* **5**, 32 min after of a pH jump from pH≈0 to pH=1.6. Decomposition of the signal of the methylene groups in Lorentzian curves is shown in the inset.

In Fig. III.18A, the mole fraction distribution of the three species, **A**H$^+$–MV–**A**H$^+$, **A**H$^+$–MV–**Ct** and **Ct**–MV–**Ct** were represented as a function of the fraction of the total **Cc→Ct** isomerization according to a stochastic behaviour, full lines.[122] In the same figure, traced lines indicate another limit situation where all-flavylium **A**H$^+$–MV–**A**H$^+$ species was completely converted into **A**H$^+$–MV–**Ct** species before the isomerization of the other branch to give all-*trans*-chalcone **Ct**–MV–**Ct** species. The experimental data indicate that the present system

deviates from the stochastic situation suggesting some influence of the first isomerization into the second. This is also in accordance with the fact that the $^1$H NMR spectra show small deviations that permitted to characterize the three species. Another confirmation of this interpretation was obtained by fitting the mole fractions of the three components as a function of time, considering **A**H$^+$–MV–**A**H$^+$ ⇆ **A**H$^+$–MV–**Ct** ⇆ **Ct**–MV–**Ct**, Fig. III.18B.[123,124] The rate constants of the first isomerization is *ca*. 3 times faster than the second one ($6.3\times10^{-4}$ s$^{-1}$ *vs*. $2.3\times10^{-4}$ s$^{-1}$, Fig. III.7B). In conclusion, the viologen bridge and the methylene spacers do not isolate both flavylium moieties from each other allowing their communication to some extent.

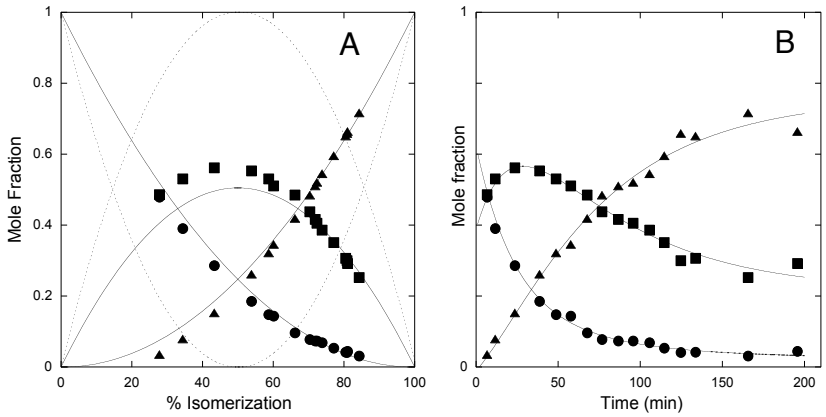


**Figure III.18** – A- Mole fraction distribution of species AH$^+$-MV-AH$^+$ (●), Ct-MV-AH$^+$ (■) and Ct-MV-Ct (▲) as a function of the total fraction of *trans*-chalcone moieties converted (A) and as a function of time (B). The fitting of the kinetic data was achieved taken into account the reverse reaction in both isomerizations: $6.3\times10^{-4}$ s$^{-1}$ and $7.2\times10^{-5}$ s$^{-1}$, respectively for the direct and reverse reactions for the conversion of AH$^+$-MV-AH$^+$ in Ct-MV-AH$^+$; $2.3\times10^{-4}$ s$^{-1}$ and $6.5\times10^{-5}$ s$^{-1}$ for the analogous processes during the conversion of Ct-MV-AH$^+$ in Ct-MV-Ct.

## III.6. Electrochemical Studies

Most viologen dications are colourless. The methylviologen ($MV^{2+}$) can be reversibly reduced to the blue cation ($MV^+$) suggesting the possibility of introducing a redox stimulus in the network of the mono and flavylium-viologen-flavylium triad reported in this work. However, the flavylium cation is usually easily irreversibly reduced and by consequence the **Ct** species was used to carry out these experiments. Cyclic voltammograms (CV) of the chalcones were run in aqueous solutions at pH=5.5 (acetate buffer 0.1M) using the classic three electrode cell with SCE as reference electrode, platinum wire as counter electrode and glassy carbon as working electrode and scanned at 100 mV s$^{-1}$. In Fig III.19 are presented the CV's of the methyl viologen (Fig III.19A), the model compound (Fig III.19B), the mono and bis flavylium in Fig III.19C and III.19D respectively.

Methyl viologen present the two oxidation and the two reduction peaks corresponding to the formation and vice versa of $MV^{+\bullet}$ from $MV^{2+}$ and $MV^0$ from $MV^{+\bullet}$. The *trans*-chalcone of

the model compound shows two reduction peaks and an oxidation peak all corresponding to poorly reversible processes.[125,126]

Regarding the **Ct**-MV and **Ct**-MV-**Ct** species of compounds **4** and **5**, they present the reduction peaks of the MV moiety and the oxidation peaks of the phenol groups on the chalcone moieties. The shape of the reduction peaks is identical to the one of the methyl viologen, although shifted to lower reduction potentials. This means that the observed peaks for **Ct**-MV and **Ct**-MV-**Ct** species are superpositions of the reduction of the methyl viologen and the two **Ct** moieties. This also explains the lack of complete reversibility found on these systems. In Fig III.20 are depicted the reduction and oxidation values obtained for the studied compounds.

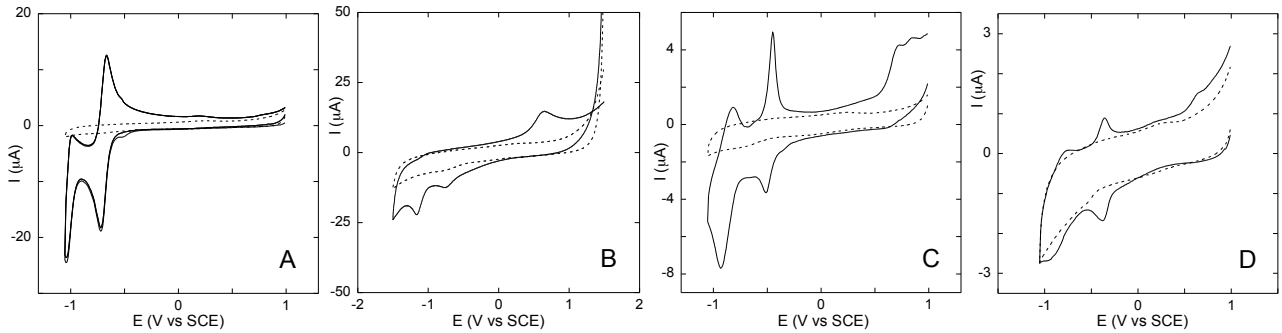


**Figure III.19**-(A) Cyclic voltammograms of methyl viologen (B) Cyclic voltammograms of model compound. (C) – Cyclic voltammograms of viologen-flavylium dyad. (D) – Cyclic voltammograms of flavylium-viologen-flavylium triad. All cyclic voltammograms (CV) were run in aqueous solutions at pH=5.5 (acetate buffer 0.1M) using the classic three electrode cell with SCE as reference electrode, platinum wire as counter electrode and glassy carbon as working electrode at 100 mV $s^{-1}$.

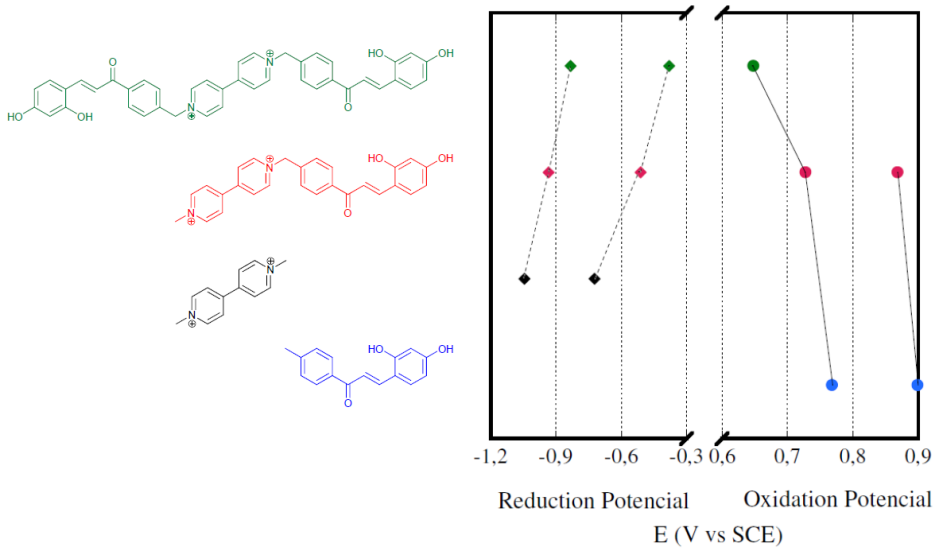


**Figure III.20** – Reduction and oxidation potentials for the model compound, MV and Ct-MV of **4** and Ct-MV-Ct species of **5**, (aqueous 0.1 M acetate buffer at pH=5.5) obtained from cyclic voltammetry carried out in a three electrode cell with SCE as reference electrode, platinum wire as counter electrode and glassy carbon as working electrode with a scan rate of 100 mV $s^{-1}$.

Analysis of the data shows that the reduction of the MV is facilitated and also the oxidation of the chalcones, showing an electron withdrawing of charge from the MV to the chalcone moiety. Due to the lack of reversibility previously mentioned, a more bluish colour was never obtained. The formation of the methyl viologen radical was finally achieved by reducing a solution of **Ct**-MV-**Ct** with dithionite, see Fig. III.21 (traced spectrum and blue-gray photo).

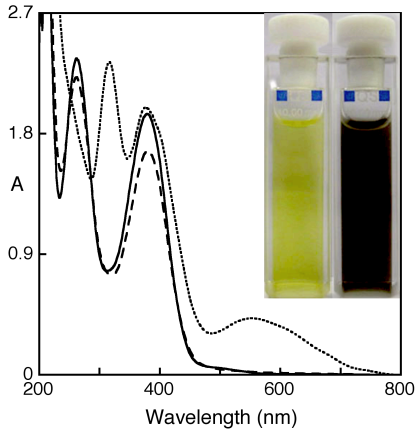


**Figure III.21** – Reduction of *bis*-chalcone, **Ct**-MV-**Ct**, of 3 at pH=4.4 in 0.1 M acetate buffer (full line, yellow colour) with sodium dithionite (pointed line, blue-gray colour); the system is partially reversible upon oxidation with potassium peroxodisulphate (traced line).

The absorption spectrum is characteristic of the methyl viologen radical cation. The reversibility of the system was also checked by addition of potassium peroxodisulphate, which recovers the absorption of the reduced form. However the system is not completely reversible and some decomposition takes place, *ca.* 12% in one cycle.

## III.7. Conclusions

The viologen unit has shown to be a peculiar bridge linking two symmetric flavylium systems. The positive charge of the bridge has a significant effect on the properties of the flavylium moieties when compared with the model compound 4'-methoxy-7-methylflavylium: it favours the deprotonation and the hydration reactions, retards the tautomerization and enhances the isomerisation. The methylene viologen bridge does not isolate both flavylium moieties from each other allowing their communication to some extent, as shown by the methylene $^{1}$H NMR signals that allow to distinguish between *flavylium-viologen-flavylium triad*, mixed flavylium-*trans*-chalcone and all-*trans*-chalcone species The bridge can also be electrochemically reduced permitting to introduce a redox stimuli on the multistate network of the *flavylium-viologen-*

*flavylium triad* system, although it was not possible to carry out the reduction reversibly, a decomposition of 12% taking place in one cycle.

## III.8. Experimental Part

*General:* All reagents and solvents were of analytical grade. NMR spectra were run on a Bruker AMX 400 instrument operating at 400.13 MHz ($^{1}$H) and 100.00 MHz ($^{13}$C). COSY, HMQC, HMBC and eventually NOESY spectra were run on each sample to allow full assignment of the NMR peaks.[127] Mass spectra were run on Micromass GCT apparatus for EI and FD ionization and on an Applied Biosystems Voyager-DE™ PRO for MALDI. Elemental analyses were obtained on a Thermofinnigan Flash EA 1112 Series instrument.

*Absorption measurements:* All spectroscopic measurements were performed using Mili-Q water and Ethanol HPLC-grade (when needed). Spectroscopic experiments were carried out in buffered solutions (Universal Buffer of Theorell and Stenhagen[128]) and pH values were measured with a MeterLab pHM240 pH meter from Radiometer Copenhagen. For solutions with HCl concentration above 0.1 M, pH was calculated from –log [HCl]. UV/Vis absorption spectra were recorded with a Varian-Cary 100 Bio spectrophotometer or in a Shimadzu VC2501-PC.

Quantum yields were determined by irradiation at 365 nm, using a medium pressure mercury arc lamp and the excitation bands were isolated with interference filters (Oriel). Actinometry was made using the ferrioxalate system.[56]

*Stopped-Flow experiments:* Stopped-flow data were acquired in an Applied Photophysics SX20 stopped flow spectrometer equipped with a PDA.1/UV photodiode array detector with a minimum scan time of 1.3 ms and a wavelength range of 200–785 nm.

### III.8.1. *Synthesis of 4'-bromomethylacetophenone*

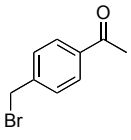


4'-bromomethylacetophenone was prepared according to the method described by *Leventis et al.*[129] 4'-methylacetophenone (14.9 mmol; 1.99 mL) was dissolved in 40 ml of $CCl_4$ (carbon tetrachloride). NBS (N-bromosuccinimide, (16.37 mmol; 2.91 g) and AIBN (2.96 mmol; 0.486 g) were added. The resulting mixture was stirred and left in reflux for 4 days. The succinimide was filtered off, and the solvent removed under reduced pressure. The residue was purified by flash chromatography in hexane/ethyl ether (8:2) to yield 2.632 g of 4'-bromomethylacetophenone (12.35 mmol; 82.9 %) as a yellow stable oil. **$^{1}$H-NMR** ($CD_3OD$, 400.13 MHz) δ (ppm): 7.93 (2H, d, $H_{2'}$, $H_{6'}$, $^{3}J_{H2',H6'- H3',H5'}$ = 8.1 Hz); 7.48 (2H, d, $H_{3'}$, $H_{5'}$, $^{3}J_{H3',H5'- H2',H6'}$ = 7.9 Hz); 4.50 (2H, s, $CH_2$); 2.60 (3H, s, $COCH_3$). **MS-**

**MALDI/TOF+**: calcd for $C_9H_9BrO^+$: 211.98 (100%); found: 211.1 $[M-H]^+$ (33.5%); 212.1 $[M]^+$ (5%).

## III.8.2. Synthesis of 1-methyl-4,4'-bipyiridyl-1-inium triflate

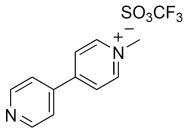


4,4'-bipyridine (0.4898g, 3.14 mmol) was dissolved in 15 mL of ethyl ether and trifluoro(methylsulfonyl)methane (0.42 mL, 3.71 mmol) was added. The resulting mixture was stirred and left at room temperature for 2h. The yellow precipitated solid was filtered off, washed with diethyl ether and dried. After recrystallization with methanol, 1-methyl-4,4'-bipyridil-1-inium triflate and 1,1'-dimethyl-4,4'-bipyridinium triflate were obtain as white solids. Was obtained 0.745 g (2.33 mmol, 74 %) of 1-methyl-4,4'-bipyridil-1-inium triflate presenting: **$^1$H-NMR** ($CD_3OD$, 400.13 MHz) δ (ppm): 7.76 (2H, d, $H_2$, $H_6$, $^3J_{H2,H6\text{-}H3,H5}$= 6.5 Hz); 7.64 (2H, d, $H_{2'}$, $H_{6'}$, $^3J_{H2',H6'\text{-}H3',H5'}$= 5.9 Hz); 7.24 (2H, d, $H_3$, $H_5$, $^3J_{H3,H3\text{-}H2,H6}$= 6.4 Hz); 6.79 (2H, d, $H_{3'}$, $H_{5'}$, $^3J_{H3',H5'\text{-}H2',H6'}$= 6.1 Hz); 3.30 (3H, s, N-$CH_3$). MS-MALDI/TOF+: calcd for $C_{11}H_{11}N_2^+$: 171.09 (100%); found: 171.5 $[M]^+$ (100%); 172.5 $[M+H]^+$ (43%). As a lateral product was obtained 0.642 g (1.33 mmol, 42.2 %) of 1,1'-dimethyl-4,4'-bipyridinium triflate presenting: **$^1$H-NMR** ($CD_3OD$, 400.13 MHz) δ (ppm): 8.96 (4H, d, $H_2$, $H_6$, $H_{2'}$, $H_{6'}$, $^3J_{H2,H6,H2',H6'\text{-}H3,H5,H3',H5'}$= 6.2 Hz); 8. 24 (4H, d, $H_3$, $H_5$, $H_{3'}$, $H_{5'}$, $^3J_{H3,H5,H3',H5'\text{-}H2,H6,H2',H6'}$= 5.9 Hz); 4.41 (6H, s, N-$CH_3$).

## III.8.3. Synthesis of 1-methyl-1'-[(acetophenone-4-il)methyl]-4,4'-bipyridinium hexafluorofosfate

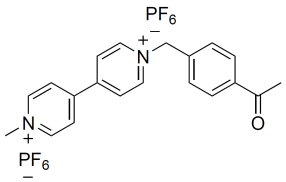


1-methyl-1'-[(acetophenone-4-il)methyl]-4,4'- bipyridinium hexafluorofosfate was prepared by an adapted method described by Porter *et al.*[117] 1-methyl-4,4'-bipyridil-1-inium triflate (0.5 mmol; 0.16 g) was dissolved in 5 mL of DMF in a round-bottom flash containing a magnetic stir bar and a reflux condenser. The solution was degassed and placed under N2. To the stirred solution, 4'-methylacetophenone (0.5 mmol; 0.106 g) previously dissolved in 2 mL of DMF was added via syringe. The resulting mixture was stirred under $N_2$ and was allowed to reflux 21h and then concentrated by distillation. The crude was dissolved in methanol, and by changing the counter ion to hexafluorofosfate, adding of ethyl ether resulted in the precipitation of a yellow solid. The solid was filtered off, washed with diethyl ether and dried, yielding 0.175 g (0.94 mmol, 58.9%) of 1-methyl-1'-[(acetophenone-4-il)methyl]-4,4'- bipyridinium hexafluorofosfate as a yellow powder. **$^1$H-NMR** ($DCl/CD_3OD$, pD≈1.0, 400.13 MHz) δ (ppm): 9.31 (2H, d, $H_2$, $H_6$, $^3$J

$H_2$,$H_6$-$H_3$,$H_5$ = 5.7 Hz); 9.15 (2H, d, $H_{2'}$, $H_{6'}$, $^3J_{H2',H6-H3',H5'}$ = 5.6 Hz); 8.64 (4H, d, $H_{3'}$, $H_{5'}$, $H_3$, $H_5$, $^3J_{H3',H5',H3,H5-H2',H6',H2,H6}$ = 5.6 Hz); 8.09 (2H, d, $H_{9'}$, $H_{13'}$, $^3J_{H9',H13'-H10',H12'}$ = 8.0 Hz); 7.65 (2H, d, $H_{10'}$, $H_{12'}$, $^3J_{H10',H12'-H9',H13'}$ = 8.0 Hz); 6.03 (2H, s, N-$CH_2$); 4.50 (3H, s, N-$CH_3$); 2.61 (3H, s, $COCH_3$). **MS-MALDI/TOF**$^+$: calcd for $C_{20}H_{20}N_2O^+$: 304.16 (100%); found: 171.6 [M-C9H9O$^{\cdot}$]$^+$ (100%); 303.7 [M-H]$^+$ (39%); 304.7 [M]$^+$ (18.8%). **EA** calcd for $C_{20}H_{20}F_{12}N_2OP_2.H_2O$: C 39.23; H 3.62; N 4.57 found: C 39.39; H 3.17; N 4.66.

## III.8.4. Synthesis of 1-methyl-1'-[(7-hydroxyflavylium-4'-il)methyl]-4,4'-bipyridinium hexafluorofosfate

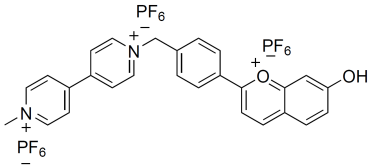


1-methyl-1'-[(acetophenone-4-il)methyl]-4,4'-bipyridinium hexafluorofosfate (0.17 mmol; 0.101 g) and 2,4-dihydroxybenzaldehyde (0.17 mmol; 0.023 g) were dissolved in 3.5 mL de glacial acetic. 1.1 mL of sulphuric acid was added and the resulting mixture was allowed to stir over night. A red-brownish solid was obtained by treating the solution with $H_2O$ and perchloric acid. The solid was filtered off, washed with ethyl acetate and dried, yielding 1-methyl-1'-[(7-hydroxyflavylium-4'-il)methyl]-4,4'- bipyridinium hexafluorofosfate quantitatively. **$^1$H-NMR** ($DCl/CD_3OD$, pD≈1.0, 400.13 MHz) δ (ppm): 9.46 (2H, d, $H_2$, $H_6$, $^3J_{H2,H6-H3,H5}$ = 5.6 Hz); 9.39 (1H, d, $H_4^f$, $^3J_{H4f-H3f}$ = 7.8 Hz); 9.19 (2H, d, $H_{2'}$, $H_{6'}$, $^3J_{H2',H6'-H3',H5'}$= 5.5 Hz); 8.75 (2H, d, $H_3$, $H_5$, $^3J_{H3,H5-H2,H6}$ = 5.6 Hz); 8.67 (2H, d, $H_{3'}$, $H_{5'}$, $^3J_{H3',H5'-H2',H6'}$ = 5.8 Hz); 8.59 (3H, d, $H_{3'}^f$, $H_{5'}^f$, $H_3^f$, $^3J_{H3'f,H5'f-H2'f,H6'f}$ = 6.9 Hz); 8.33 (1H, d, $H_5^f$, $^3J_{H5f-H6f}$ = 8.9 Hz); 7.97 (2H, d, $H_{2'}^f$, $H_{6'}^f$, $^3J_{H2'f,H6f'-H3'f,H5'f}$ = 7.9 Hz); 7.69 (1H, s, $H_8^f$); 7.56 (1H, d, $H_6^f$, $^3J_{H6f-H5f}$ = 7.6 Hz); 6.25 (2H, s, N-$CH_2$); 4.56 (3H, s, N-$CH_3$). **MS-MALDI/TOF+**: calcd for $C_{27}H_{23}N_2O_2^+$: 407.18 (100%); found: 406.6 [M-H]$^+$ (13%); 405.6 [M-2H]$^+$ (29.4%); 236.5 [M-$C_{11}H_{11}N_2^{\cdot+}$]$^+$ (16.3%); 235.5 [M-$C_{11}H_{12}N_2^{\cdot+}$]$^+$ (20.6%); 186.6 [M-$C_{15}H_9N_2^{\cdot+}$]$^+$ (3.1%); 172.5 [M-$C_{16}H_{13}O_2^{\cdot+}$]$^+$ (61.9%); 171.6 [M-$C_{16}H_{12}O_2^{\cdot+}$]$^+$ (100%).

## III.8.5. Synthesis of 1,1'-di-[(acetophenone-4-il) methyl]-4,4'-bipyridinium bromide

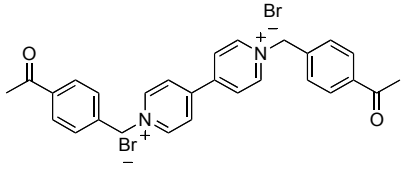


1,1'-di-[(acetophenone-4-il)methyl]-4,4'-bipyridinium bromide was prepared according to the method described by Porter *et al.*[117] 4,4'-bipyridyl (2 mmol; 0.312 g) was dissolved in 20 mL of DMF in a round-bottom flash containing a magnetic stir bar and a reflux condenser. The solution was degassed and placed under $N_2$. To the stirred solution, 4'-bromomethylacetophenone (6 mmol; 1.278 g) previously dissolved in 6 mL of DMF was added

via syringe. The resulting mixture was stirred under $N_2$ and was allowed to reflux 10h and then concentrated by distillation. The crude was dissolved in methanol, and an orange precipitated was obtained by adding ethyl ether. The solid was filtered off, washed with diethyl ether and dried, yielding 1.114 g (1.91 mmol, 95.7%) of 1,1'-di-[(acetophenone-4-il)methyl]-4,4'-bipyridinium bromide. **$^1$H-NMR** ($CD_3OD$; 400.13 MHz) δ (ppm): 9.36 (4H, d, $H_{2'}$, $H_{6'}$, $H_2$, $H_6$, $^3J_{H2',H6',H2,H6-H3',H5',H3,H5}$ = 6.6 Hz); 8.70 (4H, d, $H_{3'}$, $H_{5'}$, $H_3$, $H_5$, $^3J_{H3',H5',H2,H5-H2',H6',H2,H6}$ = 6.5 Hz); 8.09 (4H, d, $H_{9'}$, $H_{13'}$, $H_9$, $H_{13}$, $^3J_{H9',H13',H9,H13-H10',H12',H10,H12}$ = 8.2 Hz); 7.67 (4H, d, $H_{10'}$, $H_{12'}$, $H_{10}$, $H_{12}$, $^3J_{H10',H12',H10,H12-H9',H13',H9,H13}$ = 6.6 Hz); 6.05 (4H, s, N-$CH_2$); 2.60 (6H, s, $COCH_3$). **$^{13}$C-NMR** ($CD_3OD$; 400.13 MHz) δ (ppm): 151.86 ($C_4$, $C_{4'}$); 147.37 ($C_2$, $C_6$, $C_{2'}$, $C_{6'}$); 139.56 ($C_8$, $C_{8'}$); 139.04 ($C_{11}$, $C_{11'}$); 130.58 ($C_9$, $C_{13}$, $C_{9'}$, $C_{13'}$); 130.45 ($C_{10}$, $C_{12}$, $C_{10'}$, $C_{12'}$); 128.73 ($C_3$, $C_5$, $C_{3'}$, $C_{5'}$); 65.26 (CN-$CH_2$); 26.79 ($CCH_3$). **MS-MALDI/TOF+**: calcd for $C_{28}H_{26}N_2O_2^+$: 422.20 (100%); found: 289.5 [M-$C_9H_9O^{\cdot}$]+ (100%); 421.6 [M-H]+ (73%); 423.5 [M+H]+ (13%). **AE** calcd for $C_{28}H_{26}Br_2N_2O_2.H_2O$: C 56.02; H 4.70; N 4.67 found: C 56.60; H 4.64; N 4.82.

## III.8.6. Synthesis of 1,1'-di-[(7-hydroxyflavylium-4'-il) methyl]-4,4'-bipyridinium perchlorate

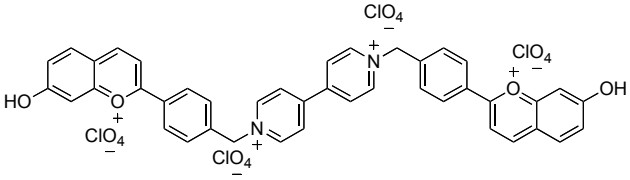


1,1'-di-[(acetophenone-4-il)methyl]-4,4'-bipyridinium bromide (0.2 mmol; 0.116 g) and 2,4-dihydroxybenzaldehyde (0.2 mmol; 0.027 g) were dissolved in 4 mL of glacial acetic acid. 1.2 mL of sulphuric acid was added and the resulting mixture was allowed to stir over night. A reddish solid was obtained by treating the solution with $H_2O$ and perchloric acid. The solid was filtered off, washed with ethyl acetate and dried, yielding 0.123 g (0.12 mmol; 59.8 %) of 1,1'-di-[(7-hydroxyflavylium-4'-il)methyl]-4,4'- bipyridinium perchlorate. **$^1$H-NMR** (DCl /$CD_3OD$, pD≈1.0, 400.13 MHz) δ (ppm): 9.47 (4H, d, $H_{2'}$, $H_{6'}$, $H_2$, $H_6$, $^3J_{H2',H6',H2,H6-H3',H5',H3,H5}$ = 6.6 Hz); 9.39 (2H, d, $H_{4f}$, $^3J_{H4f-H3f}$ = 8.3 Hz); 8.78 (4H, d, $H_{3'}$, $H_5$', $H_3$, $H_5$, $^3J_{H3',H5',H3,H5-H2',H6',H2,H6}$ = 6.6 Hz); 8.59 (4H, d, $H_{3'f}$, $H_{5'f}$, $^3J_{H3'f,H5f'-H2'f,H6'f}$ = 8.6 Hz); 8.58 (2H, d, $H_{3f}$, $^3J_{H3f-H4f}$ = 8.6 Hz); 8.33 (2H, d, $H_{5f}$, $^3J_{H5f-H6f}$ = 9.0 Hz); 7.96 (4H, d, $H_{2'f}$, $H_{6'f}$, $^3J_{H2'f,H6f'-H3'f,H5'f}$ = 8.2 Hz); 7.67 (2H, s, $H_{8f}$); 7.55 (2H, d, $H_{6f}$, $^3J_{H6f-H5f}$ = 9.0 Hz, $^4J_{H6f-H8f}$ = 2.2 Hz); 6.23 (4H, s, N-$CH_2$). **MS-MALDI/TOF+**: calcd for $C_{42}H_{32}N_2O_4^+$: 628.24 (100%); found: 627.7 [M-H]+ (32.8%); 391.7 [M- $C_{16}H_{13}O_2^{\cdot}$+]+ (25%); 235.6 [M-$C_{26}H_{20}N_2O_2^{\cdot 3+}$]$^+$ (100%). **ESI-MS** m/z (%): 787.6 [M + $ClO^{4-}$ + 2$OCH_3^-$ -2H]$^+$, 688.1 [M + 2$OCH_3^-$ -2H]$^{2+}$, 422.4 [M -7OH-4'Me-flav + $OCH_3^-$ -H]$^{2+}$, 390.8 [M -7OH-4'Me-flav -2H]$^{3+}$, 266.9 [7OH-4'Me-flav + OCH3$^-$ -H]$^{2+}$, 235.9 [7OH-4'Me-flav]$^+$. **EA** calcd for $C_{42}H_{32}Cl_4N_2O_{20}$.(3)$H_2O$: C 46.68; H 3.54; N 2.59 found: C 46.48; H 3.13; N 2.70.

## III.8.7. Synthesis of 7-hydroxy-4'-methylflavylium tetrafluoroborate

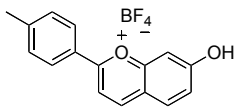


7-hydroxy-4'methylflavylium tetrafluoroborate was prepared according to a procedure adapted from Katritzky. 2,4-dihydroxybenzaldehyde (10 mmol, 1.38 g) and 4-methylacetophenone (10 mmol, 1.34 g) were dissolved in 10 ml of acetic acid and 2 ml of $HBF_4$. 10 ml of acetic anhydride were then added dropwise and the temperature of the reaction raised. The reaction mixture was stirred overnight. By the following day diethyl ether and ethyl acetate was added and a orange solid precipitated, was filtered off and carefully washed with diethyl ether and dried yielding 0.57 g (1.78 mmol, 18%) of 7-hydroxy-4'methylflavylium tetrafluoroborate. **$^{1}$H-NMR** (DCl /$CD_3OD$, pD≈1.0, 400.13 MHz) δ (ppm): 9.27 (1H, d, $H_{4,}$ $^{3}J_{H4\ H3}$ = 8.5 Hz), 8.48 (1H, d, $H_{4,}$ $^{3}J_{H3\ H4}$ = 8.5 Hz), 8.39 (2H, d, $H_{2'6',}$ $^{3}J_{H2',H6'-\ H3',H5'}$ = 8.3 Hz), 8.25 (1H, d, $H_{5,}$ $^{3}J_{H5\ H6}$ = 9.0 Hz), 7.62 (1H, d, $H_{8,}$ $^{4}J_{H8\ H6}$ = 1.6 Hz), 7.56 (2H, d, $H_{3'5',}$ $^{3}J_{H3',H5'-\ H2',H6'}$ = 8.2 Hz), 7.49 (1H, d, $H_{6,}$ $^{3}J_{H6\ H5}$ = 9.0 Hz, $^{3}J_{H6\ H8}$ = 2.0 Hz), 2.54 (3H, s, $CH_3$). **$^{13}$C-NMR** (DCl /$CD_3OD$, pD≈1.0, 400.13 MHz) δ (ppm): 173.55 ($C_2$); 171.36 ($C_7$); 161.15 ($C_{8a}$); 156.21 ($C_4$); 149.75 ($C_{4'}$); 134.44 ($C_5$); 132.05 ($C_{3'}$, $C_{5'}$); 130.61($C_{2'}$, $C_{6'}$); 127.81 ($C_1$); 123.46 ($C_6$); 121.29 ($C_{4a}$); 114.07 ($C_3$); 103.74 ($C_8$); 22.13 ($C_{CH3}$). **MS-MALDI/TOF+**: calcd for $C_{16}H_{13}O_2^+$: 237.09 (100%); found: 237.1 $[M]^+$ (100%); 135.1 $[M-C_8H_6O + H^{\cdot}]^+$ (65%). 119.07 $[M- C_8H_6O+ H^{\cdot}]^+$ (100%).

# CHAPTER IV. Metal Complexing Units

# IV. Metal Complexing Units

In this chapter, directional synthesis of polypyridine ligands as building blocks to supramolecular systems containing flavylium salts is discussed. Characterization of one of the synthesized compounds is also presented.

## IV.1. Introduction

Polypyridine Ru(II) complexes have long been used as components to build up supramolecular species due to a unique combination of chemical stability, redox properties, excited-state properties and lifetimes.[130] In this chapter, dyads and triads constituted by flavylium systems containing a central phenantroline and/or 2,2'-bipyridine unit are presented.

1,10-Phenanthroline is a planar molecule thus more rigid than 2,2'-bipyridne making it entropically a better chelating molecule[131], but at the same time and from the synthetic point of view is more difficult to handle. Both units possess high affinity to several metal cations[132] making it possible a wide range of luminescent compounds.

These build up of supramolecular dyads and triads involving flavylium cations and polypyridine Ru(II) complexes allows the possibility of introducing new processes in the flavylium systems such as electric inputs, energy processes and electron transfer processes.

## IV.2. Phenanthroline as a building block

The aim of this work is the synthesis of supramolecular dyads and triads constituted by flavylium moieties covalently linked to the phenanthroline as a building block and finally to complex with a $Ru(bpy)_2$ moiety.

The synthetic strategy chosen is presented in Scheme IV.1. There are several factors to take into account for this synthetic pathway. The substitutions at positions 3 and 8 on the phenanthroline core are due to steric hindrance since the required ligand itself would be bulky, especially when complexed with $Ru(bpy)_2$. The choice of building from the central unit is due to the reaction last step, since the formation of the desired flavylium is formed under extremely acidic conditions. If on the other hand we synthesize the flavylium previously, purifications in any further synthetic step would imply the use of rather acidic pH values to avoid the many equilibria originated by flavylium under less acidic conditions.

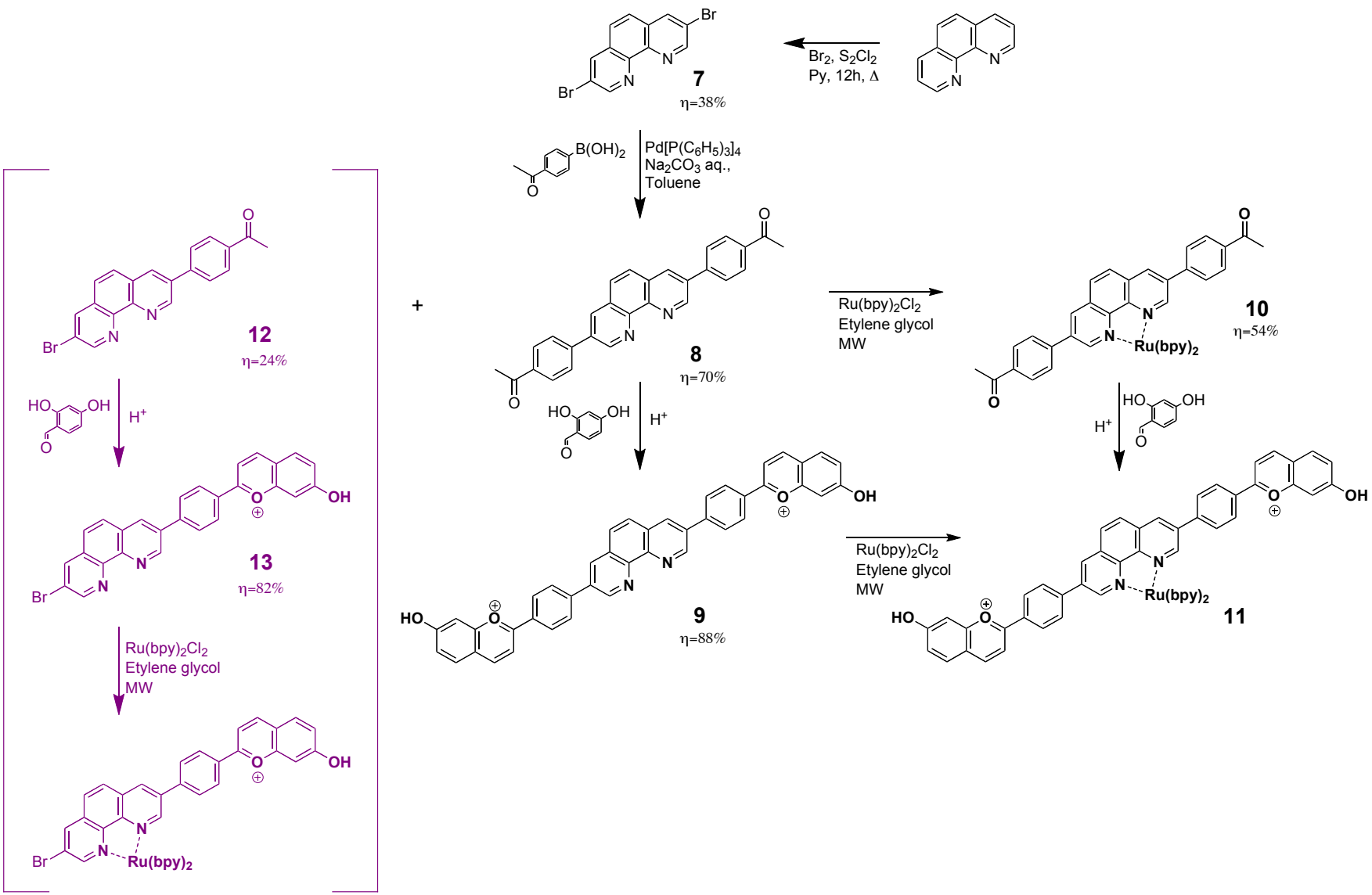


**Scheme IV.1 –** Synthetic path proposed to obtain complex 11

So the synthesis started with bromination of 1,10-phenantroline, which was treated with $Br_2$ in the presence of $S_2Cl_2$ and pyridine.[136]

The yields of compound **7** are usually low due to the *work-up* process but the compound can nevertheless be obtained in large quantities and high purity. Palladium-catalysed cross coupling between 3,8-dibromo-1,10-phenantroline (**7**) and 4-acetylboronic acid leads to 3,8-bis(4-acetylphenyl)-1,10-phenantroline (**8**). When extensive deaeration for oxygen removal and fresh Pd(0) are used the reaction goes smoothly also with high yields and excelent purity. Having obtained compound **8,** a simple aldol condensation under acidic conditions with any chosen salicylaldehyde would allow to obtain symmetric triad ligand**s** with two flavylium units. In this case and using the know-how of the group with this type of compounds, 2,4-dihydroxybenzaldehyde was chosen, originating 3,8-bis-(7-hydroxyflavylium)-1,10-phenanthroline, compound **9**. All the details for the synthesis and characterization can be found in the experimental part, page 97.

Prior to attempting the synthesis of metal complexes of **9**, the compound was studied in solution, see section IV.4 page 94.

The synthesis of the final complex **11** has proved to be more difficult than expected.

Initially microwave synthesis was tried by adding together compound **9** and $Ru(bpy)_2Cl_2$ in ethylene glycol. By TLC (thin layer chromatography) it was possible to observe the formation of new products even the ligand was not totally consumed. The product that formed shows an orange fluorescence, characteristic of polypyridine Ru(II) complexes. The problems arose during the purification process. Several purification procedures using silica gel, reversed phase silica, alumina and size exclusion chromatography were made, but even in the rare cases where a single spot was obtained the NMR showed poor purity and eventually no signals of the desired product. Several factors may explain these results, e.g., microwave degradation of the ligand or equilibria in solution originating several species with different abilities to form Ru(II) complexes. To overcome this last interference, the synthesis was attempted in the presence of catalytic amounts of a strong acid, since it helps dissolving the ligand and allows a better control of species in solution by shifting the multiequilibria system to the flavylium form. Several attempts were also made in the presence of $AgNO_3$ to help removing the chlorides through precipitation of AgCl and facilitate the complexation to Ru(II). Neither of these attempts led to the formation of the pure desired compound. Performing the same synthesis under milder conditions, by refluxing in DMF or ethanol had the same outcome.

From all the attempts carried out to obtain complex **11**, only the syntheses in DMF under reflux and in microwave oven with ethylene glycol showed an interesting pattern in NMR. In both cases, four different sets of pyridine protons were identified to which however no plausible justification could be found (see Supplementary Material, Page 122, Figure VI.19, complex **11**). From MALDI-TOF analysis only bipyridine fragments were identified.

Due to all the difficulties presented, the synthetic pathway to obtain compound **11** from compound **9** was left aside. It was decided to abandon the initial idea of synthesizing a triad ligand that could be used to form complexes with different metal ions, e.g., inert metal ions from groups 8-10, labile metal ions from groups 9-10 or lanthanide ions, and proceed with a synthetic strategy where an inert metal complex is initially formed and the flavylium/chalcone moieties are introduced in a second step.

A new synthetic route was pursued starting with compound **8**. Microwave synthesis was tried by adding together compound **8** and $Ru(bpy)_2Cl_2$ in ethylene glycol and after flash chromatography in $CH_3COCH_3$:$CH_3OH$:$H_2O$:$KNO_3$ (40:10:10:1) compound **10** was obtained. Pure crystals suitable for x-ray crystallography were obtained by recrystallization in a mixture of acetonitrile:diethyl ether.

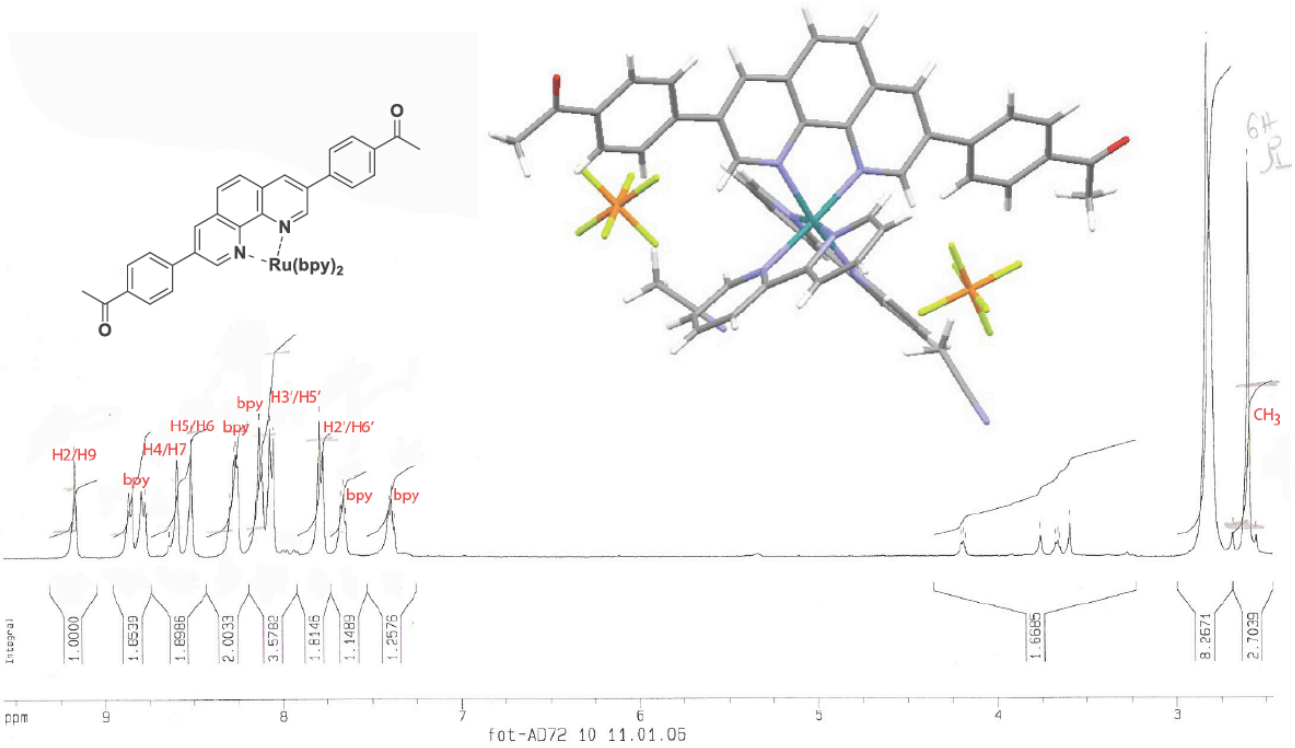


**Figure IV.1 –** NMR data and x-ray of compound [(3,8-Bis(p-oxophenyl-1,10-phenanthroline))$Ru(bpy)_2$]$(PF_6)_2$ **(10)**

Having obtained compound **10,** the synthesis of the final compound **11** was again attempted through aldol condensation with 2,4-dihydroxybenzaldehyde under acidic conditions. Previous tests were made in order to verify the stability of $Ru(bpy)_2Cl_2$ in extremely acidic conditions (10 M HCl), which proved to be stable.

This synthetic method is rather drastic and usually the compounds are obtained through precipitation. Any attempt of purification in this case is extremely difficult since flavylium purification is usually done by recrystallization and no pure compound could be obtained under these conditions.

But obtaining compound **10** does allow more than one synthetic pathway up to the final compound. Since no product could be obtained in acidic conditions, attempts were made in basic medium to obtain the chalcone. This method is more feasible because after neutralization the chalcones will be neutral and the overall charge is that of the Ru(II) complex facilitating purification.

An initial attempt was made by reacting compound **10** with 4-dimethylaminobenzaldehyde in ethanol and KOH at room temperature, Scheme IV.2. The product would not form a flavylium since the OH group in position 2 is missing but the success of the reaction would encourage to proceed with this strategy.

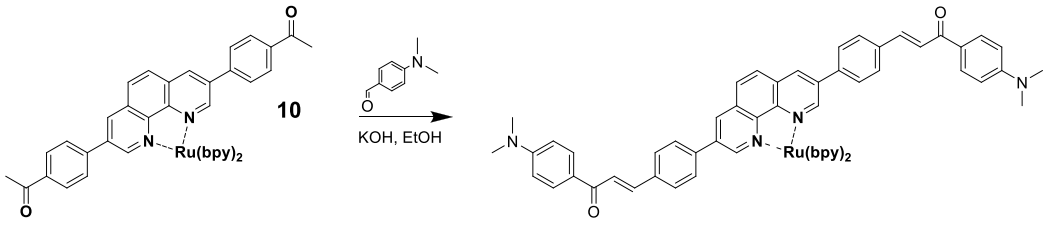


**Scheme IV.2 –** Synthesis of [(3,8-Bis-(E)-1-((4-(dimethylamino)phenyl)-3-phenylprop-2-en-1-one)-1,10-phenanthroline))$Ru(bpy)_2$] $(PF_6)_2$ or [(3,8-Bis-(4'- dimethylaminochalcone-1,10-phenanthroline))$Ru(bpy)_2$]$(PF_6)_2$

After flash chromatography the NMR was a good surprise, see Figure IV.2. It is clear the presence of news picks in comparison with the starting material in Figure IV.1.

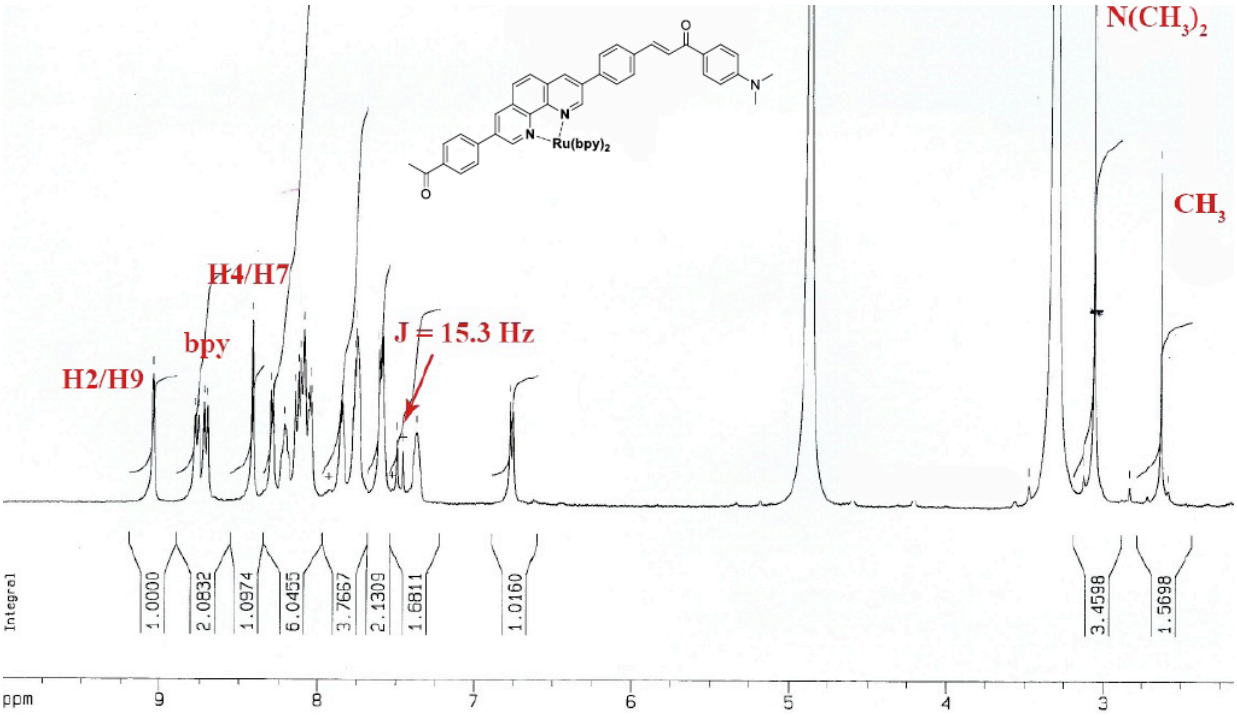


**Figure IV.2 –** NMR data obtained of compound [(3,8-Bis-(4'- dimethylaminochalcone-1,10-phenanthroline))$Ru(bpy)_2$]$(PF_6)_2$

Looking at high field the methyl singlet characteristic of acetophenone is easily identified even if the corresponding singlet of the dimethylamino group of the starting material is also present. But the most significant point is the presence of doublets with $J$ = 15.3 Hz, characteristic of the vicinal ($^3J$) coupling between two hydrogens in a trans double bond, indicating that the reaction occurred but was not complete (ca. 50% conversion was observed from NMR).

In the light of these results a similar experiment was carried out under the same conditions but in the presence of 2,4-dihydroxybenzaldehyde. Unfortunately, in this case, no product could be isolated.

Taking into account that the synthesis was effective in the absence of OH group in position 2, it was decided to proceed with the protection of the hydroxyl groups of benzaldehyde, initially with *p*-toluenesulfonic acid which was unsuccessful probably due to steric hindrance and finally with chloromethyl methyl ether (MOMCl). In both of these cases no product was obtained either in acidic or basic conditions. Regarding the acidic conditions some orange fluorescence was verified but the same problems in the purification were encountered. Under basic conditions no reaction occurred. MOMCl should not decompose either in extreme acid or basic conditions above 100ºC so it is unclear why the reaction did not occur.

Another new perspective was again searched for. If the problem is always the final step of synthesis, either flavylium/chalcone formation or metal complexation, would it be possible to covalently link the complex to the flavylium?

In Scheme IV.3 is depicted the synthetic path planned. Starting with compound **7** by microwave irradiation with $Ru(bpy)_2Cl_2$ in ethylene glycol, compound **14** was easily obtained in high yield.

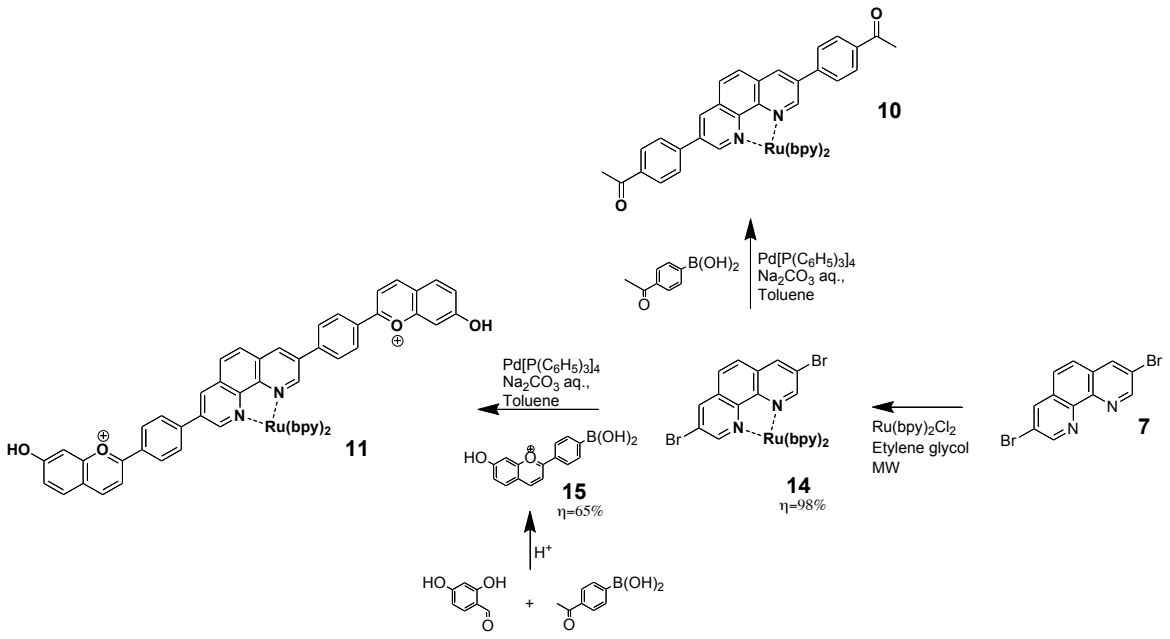


**Scheme IV.3 -** Synthetic path proposed to obtain complex **11**

Compound **15** was also easily obtained. Palladium-catalysed cross coupling in the same conditions as in previous cases between **14** and **15** should provide us with compound **11** but once again the reaction did not occur. The synthesis of **10** through **14** was to make sure that Suzuki coupling was possible with ruthenium complexes.

In parallel with all the reactions described it was also tried to obtain the dyad depicted in Scheme IV.1 in purple. Actually this synthetic pathway gave us a breakthrough. Not depicted in the scheme, but also tried was the formation of the ruthenium complex of compound **12**. This compound was obtained and after recrystallization, crystals were obtained suitable for x-ray crystallography, Figure IV.3.

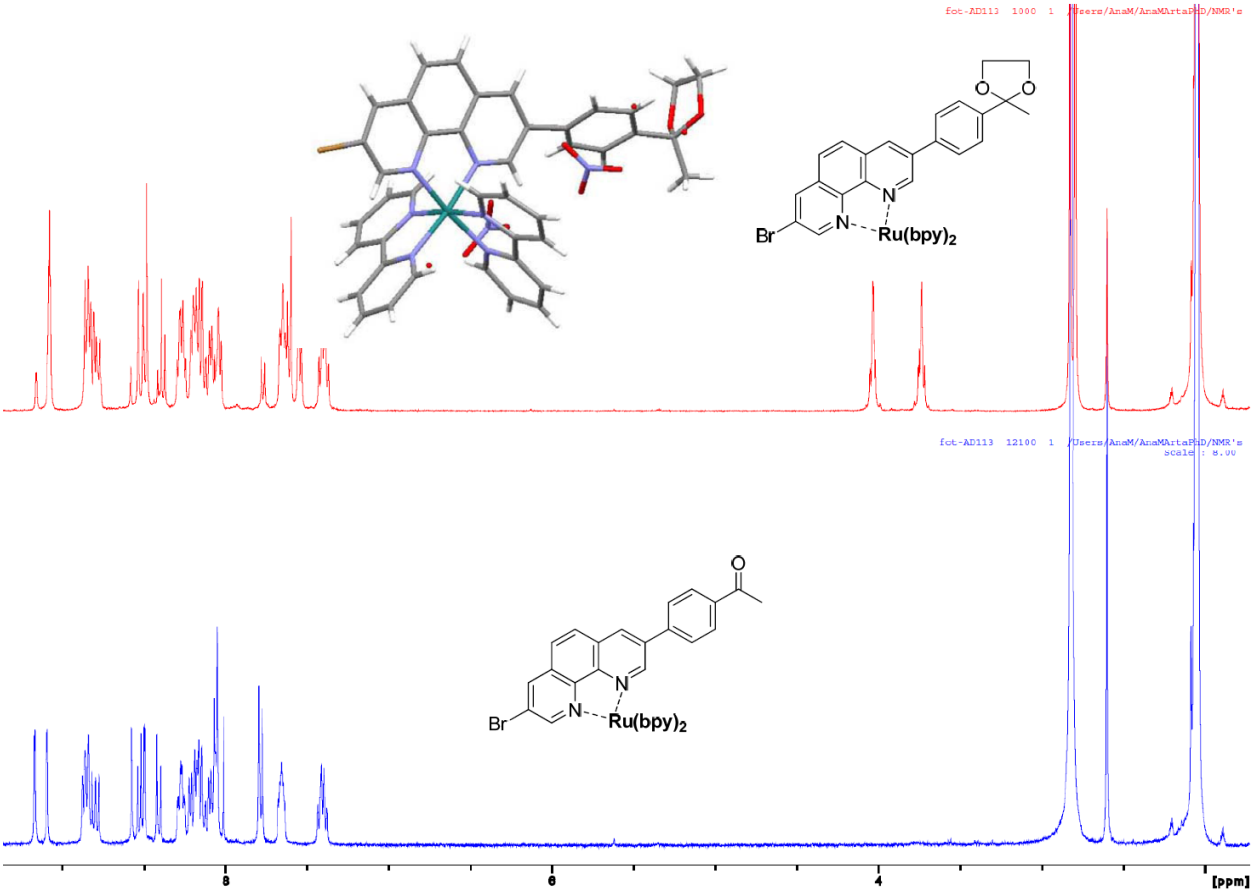


**Figure IV.3** -NMR data and x-ray of compound [(3-Bromo-8-p-oxophenyl -1,10-phenanthroline))$Ru(bpy)_2$]$(PF_6)_2$

Both $^1H$ NMR spectra's depicted are from the compound obtained. The main difference is around 4 ppm. In the red spectra there are two triplets corresponding to the ethylene group that is protecting the carbonyl that does not exist in the blue spectra. Initially those signals were thought to be an impurity but the x-ray structure showed the protection of the carbonyl group

after complex formation in the microwave in the presence of ethylene glycol. By deprotection of the carbonyl group in perchloric acid adsorbed on silica gel[133] the blue spectra is obtained.

This fact could be one of the reasons why no product formation was verified in some cases. All the $^{1}H$ NMR data obtained from the previous compounds were reviewed and the protection of the carbonyl group in the microwave reaction is not a rule, it probably depends on the microwave power used and on the reaction time. Nevertheless all the reactions were repeated with the same outcome.

## IV.3. 2,2'-Bipyridine as a building block

Like in the phenanthroline case, a synthetic strategy was chosen and is presented in Scheme IV.4. Initially there were two possibilities, by covalently linking the flavylium moiety to the bipyridine or synthesizing one flavylium with one pyridine and finally linking the pyridines covalently to obtain a disubstituted bipyridine. The first hypothesis was the one chosen.

Like in the viologen triad, the easiest way to covalently link the central unit to the acetophenone that allows the flavylium formation is by nucleophilic substitution. The reasoning in this case was the same with some mitigating circumstances. The objective was a reductive amination between an aminoacetophenone and 4,4'-diformyl-2,2'-bipyridine (compound **16**), a procedure described in the literature.[135]

By treating 4,4'-dimethyl-2,2'-bipyridine with Bredereck's reagent, 4,4'-dienamine-2,2'-bipyridine was obtained in high yields. The diformyl bipyridine (**16**) was then easily obtained by oxidative cleavage of the enamine groups by sodium periodate in aqueous THF also with high yield.[134]

Compound **17** also known as Hantzsch reagent was very important in the reductive amination step. Hantzsch dihydropyridine reduces imines to the corresponding amines in the presence of a catalytic amount of an acid and the reduction is completely selective to imines in the presence of aldehydes or ketones,[135] which was crucial to maintain the acetophenones intact for flavylium/chalcone formation.

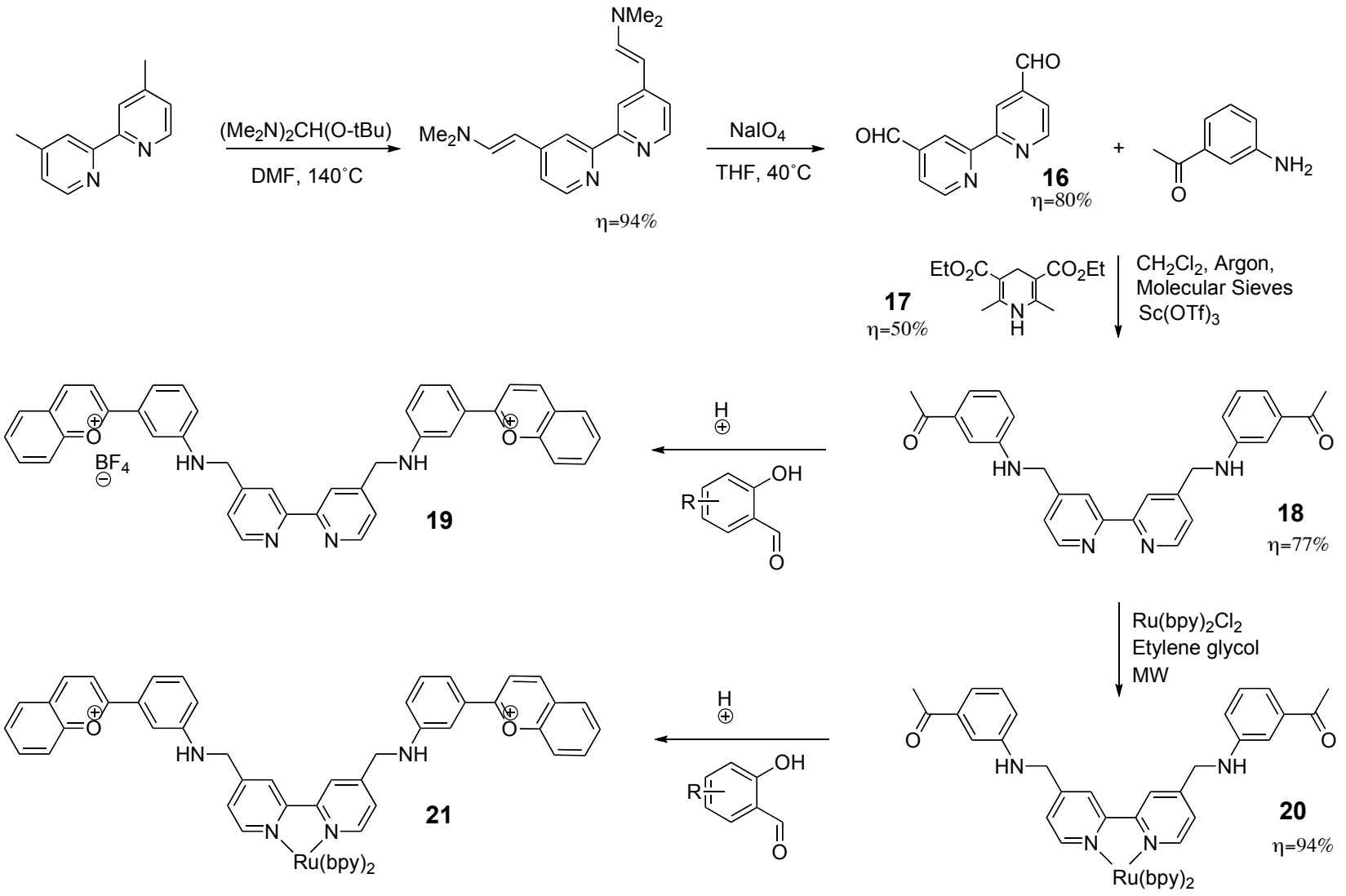


**Scheme IV.4 -** Synthetic path proposed to obtain complex **21**

The reductive amination was initially performed following a procedure described by Ohsawa *et al* [136] using the conditions described in Scheme IV.4 with 4,4 '-diformyl-2,2'-bipyridine, Hantzsch reagent and the 4-aminoacetophenone. After the work-up a yellow powder was obtained but the $^1$H-NMR reveals the presence of the 4-aminoacetophenone and the Hantzsch reagent in the reduced and oxidized form, all in different proportions. The fact that no reaction occurs with 4-aminoacetophenononone is due to the deactivation of the amino group by resonance effect. These syntheses only succeeded in the presence of 3-aminoacetophenone allowing to obtain compound **18** in high yield.

From compound **18** it should be straightforward to obtain the final ligand **19** but the reaction did not succeed either under acidic or basic conditions. In extreme acid conditions necessary to obtain the flavylium all the amino groups are protonated which probably deactivates de carbonyl group this time by inductive effect. In basic pH the solubility was the problem. Compound **18** was only soluble in organic solvents and the normal aqueous bases used to synthesize chalcones were immiscible. Several organic bases were tested but no product was formed.

Following the path to compound **20**, formation of the complex was easy and with high yield but once more the synthesis to obtain the supramolecular triad did not result.

## IV.4. The Reaction network of Ligand 9

### IV.4.1. *The reaction network*

The network of chemical reactions of ligand **9** was characterized following the same strategy as in the previous chapters and several thermodynamic constants were obtained by UV-Vis spectrophotometric titrations. Due to extreme problems in solubilisation the compound was previous dissolved in concentrated $HClO_4$ and only after the mother solution prepared. All prepared solutions were in buffered solutions in methanol with 10% $H_2O$.

The changes in absorption spectra taken 1 min after direct pH jumps from stock solutions of ligand **9** at pH= 0 ($AH^+$) to higher pH values are shown in Figs. IV.4A. The shape and position of the bands clearly indicate the formation of the quinoidal base allowing to calculate p$K_{a1}$= 1.9 and p$K_{a1}$= 3.5, Scheme I.5. Figure IV.4B shows the pH dependent absorption of the equilibrated solutions after 1 day in the dark, leading to p$K'_a$= 1.6. Taking into account that ligand **9** is constituted by two flavylium (7-hydroxyflavylium) covalently linked to phenanthroline it is possible to compare once again the thermodynamic constants obtained to their relative 7-hydroxyflavylium.

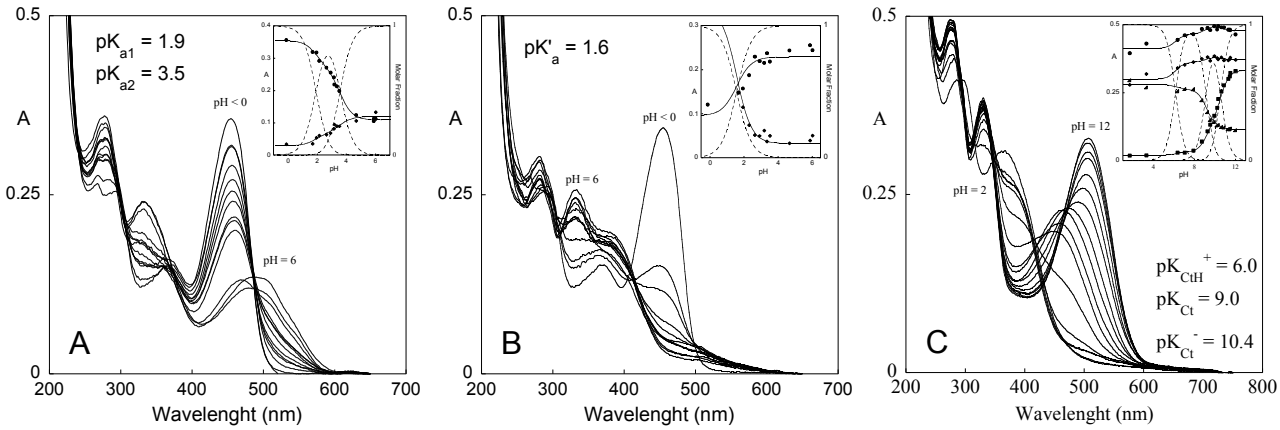


**Figure IV.4** - **A** – Spectral variations obtained immediately upon pH jumps from equilibrated solutions at pH=0 to higher values. **B**- Absorption spectra of dark equilibrated solution as function of pH. **C** - Spectral variations obtained immediately upon pH jumps from equilibrated solutions at pH=12 to lower pH's values. Inset's: Equilibrium distribution of the equilibrated species and molar fraction as a function of pH.

These values of p$K_a$=3.55 and p$K'_a$=2.70 for 7-hydroxyflavylium[118] compare with the ones obtained for ligand **9** of p$K_{a1}$= 1.9, p$K_{a1}$= 3.5 and p$K'_a$= 1.6. The p$K$a's of the flavylium moieties to form quinoidal bases are lower than usual, probably due to the stabilization by conjugation with the phenanthroline moiety. The global p$K$'a is also low showing that the phenanthroline moiety facilitates the hydration reactions.

The existence of two p$K_a$ as opposed the observed for triad **5** of the previous chapter is probably due to a higher communication between the two flavylium units influencing the p$K_a$ differing by more than one pH unit.[121]

Regarding the basic region formation of the ionized *trans*-chalcone $\mathbf{Ct}^{2-}$ is verified. This species can be titrated back to acidic pH, forming $\mathbf{Ct}^-$ and **Ct** with p$K_a$'s of 10.4 and 9.0 respectively, as shown in Fig. IV.4C. If the titration continues to more acidic pH values formation of $\mathbf{CtH}^+$ takes place with p$K_a$ of 6.0.

Unfortunately no kinetic information about the system was taken, but is possible to say that thermodynamically has the same behaviour as synthetic flavylium.

## IV.4.2. *Photochemistry*

As showed in the previous chapters chalcones can show efficient photoisomerization allowing exploring the compounds as photochromic systems. In this case a stock solution at pH = 1.9 was irradiated at 366 nm, Figure IV.5.

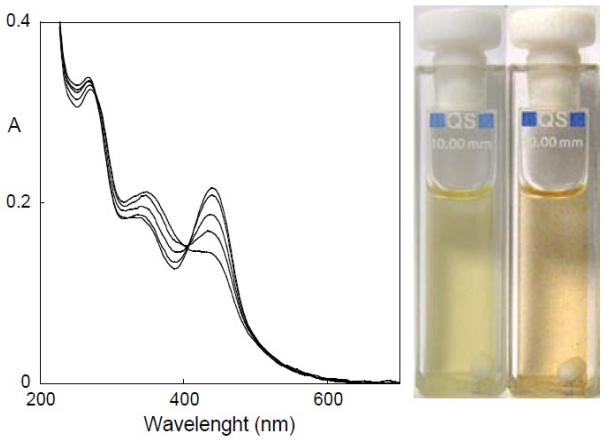


**Figure IV.5 -** Irradiation of an equilibrated solution at 366 nm, pH = 1.9

At this pH only a small amount of **AH**$^+$ is present and after irradiation is clear the conversion of **Ct** into **AH**$^+$. Despite not being an efficient system, orange colour was obtained being a mixture of the remaining *trans*-chalcone with the yellow of the flavylium.

## IV.4.3. *Conclusions*

Preliminary studies shows that the supramolecular system containing two flavylium moieties linked through a phenanthroline keep their usual reaction network, addressable through pH jumps and light. In the Figure IV.6 are depicted the absorption spectra of the Ru(Phen)(bpy) –black-, Ru(Phen)(acetophenone)(bpy) or compound **8** – red– the ligand **9** – orange – and the obtained crude for complex **11** – brown.

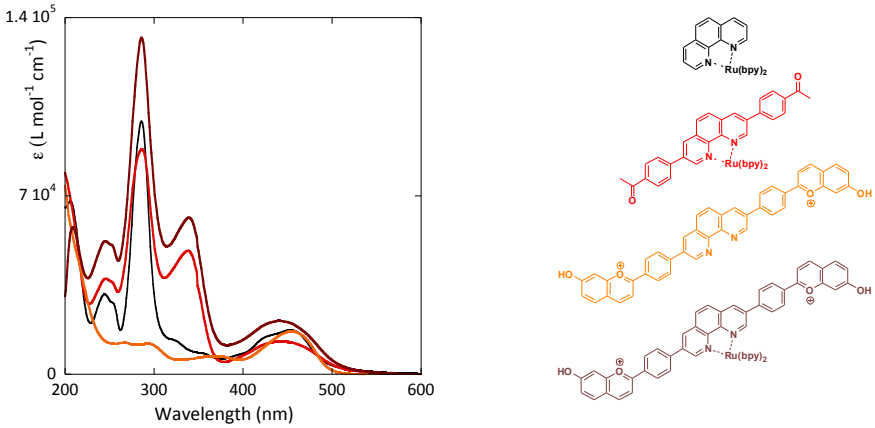


**Figure IV.6 –** Absorption spectra and corresponding molecules

It can be seen the contribution of every moiety in the construction of the supramolecular triad. From the H-NMR of **11** it was not possible to confirm if the desired compound was in fact obtained. By observing the absorption spectra, it would be expected a higher contribution of the flavylium moieties on the triad **11**, and a red shift of the band at 450 nm when the pH is increased. Since none of the referred phenomena were registered, further insight on the chemical/ photochemical and photophysical studies are expected in the short term in order to more accurately determine whether or not the synthesis was successful and to explain the overall processes.

## IV.5. Experimental Part

All reagents and solvents used were of analytical grade. NMR spectra were run on a Bruker AMX 400 instrument operating at 400.13 MHz ($^{1}H$) and 100.00 MHz ($^{13}C$). COSY, HMQC, HMBC and eventually NOESY spectra were run on each sample to allow full assignment of the NMR peaks.[127] NMR numeration for the complexes followed Yitzhak Tor *et al.*[137] Mass spectra were run on Micromass GCT apparatus for EI and FD ionization and on an Applied Biosystems Voyager-DE™ PRO for MALDI. Elemental analyses were obtained on a Thermofinnigan Flash EA 1112 Series instrument.

### IV.5.1. Synthesis of 3,8-dibromo-1,10-phenanthroline

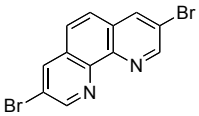


3,8-dibromo-1,10-phenanthroline was prepared according to a procedure adapted from Sauvage *et al*[138]. A stirred 1-chlorobutane solution containing 1,10-Phenanthroline-hydrochloride monohydrate (23 mmol, 4.56 g), $S_2Cl_2$ (75.4 mmol, 6.03 mL), pyridine (74.3 mmol, 5.9 mL) and $Br_2$ (72.5 mmol, 3.7 mL) was refluxed for 15h. After cooling to room temperature, the solid formed was separated, and an aqueous solution of NaOH and $CHCl_3$ was added to the solid. The $CHCl_3$ solution was separated and purified by column chromatography ($SiO_2$, chloroform). Recrystallization over 1,2-dichloroethane yield 3.05 g (9 mmol, 39%) of 3,8-dibromo-1,10-phenanthroline. **$^{1}$H-RMN** ($CDCl_3$, 400.13 MHz) δ (ppm): 9.17 (2H, s, $H_2$, $H_9$), 8.39 (s, 2H, $H_4$, $H_7$), 7.74 (s, 2H, $H_5$, $H_6$).

## IV.5.2. Synthesis of 3,8-Bis(p-oxophenyl) - 1,10 -phenanthroline

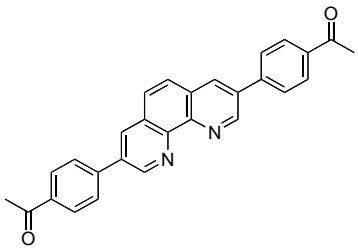

3,8-bis(p-oxophenyl)-1,10-phenanthroline was prepared according to a procedure adapted from Sauvage *et al.*[139] A degassed solution of $Na_2CO_3$ (2M, 50 mL) and subsequently a degassed solution of the 4-acetylphenyl boronic acid (10.2 mmol, 1.67 g) in a $C_6H_5CH_3/CH_3OH$ (60/10, 15 mL) were added to a degassed solution of 3,8-dibromo-1,10-phenanthroline (4.76 mmol, 1.6 g) and $Pd(PPh_3)_4$ (47.6 mmol, 0.55 g) in toluene (86 mL). After 24h under reflux, the reaction mixture was cooled to room temperature during which process, a precipitated appeared. This was filtered on a sintered disk funnel (porosity 4) and washed with cold toluene. Fast filtration over alumina ($CHCl_3$ as eluent) gave 1.38 g (3.31 mmol) of 3,8-bis(p-oxophenyl)-1,10-phenanthroline in 69.5 % yield. **$^1$H-NMR** ($CDCl_3$, 400.13 MHz) δ (ppm): 9.48 (2H, d, $H_2$, $H_9$, $^4J_{H2\text{-}H4,\ H9\text{-}H7}$ = 1.6 Hz), 8.48 (2H, d, $H_4$, $H_7$, $^4J_{H4\text{-}H2,\ H7\text{-}H9}$ = 1.6 Hz), 8.16 (2H, d, $H_{2'}$, $H_{6'}$, $^3J_{H2'\text{-}H3',\ H6'\text{-}H5'}$ = 8.0 Hz), 7.95 (2H, s, $H_5$, $H_6$), 7.91 (2H, d, $H_{3'}$, $H_{5'}$, $^3J_{H2'\text{-}H3',\ H6'\text{-}H5'}$ = 8.0 Hz), 2.69 (6 H, s, $CH_3$). **$^{13}$C-RMN** ($CD_3OD$, 100.62 MHz) δ (ppm): 149.4, 136.8, 133.9, 129.3, 128.6, 127.7, 127.4, 26.8 ($CH_3$). **MS-MALDI/TOF+**: *m/z*: calcd (%) for $C_{28}H_{20}N_2O_2^+$: 416.15 (100); found: 417.18 $[M+H]^+$ (97); 439.16 $[M+Na]^+$(20). **ESI-MS**: *m/z*: calcd (%) for $C_{28}H_{20}N_2O_2^+$: 416 (100); found: 417.3 $[M+H]^+$ (97); 439.2 $[M+Na]^+$(40).

## IV.5.3. Synthesis of (3-Bromo-8-p-oxophenyl)-1,10-phenanthroline

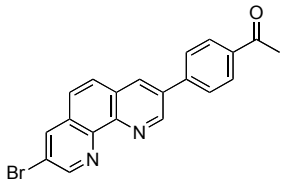

(3-Bromo-8-*p*-oxophenyl)-1,10-phenanthroline was prepared according to a procedure adapted from Sauvage *et al.*[139] A degassed solution of $Na_2CO_3$ (2M, 50 mL) and subsequently a degassed solution of the 4-acetylphenyl boronic acid (4.76 mmol, 0.78 g) in a $C_6H_5CH_3/CH_3OH$ (60/10, 7 mL) were added to a degassed solution of 3,8-dibromo-1,10-phenanthroline (4.76 mmol, 1.6 g) and $Pd(PPh_3)_4$ (47.6 mmol, 0.55 g) in toluene (86 mL). After 24h under reflux, the reaction mixture was cooled to room temperature during which process, a precipitated appeared. This was filtered on a sintered disk funnel (porosity 4) and washed with cold toluene. Fast filtration over alumina ($CHCl_3$ as eluent) gave 670 mg (1.78 mmol) of (3-Bromo-8-*p*-oxophenyl)-1,10-phenanthroline in 37.5 % yield. **$^1$H-NMR** ($CDCl_3$, 400.13 MHz) δ (ppm): 9.43 (1H, s, $H_2$), 9.19 (1H, s, $H_9$), 8.43 (2H, d, $H_4$, $H_7$, $^4J_{H4\text{-}H2,\ H7\text{-}H9}$ = 1.6 Hz), 8.13 (2H, d, $H_{2'}$, $H_{6'}$, $^3J_{H2'\text{-}H3',\ H6'\text{-}H5'}$ = 7.5 Hz), 7.88 (2H, d, $H_{3'}$, $H_{5'}$, $^3J_{H3'\text{-}H2',\ H5'\text{-}H6'}$ = 7.5 Hz), 7.76 (2H, d, $H_5$, $H_6$, $^3J_{H5\text{-}H6}$ = 8.6 Hz), 2.69 (6 H, s, $CH_3$). **$^{13}$C-RMN** ($CDCl_3$, 100.62 MHz) δ (ppm): 197.4

(C=O), 151.4 ($C_9$), 149.4 ($C_2$), 145.4, 144.4, 141.7, 137.5 ($C_7$), 136.7, 134.8, 133.8 ($C_4$), 129.8, 129.2 ($C_{2'}$, $C_{6'}$), 128.3, 127.9, 127.6 ($C_{3'}$, $C_{5'}$), 126.1 ($C_5$, $C_6$), 26.6 ($CH_3$).

## IV.5.4. Synthesis of 3,8-Bis-(7-hydroxiflavylium)-1,10-phenanthroline perchlorate

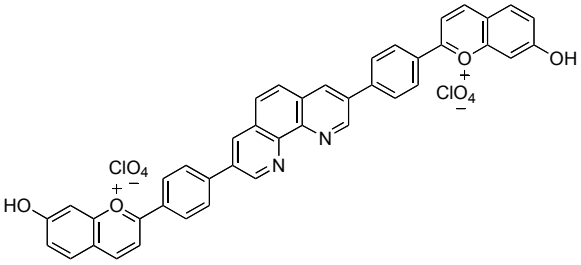


3,8-Bis(7-dihydroxiflavylium)-1,10-phenanthroline perchlorate was prepared according to a procedure adapted from Katritzky.[116] 2,4-dihydroxybenzaldehyde (0.58 mmol, 80 mg) and 3,8-bis(p-oxophenyl)-1,10-phenanthroline (0.28 mmol, 115 mg) was dissolved in 10 ml of acetic acid and 3 ml of $HClO_4$. The reaction mixture was stirred overnight in reflux. By the following day diethyl ether was added and a red solid precipitated, was filtered off and carefully washed with diethyl ether and dried yielding 199 mg (0.42 mmol, 87.7%) of 3,8-Bis(7-dihydroxiflavylium)-1,10-phenanthroline perchlorate. **$^1$H-NMR** (DCl /DMSO, pD≈1.0, 400.13 MHz) δ (ppm): 9.78 (2H, s, $H_2$, $H_9$), 9.65 (2H, s, $H_4$, $H_7$), 8.68 (2H, s, $H_5$, $H_6$), 8.23 (8H, s, $H_{2f'}$, $H_{3f'}$, $H_{5f'}$, $H_{6f'}$), 7.99 (2H, d, $H_{4f}$, $^3J_{H4f\text{-}H3f}$ = 7.0 Hz), 7.86 (4H, m, $H_{3f}$, $H_{5f}$), 6.47 (2H, s, $H_8$), 6.34 (2H, d, $H_6$, $^3J_{H6f\text{-}H5f}$ = 8.2 Hz). **MS-MALDI/TOF+**: *m/z*: calcd (%) for $[C_{42}H_{26}N_2O_4]^{2+}$: 311.09 (100); found: 200.18 $[M\text{-}C_{15}H_{11}O_2]^{2+}$ (72); 401.18 $2[M\text{-}C_{15}H_{11}O_2]^{2+}$ (15); 519 $[C_{35}H_{23}N_2O_3]^+$ (23). **ESI-MS**: *m/z*: calcd (%) for $[C_{42}H_{26}N_2O_4]^{2+}$: 311.09 (100); found: 311.2 $[M]^{2+}$ (100); 621.5 $[2M]^+$ (33); 519 $[C_{35}H_{23}N_2O_3]^+$ (30).

## IV.5.5. Synthesis of [(3,8-dibromo-1,10-phenanthroline)Ru(bpy)$_2$](PF$_6$)$_2$

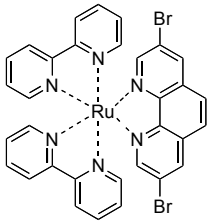


A mixture of 3,8-dibromo-1,10-phenanthroline (1.54 mmol, 520 mg) and $Ru(bpy)_2Cl_2$ (1.54 mmol, 0.79 g) in 40 mL of ethylene glycol was refluxed in a microwave for 2 min. After total consumption verified by TLC (eluent: $CH_3COCH_3$:$CH_3OH$:$H_2O$:$KNO_3$, 40:10:10:1) ethylene glycol was removed by distillation at reduced pressure. The mixture was dissolve in water and 1.2 g $NH_4PF_6$ was added to precipitate the orange complex, which was subsequently filtered off, rinsed with diethyl ether, and dried, yielding 1.58 g (1.52 mmol, 98%) of [(3,8-dibromo-1,10-phenanthroline)Ru(bpy)$_2$](PF$_6$)$_2$.**$^1$H-NMR** ($CD_3COCD_3$, 400.13 MHz) δ (ppm): 9.07 (2H, s, $H_{2Phen}$, $H_{9Phen}$), 8.83 (2H, d, $H_{6'bpy}$, $^3J_{H6'bpy\text{-}H5'bpy}$ = 8.1 Hz), 8.79 (2H, d, $H_{6bpy}$, $^3J_{H6bpy\text{-}H5bpy}$ = 8.1 Hz), 8.48 (2H, s, $H_{4Phen}$, $H_{7Phen}$), 8.40 (2H, s, $H_{5Phen}$, $H_{6Phen}$), 8.25 (2H, t, $H_{5'bpy}$, $^3J_{H5'bpy\text{-}H6'bpy}$ = 8.1 Hz, $^3J_{H5'bpy\text{-}H4bpy}$ = 6.2 Hz), 8.16 (2H, t, $H_{5bpy}$, $^3J_{H5bpy\text{-}H6bpy}$ = 8.1 Hz, $^3J_{H5bpy\text{-}H4bpy}$ = 6.2 Hz), 8.12

(2H, d, $H_{\alpha\ bpy}$, $^3J_{H\alpha\ bpy\text{-}H\beta\ bpy}$ = 6.0 Hz), 8.01 (2H, d, $H_{\alpha\ bpy}$, $^3J_{H\alpha\ bpy\text{-}H\beta\ bpy}$ = 6.0 Hz), 7.63 (2H, t, $H_{\beta\ bpy}$, $^3J_{H\beta\ bpy\text{-}H\delta\ bpy}$ = 6.0 Hz, $^3J_{H\beta\ bpy\text{-}H\delta\ bpy}$ = 6.2 Hz), 7.39 (2H, t, $H_{\beta\ bpy}$, $^3J_{H\beta\ bpy\text{-}H\delta\ bpy}$ = 6.0 Hz, $^3J_{H\beta\ bpy\text{-}H\delta\ bpy}$ = 6.2 Hz). **$^{13}$C-NMR** ($CD_3COCD_3$, 100.62 MHz) δ (ppm): 158.5, 158.1 ($C_{15}$), 154.7 ($C_4$, $C_7$), 153.4, 153.1 ($C_{10}$), 147.2, 140.0 ($C_2$, $C_9$), 139.3, 139.2 (C12), 132.6 ($C_6$-C-$C_7$), 129.5 ($C_6$, $C_3$), 128.8, 128.6 ($C_{11}$), 125.4 ($C_{13}$), 121.9 (C-Br). **MS-MALDI/TOF+**: *m/z*: calcd (%) for $[C_{32}H_{22}Br_2N_6Ru]^{2+}$: 376.0 (100); found: 413.02 2$[Ru(bpy)_2]^{2+}$ (100); 594.84 2$[M\text{-}bpy]^{2+}$ (98).

## IV.5.6. Synthesis of [((3-Bromo-8-p-oxophenyl)-1,10-phenanthroline)Ru(bpy)$_2$] $(PF_6)_2$

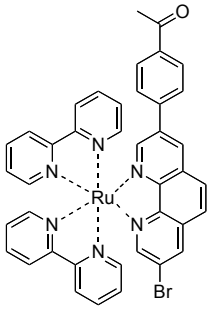


A mixture of (3-Bromo-8-*p*-oxophenyl)-1,10-phenanthroline (0.26 mmol, 100 mg) and $Ru(bpy)_2Cl_2$ (0.26 mmol, 0.14 g) in 10 mL of ethylene glycol was refluxed in a microwave for 2 min. After total consumption verified by TLC (eluent: $CH_3COCH_3$:$CH_3OH$:$H_2O$:$KNO_3$, 40:10:10:1) ethylene glycol was removed by distillation at reduced pressure. The mixture was dissolved in water and an excess of $NH_4PF_6$ was added to precipitate the orange complex, which was subsequently filtered off, rinsed with diethyl ether, and dried. After flash chromatography (Silica gel 60, $CH_3COCH_3$:$CH_3OH$:$H_2O$: $KNO_3$, 40:10:10:1), 0.27 g of [((3-Bromo-8-*p*-oxophenyl)-1,10-phenanthroline) $Ru(bpy)_2$]$(PF_6)_2$ were obtained yielding (0.25 mmol, 93%) **$^1$H-NMR** ($CD_3COCD_3$, 400.13 MHz) δ (ppm): 9.17 (1H, d, $H_{2Phen}$, $^4J_{H2Phen\ –\ H4Phen}$ = 1.7 Hz), 9.09 (1H, d, $H_{9Phen}$, $^4J_{H9Phen\ –\ H7Phen}$ = 1.8 Hz,), 8.81 (4H, m, $H_{\gamma bpy}$), 8.57 (1H, d, $H_{4Phen}$, $^4J_{H4Phen\ –\ H2Phen}$ = 1.7 Hz), 8.52 (1H, d, $H_{5Phen}$, $^3J_{H5Phen\ –\ H6Phen}$ = 8.9 Hz), 8.49 (1H, d, $H_{7Phen}$, $^4J_{H7Phen\ –\ H9Phen}$ = 1.8 Hz), 8.41 (1H, d, $H_{6Phen}$, $^3J_{H6Phen\ –\ H5Phen}$ = 8.9 Hz), 8.29 – 8.22 (2H, m, $H_{\delta\ bpy}$), 8.21 (1H, d, $H_{\alpha\ bpy}$, $^3J_{H\alpha\ bpy\text{-}H\beta\ bpy}$ = 5.5 Hz), 8.18 – 8.14 (3H, dd, 2$H_{\alpha\ bpy}$, 1$H_{\delta\ bpy}$), 8.09 (1H, d, $H_{\alpha\ bpy}$, $^3J_{H\alpha\ bpy\text{-}H\beta\ bpy}$ = 5.5 Hz), 8.07 – 8.04 (3H, m, $H_{2'}$, $H_{6'}$, $H_{\delta\ bpy}$), 7.78 (2H, d, $H_{3'}$, $H_{5'}$, $^3J_{H3'\text{-}H2',\ H5'\text{-}H6'}$ = 8.4 Hz), 7.67 – 7.63 (2H, m, $H_{\beta\ bpy}$), 7.40 (2H, dd, $H_{\beta\ bpy}$), 2.60 (3H, s, $CH_3$). **$^{13}$C-NMR** ($CD_3COCD_3$, 100.62 MHz) δ (ppm): 158.5, 154.3 ($C_{7Phen}$), 153.5, 153.4 ($C_{\alpha\ bpy}$), 153.2 ($C_{\alpha\ bpy}$), 152.2 ($C_{4Phen}$), 139.9, 139.1 ($C_{9Phen}$), 138.9 ($C_{\delta\ bpy}$), 135.9 ($C_{2Phen}$), 130.5, 129.9, 128.8 ($C_{3'}$, $C_{5'}$), 128.7 ($H_{6Phen}$), 128.6 ($H_{5Phen}$), 128.5 ($C_{\beta\ bpy}$), 125.4 ($C_{\gamma bpy}$), 23.2 (**C**H3).

## IV.5.7. Synthesis of [((3,8-Bis(p-oxophenyl-1,10-phenanthroline)Ru(bpy)$_2$](PF$_6$)$_2$

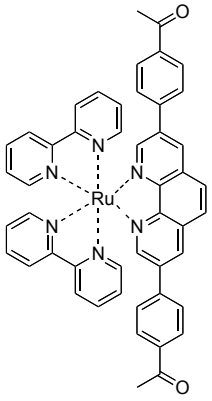

[(3,8-Bis(p-oxophenyl-1,10-phenanthroline))Ru(bpy)$_2$](PF$_6$)$_2$ was prepared according to a procedure adapted from Sauvage *et al.*[139] A degassed solution of $Na_2CO_3$ (2M, 5.1 mL) and subsequently a degassed solution of the 4-acetylphenyl boronic acid (0.96 mmol, 0.16 g) in a $C_6H_5CH_3/CH_3OH$ (60/10, 1.5 mL) were added to a degassed solution of [(3,8-dibromo-1,10-phenanthroline)Ru(bpy)$_2$](PF$_6$)$_2$ (0.48 mmol, 0.5 g) and Pd(PPh$_3$)$_4$ (0.048 mmol, 0.054 g) in toluene (10 mL). After 24h under reflux, the reaction mixture was cooled to room temperature during which process, a precipitated appeared. This was filtered on a sintered disk funnel (porosity 4) and washed with cold toluene. The residue was purified by flash chromatography in $CH_3COCH_3$:$CH_3OH$:$H_2O$:$KNO_3$ (40:10:10:1) to yield 0.29 g (0.26 mmol, 54%) of [(3,8-Bis(*p*-oxophenyl-1,10-phenanthroline))]Ru(bpy)$_2$(PF$_6$)$_2$. **$^1$H-NMR** ($CD_3COCD_3$, 400.13 MHz) δ (ppm): 9.17 (2H, s, $H_{2Phen}$, $H_{9Phen}$), 8.86 (2H, d, $H_{\gamma bpy}$, $^3J_{H\gamma bpy\text{-}H\delta bpy}$ = 7.8 Hz), 8.79 (2H, d, $H_{\gamma bpy}$, $^3J_{H\gamma bpy\text{-}H\delta bpy}$ = 7.5 Hz), 8.59 (2H, s, $H_{4Phen}$, $H_{7Phen}$), 8.51 (2H, s, $H_{5Phen}$, $H_{6Phen}$), 8.27 (2H, m, $H_{\delta bpy}$), 8.13 (4H, d, $H_{\alpha bpy}$, $^3J_{H\alpha bpy\text{-}H\beta bpy}$ = 6.7 Hz), 8.06 (4H, d, 2H$_{3'}$, 2H$_{5'}$, $^3J_{H3'\text{-}H2',\ H5'\text{-}H6'}$ = 8.1 Hz), 7.79 (2H, d, 2H$_{2'}$, 2H$_{6'}$, $^3J_{H2'\text{-}H3',\ H6'\text{-}H5'}$ = 8.1 Hz), 7.66 (2H, t, $H_{\beta bpy}$), 7.39 (2H, t, $H_{\beta bpy}$), 2.55 (6H, s, $CH_3$). **$^{13}$C-RMN** ($CD_3COCD_3$, 100,62 MHz) δ (ppm): 197.4, 158.6, 158.1, 153.3 ($C_{\beta bpy}$, $C_{\gamma bpy}$), 151.9 ($C_{4Phen}$, $C_{7Phen}$), 147.7, 140.48, 139.0, 138.8, 138.7, 138.4, 135.8 ($C_{2Phen}$, $C_{9Phen}$), 132.0, 129.9 ($C_{3'}$, $C_{5'}$), 129.7 ($C_{5Phen}$, $C_{6Phen}$), 128.7 ($C_{2'}$, $C_{6'}$), 128.6 ($C_{\delta}$), 125.3 ($C_{\alpha}$), 26.8 (**C**H3). **MS-MALDI/TOF+**: *m/z*: calcd (%) for $[C_{48}H_{36}N_6O_2Ru]^{2+}$: 415.09 (100); found: 413.07 $[M\text{-}2H]^{2+}$ (85); 673.18 $[M\text{-}bpyH]^{2+}$ (100).

## IV.5.8. Synthesis of 4'-boronic acid-7-hydroxyflavylium hydrogensulphate

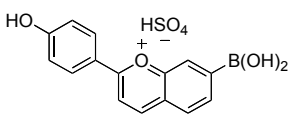

4'-boronic acid-7-hydroxyflavylium hydrogensulphate was prepared according to a procedure adapted from Katritzky.[116] 2,4-dihydroxybenzaldehyde (1.45 mmol, 200 mg) and 4-acetylphenyl boronic acid (1.45 mmol, 237 mg) were dissolved in 10 ml of acetic acid and 2 ml of $H_2SO_4$. The reaction mixture was stirred overnight in reflux. By the following day diethyl ether was added and a red solid precipitated, was filtered off and carefully washed with diethyl ether and dried yielding 339 mg (0.93 mmol, 64.3%) of 4'-boronic acid-7-hydroxyflavylium hydrogensulphate. **$^1$H-NMR** (DCl /$CD_3OD$, pD≈1.0, 400.13 MHz) δ (ppm): 8.07 (1H, d, $H_{4,}$ $^3J_{H4\ H3}$ = 8.4 Hz), 7.28 (1H, d, $H_{3,}$ $^3J_{H3\ H4}$ = 8.5 Hz), 7.17 (2H, d, $H_{2'6',}$ $^3J_{H2',H6'\text{-}\ H3',H5'}$ = 8.4 Hz),

7.03 (1H, d, $H_{5,}$ $^{3}J_{H5\ H6}$ = 9.0 Hz), 6.79 (2H, d, $H_{3'5',}$ $^{3}J_{H3',H5'-\ H2',H6'}$ = 8.4 Hz), 6.37 (1H, d, $H_{8,}$ $^{3}J_{H6\ H5}$ = 1.9 Hz), 6.26 (1H, d, $H_{6,}$ $^{3}J_{H6\ H5}$ = 9.0 Hz, $^{3}J_{H6\ H8}$ = 2.0 Hz).

## IV.5.9. Synthesis of 4,4'-dienamine-2,2'-bipyridine

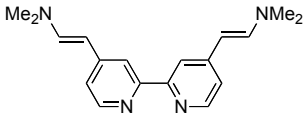


4,4'-dienamine-2,2'-bipyridine was prepared according to a procedure adapted from Bozec *et al.*[134] In a typical reaction, a degassed solution of 4,4'-dimethyl-2,2'-bipyridine (1 g, 5.4 mmol) and tert-butoxybis(dimethylamino)methane (4.7 ml, 22.7 mmol) in dry DMF (5 ml) was heated under argon for 18 h. The reaction mixture was cooled to RT and water (50 ml) was added. The mixture was then extracted with dichloromethane (5 x 15 ml). The organic layers were dried over $MgSO_4$, concentrated in vacuum and precipitated by adding $Et_2O$ to give pure 4,4'-dienamine-2,2'-bipyridine as a yellow powder yielding 1.49 g (5.1 mmol, 94%). **$^{1}$H-NMR** ($CDCl_3$, 400.13 MHz) δ (ppm): 8.33 (2H, d, $H_{6bpy,}$ $^{4}J_{H6bpy\ -H5bpy}$ = 5.2 Hz), 8.13 (2H, s, $H_{3bpy}$), 7.24 (d, 2H, $H_{\alpha,}$ $^{3}J_{H\alpha-H\beta}$ = 14 Hz), 6.94 (2H, d, $H_{5bpy,}$ $^{3}J_{H5bpy\ -H6bpy}$ = 5.1 Hz), 5.08 (2H, d, $H_{\beta,}$ $^{3}J_{H\beta-H\alpha}$ = 14 Hz), 2.88 (6H, s, $NMe_2$).

## IV.5.10. Synthesis of 4,4'-diformyl-2,2'-bipyridine

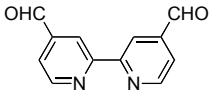


4,4'-diformyl-2,2'-bipyridine was prepared according to a procedure adapted from Bozec *et al.*[134] In a typical reaction, 4,4'-dienamine-2,2'-bipyridine (1.4 g, 4.75 mmol) was dissolved in THF. An aqueous solution of $NaIO_4$ (7.9 g, 37.1 mmol) was added dropwise at RT and the reaction mixture was stirred for 18 h. The insolubles were removed by filtration and washed with THF. The solvent was evaporated in vacuum and dichloromethane (60 ml) was added. The organic layer was washed with saturated $NaHCO_3$ solution (3 x 20 ml), dried over $MgSO_4$ and then evaporated to dryness to give pure 4,4'-diformyl-2,2'-bipyridine as a white powder yielding 0.8 g (3.78 mmol, 80 %). **$^{1}$H-NMR** ($CDCl_3$, 400.13 MHz) δ (ppm): 10.2 (2H, s, CHO), 8.96 (2H, d, $H_{6bpy,}$ $^{3}J_{H6bpy\ -H5bpy}$ = 4 Hz), 8.893 (2H, s, $H_{3bpy}$), 7.79 (d, 2H, $H_{5bpy,}$ $^{3}J_{H5bpy\ -H6bpy}$ = 4 Hz).

## IV.5.11. Synthesis of Hantzsch 1,4-DHP

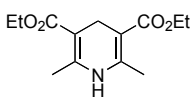


Diethyl-2,6-dimethyl-1,4-dihydropyridine-3,5-dicarboxylate (Hantzsch 1,4-DHP) was prepared according to a procedure from Perumal *et al.*[140,141] A mixture of formaldehyde (2mL, 54.3 mmol), ethyl acetoacetate (9.18 mL, 72.6 mmol) and ammonium hydroxide (3.77 mL, 96.8 mmol) in 5 mL of ethanol were refluxed in a microwave for 1 min to an output power of 400 W. The reaction mixture was cooled to room temperature

during which process, a precipitated appeared. This was filtered on a sintered disk funnel (porosity 4) and washed with pet-ether. Diethyl-2,6-dimethyl-1,4-dihydropyridine-3,5-dicarboxylate was obtained as a yellow solid yielding 6.83 g (27 mmol, 50%). **$^1$H-NMR** ($CDCl_3$, 400.13 MHz) δ (ppm): 4.91 (1H, s, NH), 4.18 (4H, d, $H_2$, $^3J_{H2-H1}$ = 6.9 Hz), 3.24 (2H, s, $H_4$), 2.17 (6H, s, $H_3$), 1.26 (6H, t, $H_1$, $^3J_{H1-H2}$ = 6.9 Hz).

## IV.5.12. 4,4'-Tri-[*N,N'*-(3-methylamino)acetophenone]-2,2'-bipyridine

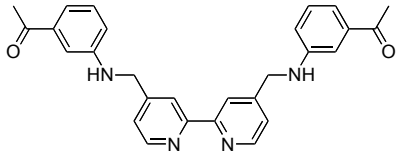

4,4'- Tri-[*N,N'*-(3-methylamino)acetophenone]-2,2'-bipyridine was prepared according to a procedure adapted from Ohsawa *et al.*[136] In a typical reaction, to a degassed solution of 4,4'-diformyl-2,2'-bipyridine (1.5 g, 7.07 mmol), 3-aminoacetophenone (2.29 g, 16.9 mmol), Hantzsch reagent (4.3 g, 16.9 mmol) and $Sc(OTf)_3$ (69.6 mg, 0.14 mmol) in dry THF (90 ml) were allowed to react at RT under argon for 24 h. After AcOEt was added, the mixture was washed with 5% aqueous $Na_2CO_3$ solution and brine. The organic layers were dried over $MgSO_4$ and concentrated in vacuum yielding 2.45 g (5.45 mmol, 77%) as a yellowish powder of 4,4'- Tri-[*N,N'*-(3-methylamino)acetophenone]-2,2'-bipyridine. **$^1$H-NMR** ($CDCl_3$, 400.13 MHz) δ (ppm): 8.61 (2H, d, $H_{6bpy}$, $^4J_{H6bpy-H5bpy}$ = 4.9 Hz), 8.40 (2H, s, $H_{3bpy}$), 7.32 (d, 2H, $H_{5bpy}$, $^3J_{H5bpy-H6bpy}$ = 4.9 Hz), 7.28 (2H, d, $H_{5'}$, $^3J_{H5'-H4'}$ = 7.8 Hz, $^3J_{H5'-H6'}$ = 7.8 Hz), 7.24 (2H, d, $H_{4'}$, $^3J_{H4'-H5'}$ = 7.8 Hz), 7.22 (2H, d, $H_{2'}$, $^4J_{H2'-H6'}$ = 1.9 Hz, $^4J_{H2'-H4'}$ = 2.1 Hz), 6.77 (2H, d, $H_{6'}$, $^3J_{H6'-H5'}$ = 7.8 Hz, $^4J_{H6'-H2'}$ = 1.9 Hz), 4.50 (4H, s, $CH_2NH$), 2.53 (6H, s, $CH_3$). **$^{13}$C-NMR** ($CDCl_3$, 100,62 MHz) δ (ppm): 231.2, 198.41, 156.3, 149.6 ($C_{6bpy}$), 147.65, 138.2, 129.5 ($C_9$), 122.2 ($C_{5bpy}$), 119.6 ($C_{3bpy}$), 118.41 ($C_8$), 117.4 ($C_7$), 111.88 ($C_{11}$), 47.2 (**C**$H_2$NH), 26.7 (**C**H3). **MS-MALDI/TOF+**: *m/z*: calcd (%) for $C_{28}H_{26}N_4O_2$: 450.21 (100); found: 451.2 $[M+H]^+$ (55).

## IV.5.13. Synthesis of [(4,4'-Tri-(*N,N'*-(3-methylamino)acetophenone)-2,2'-bipyridine)]$Ru(bpy)_2(PF_6)_2$

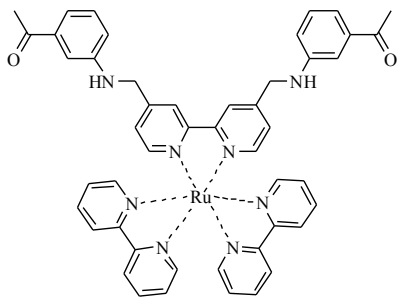

A mixture of 4,4'- Tri-[*N,N'*-(3-methylamino)acetophenone]-2,2'-bipyridine (0.66 mmol, 302.3 mg) and $Ru(bpy)_2Cl_2$ (0.66 mmol, 347.4 mg) in 35 mL of ethylene glycol was refluxed in a microwave for 2 min. After total consumption verified by TLC (eluent: $CH_3COCH_3$:$CH_3OH$:$H_2O$:$KNO_3$, 40:10:10:1) ethylene glycol was removed by distillation at

reduced pressure. The mixture was dissolve in water and an excess of $NH_4PF_6$ was added to precipitate the red complex, which was subsequently filtered off, rinsed with diethyl ether, and dried. After flash chromatography (Silicagel 60, $CH_3COCH_3$:$CH_3OH$:$H_2O$:$KNO_3$, 40:10:10:1), [(4,4'- Tri-(*N,N'*-(3-methylamino)acetophenone) -2,2'-bipyridine)]$Ru(bpy)_2(PF_6)_2$ was obtained yielding 0.72 g (0.62 mmol, 94%). **$^1$H-RMN** ($CD_3COCD_3$, 400.13 MHz) δ (ppm): 8.85 (2H, s, $H_{6bpy}$), 8.77 (4H, d, $H_{\gamma bpy}$, $^3J_{H\gamma bpy\text{-}H\delta bpy}$ = 7.7 Hz), 8.18 (4H, dd, $H_{\delta bpy}$, $^3J_{H\delta bpy\text{-}H\gamma bpy}$ = 7.8 Hz), 8.02 (2H, d, $H_{\beta bpy}$, $^3J_{H\beta bpy\text{-}H\alpha bpy}$ = 5.1 Hz), 7.95 (4H, t, $H_{\alpha bpy}$, $^3J_{H\alpha bpy\text{-}H\beta bpy}$ = 5.3 Hz), 7.55 (6H, m, $2H_{4'}$, $2H_{5'}$, $2H_{3bpy}$), 7.24 (4H, m, $2H_{\beta bpy}$, $2H_{5bpy}$), 7.17 (2H, s, $H_{2'}$), 6.91 (2H, d, $H_{4'}$, $^3J_{H4'\text{-}H5'}$ = 7.0 Hz), 6.0 (2H, s, NH), 4.71 (4H, s, $CH_2NH$), 2.46 (6H, s, $CH_3$).

# CHAPTER V. Conclusions

# V. Conclusions

In this thesis, the network of chemical reactions of flavylium ions was extended to multiresponsive covalently linked supramolecular systems.

When metal-complexing groups like catechol or carboxylic groups were covalently linked to the flavylium moiety it was possible to address the system through new stimul, achieving this way the extension of the network of chemical reactions characteristic of flavylium compounds.

The redox stimulus - viologen - introduced in the system allowed the electrochemical reduction of the same, although it was not possible to define a total reversible system due to decomposition in every cycle. Nevertheless the results obtained are very encouraging in the persuit of a completely reversible and electrically addressable system.

Major breakthroughs were made in the synthesis to covalently link flavylium systems to metal-complexing units, although they were very ambitious and extremely demanding. Despite the stability of the complexes prevented the obtaining of the final compounds, the Ru(II) polypyridyl was introduced for the first time in the flavylium system. The know-how achieved from this research will allow redesign the synthetic approach in order to facilitate the preparation of such compounds and also to increase their water solubility, which is a major factor to consider when working with flavylium systems.

# CHAPTER VI. Supplementary Material

# VI. Supplementary Material

## VI.1. Kinetics of thermal reaction – deduction of Equation I-13

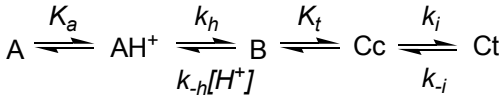


**Equation I-12**

Assuming that **B** and **Cc** are in fast equilibrium, we can simplify the problem:

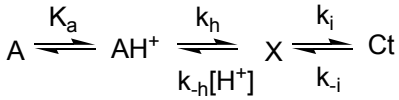


(S1)

$$[X]=[B]+[Cc] \tag{S2}$$

$$[X]=[B]+K_t[B] \tag{S3}$$

$$\chi_B=\frac{1}{1+K_t};\chi_{Cc}=\frac{K_t}{1+K_t} \tag{S4,S5}$$

And we obtain the following differential equations:

$$\frac{d([AH^+]+[A])}{dt}=-k_h\frac{[H^+]}{[H^+]+K_a}([AH^+]+[A])+k_{-h}[H^+]\chi_B[X] \tag{S6}$$

$$\frac{d([X])}{dt}=k_h\frac{[H^+]}{[H^+]+K_a}([AH^+]+[A])+k_{-i}[Ct]-(k_{-h}[H^+]\chi_B+k_i\chi_{Cc})[X] \tag{S7}$$

$$\frac{d([Ct])}{dt}=k_i\chi_{Cc}[X]-k_{-i}[Ct] \tag{S8}$$

Applying the steady state approximation:

$$[X]=\frac{k_h\frac{[H^+]}{[H^+]+K_a}([AH^+]+[A])+k_{-i}[Ct]}{k_{-h}[H^+]\chi_B+k_i\chi_{Cc}} \tag{S9}$$

And finally, substituting [X] one obtains,

$$\frac{d([AH^+]+[A])}{dt}=-k_h\frac{[H^+]}{[H^+]+K_a}([AH^+]+[A])+k_{-h}[H^+]\chi_B\frac{k_h\frac{[H^+]}{[H^+]+K_a}([AH^+]+[A])+k_{-i}[Ct]}{k_{-h}[H^+]\chi_B+k_i\chi_{Cc}}$$

$$\frac{d([AH^+]+[A])}{dt} = -\frac{k_i \chi_{Cc} k_h \frac{[H^+]}{[H^+]+K_a}([AH^+]+[A])}{k_{-h}[H^+]\chi_B + k_i \chi_{Cc}} + \frac{k_{-i}k_{-h}[H^+]\chi_B[Ct]}{k_{-h}[H^+]\chi_B + k_i \chi_{Cc}} \quad \text{(S10)}$$

$$\frac{d([Ct])}{dt} = k_i \chi_{Cc} \frac{k_h \frac{[H^+]}{[H^+]+K_a}([AH^+]+[A]) + k_{-i}[Ct]}{k_{-h}[H^+]\chi_B + k_i \chi_{Cc}} - k_{-i}[Ct]$$

$$\frac{d([Ct])}{dt} = \frac{k_i \chi_{Cc} k_h \frac{[H^+]}{[H^+]+K_a}([AH^+]+[A])}{k_{-h}[H^+]\chi_B + k_i \chi_{Cc}} - \frac{k_{-i}k_{-h}[H^+]\chi_B[Ct]}{k_{-h}[H^+]\chi_B + k_i \chi_{Cc}} \quad \text{(S11)}$$

Now it is easy to account for first order kinetic constant observed:

$$k_{obs} = \frac{\frac{[H^+]}{[H^+]+K_a} k_i \chi_{Cc} k_h + k_{-i}k_{-h}[H^+]\chi_B}{k_{-h}[H^+]\chi_B + k_i \chi_{Cc}} \quad \text{(S12)}$$

$$k_{obs} = \frac{\frac{[H^+]}{[H^+]+K_a} k_i \frac{K_T}{1+K_T} k_h + k_{-i}k_{-h}[H^+]\frac{1}{1+K_T}}{k_{-h}[H^+]\frac{1}{1+K_T} + k_i \frac{K_T}{1+K_T}}$$

(S13)

Rearranging, one obtains:

$$k_{obs} = \frac{\frac{[H^+]}{[H^+]+K_a} k_i K_t k_h + k_{-i}k_{-h}[H^+]}{k_{-h}[H^+] + k_i K_t}$$

$$k_{obs} = \frac{\frac{[H^+]}{[H^+]+K_a} k_i K_t K_h + k_{-i}[H^+]}{[H^+] + \frac{k_i K_t}{k_{-h}}} \quad \textbf{Equation I-13}$$

## VI.2. Quantum yields – Equation I-15

The quantum yield of formation of $\mathbf{AH}^+$ is pH dependent, and in the case of a low thermal barrier it can be given by equation 1.48, in which the numerator accounts for the formation of $\mathbf{AH}^+$ and the denominator is simply a sum of the two processes. That is, the observed quantum yield is given by the product of the intrinsic quantum yield of the reaction by the efficiency of formation of $\mathbf{AH}^+$.

$$\Phi = \Phi_{Ct-Cc}\frac{k_{-h}\left[H^+\right]}{k_{-h}\left[H^+\right]+k_iK_t} = \Phi_{Ct-Cc}\frac{\left[H^+\right]}{\left[H^+\right]+\frac{k_iK_t}{k_{-h}}} \qquad \textbf{Equation I-15}$$

## VI.3. NMR data and compounds numeration for NMR assignment

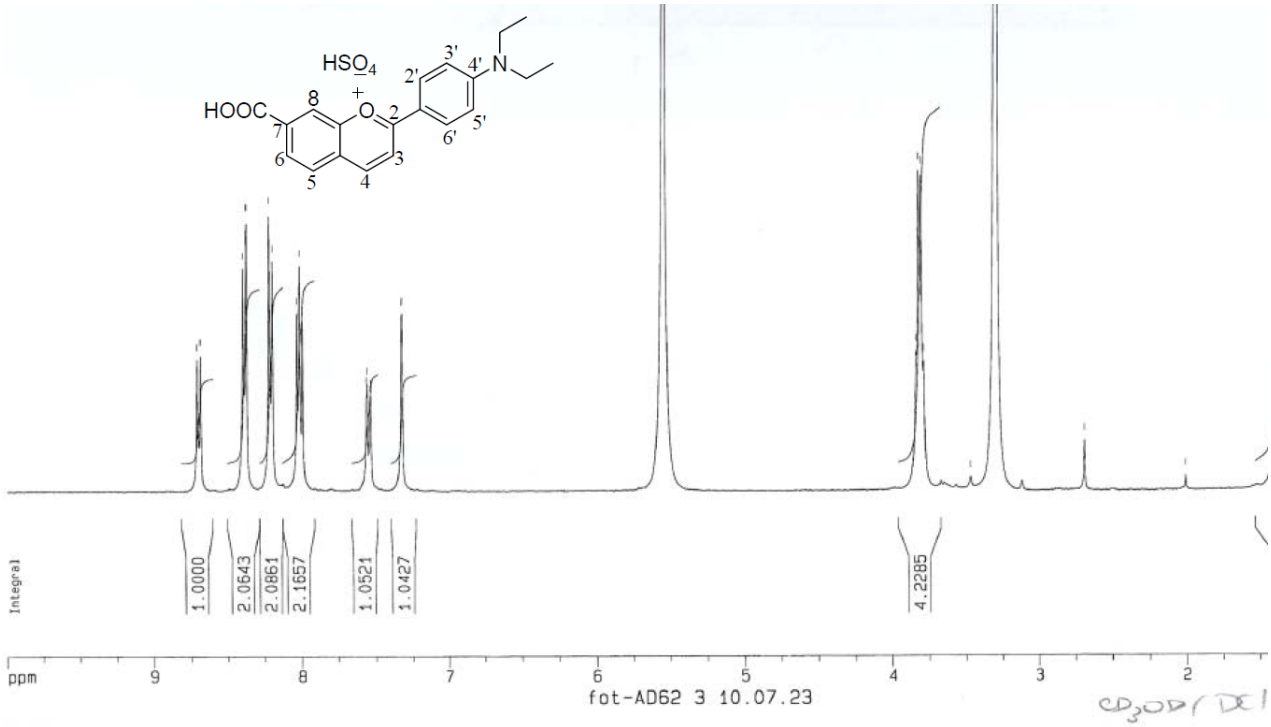


**Figure VI.1 –** $^1$H-NMR data and numeration for compound 2-(4-carboxyphenyl)-7-diethylamino-1-benzopyrylium hydrogensulfate

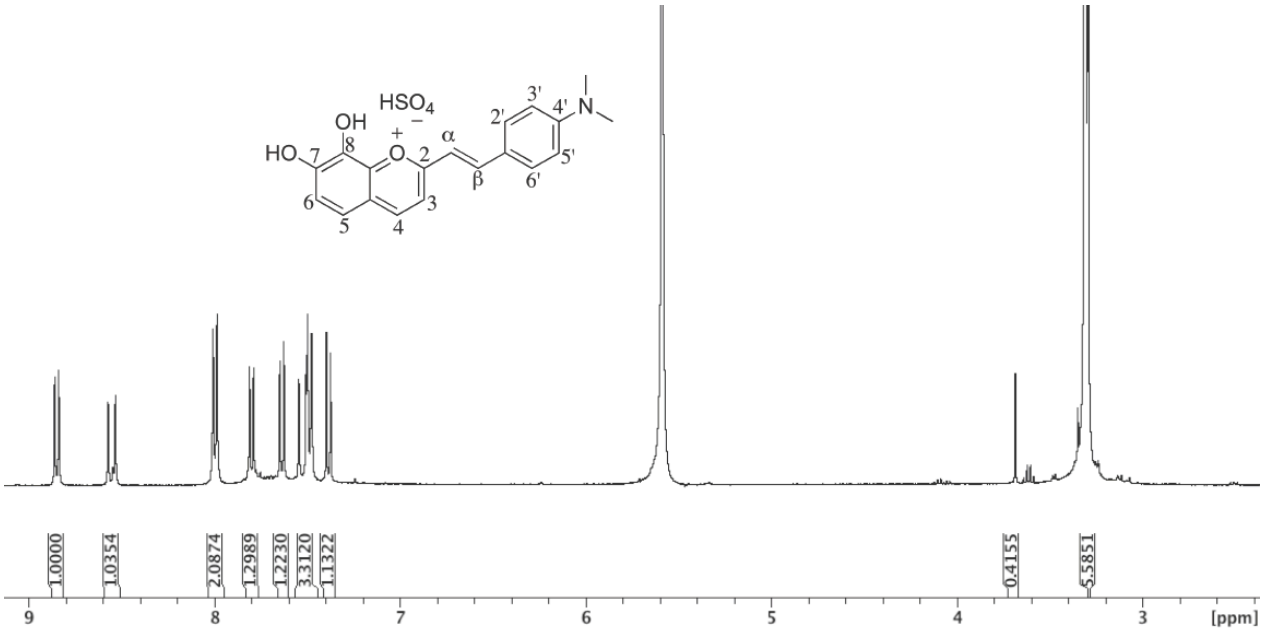


**Figure VI.2 –** $^{1}$H-NMR data and numeration for compound 7,8-dihydroxy-2-(4-dimethylaminostyryl)-1-benzopyrylium hydrogensulfate

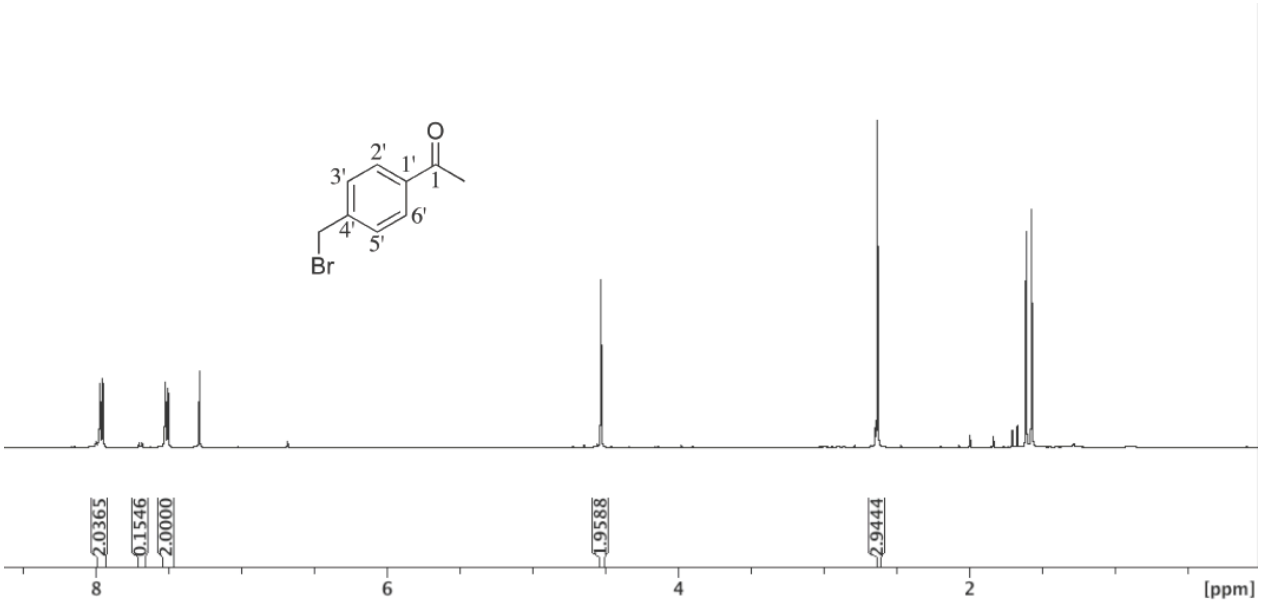


**Figure VI.3 -** $^{1}$H-NMR data and numeration for compound 4'-bromomethylacetophenone **(1)**

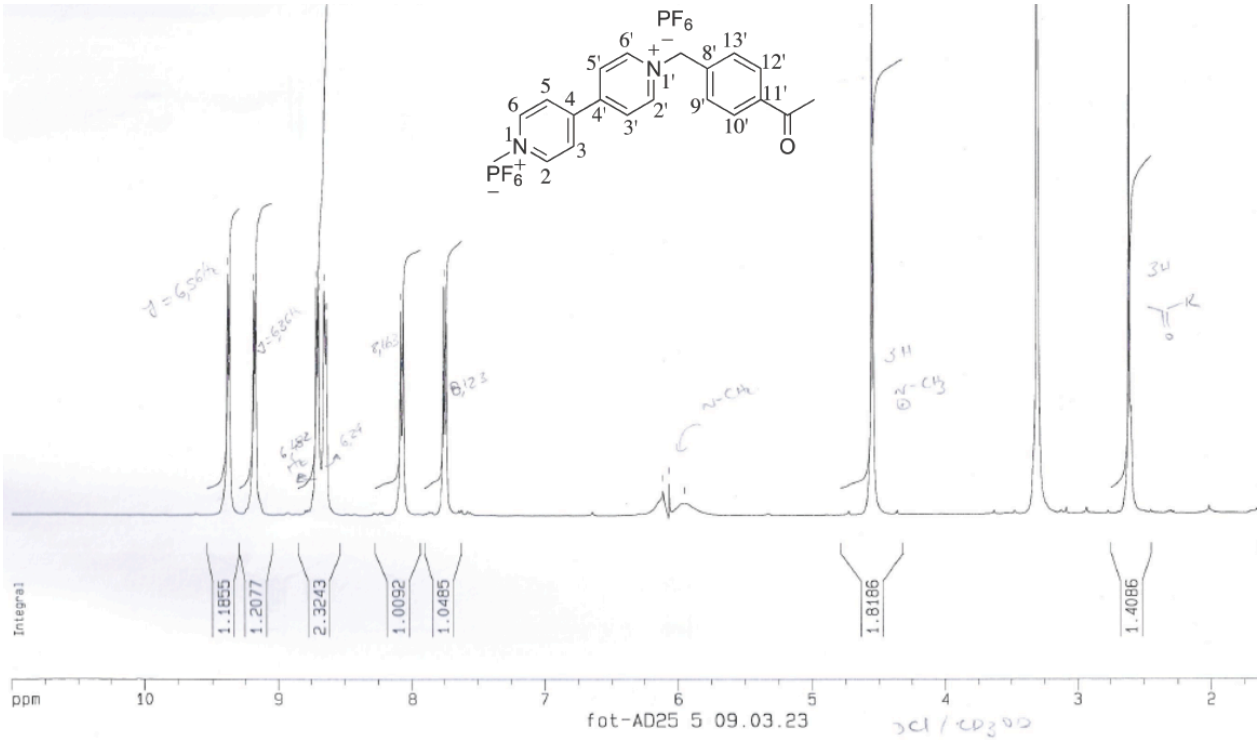


**Figure VI.4 -** $^{1}$H-NMR data and numeration for compound 1-methyl-1'-[(acetophenone-4-il))methyl]-4,4'bipyridinium hexafluorofosfate **(2)**

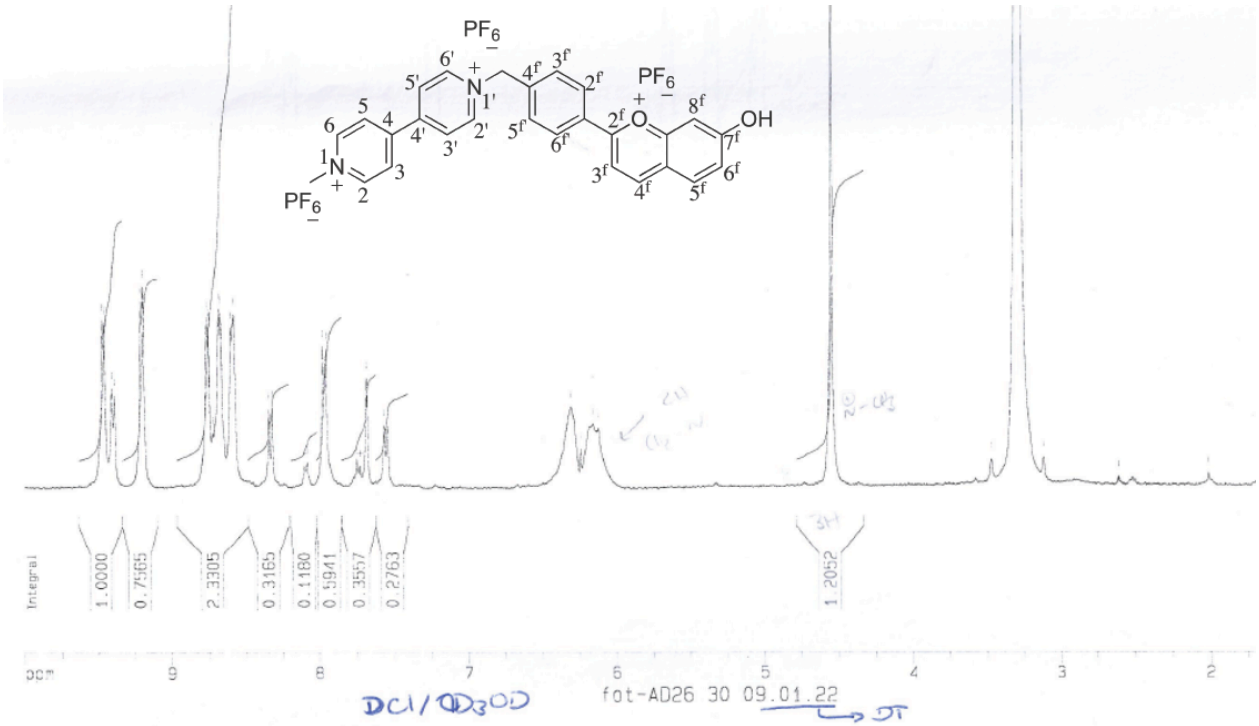


**Figure VI.5 -** $^{1}$H-NMR data and numeration for compound 1-methyl-1'-[(7-hydroxyflavylium-4'-il)methyl]-4,4'bipyridinium hexafluorofosfate **(4)**

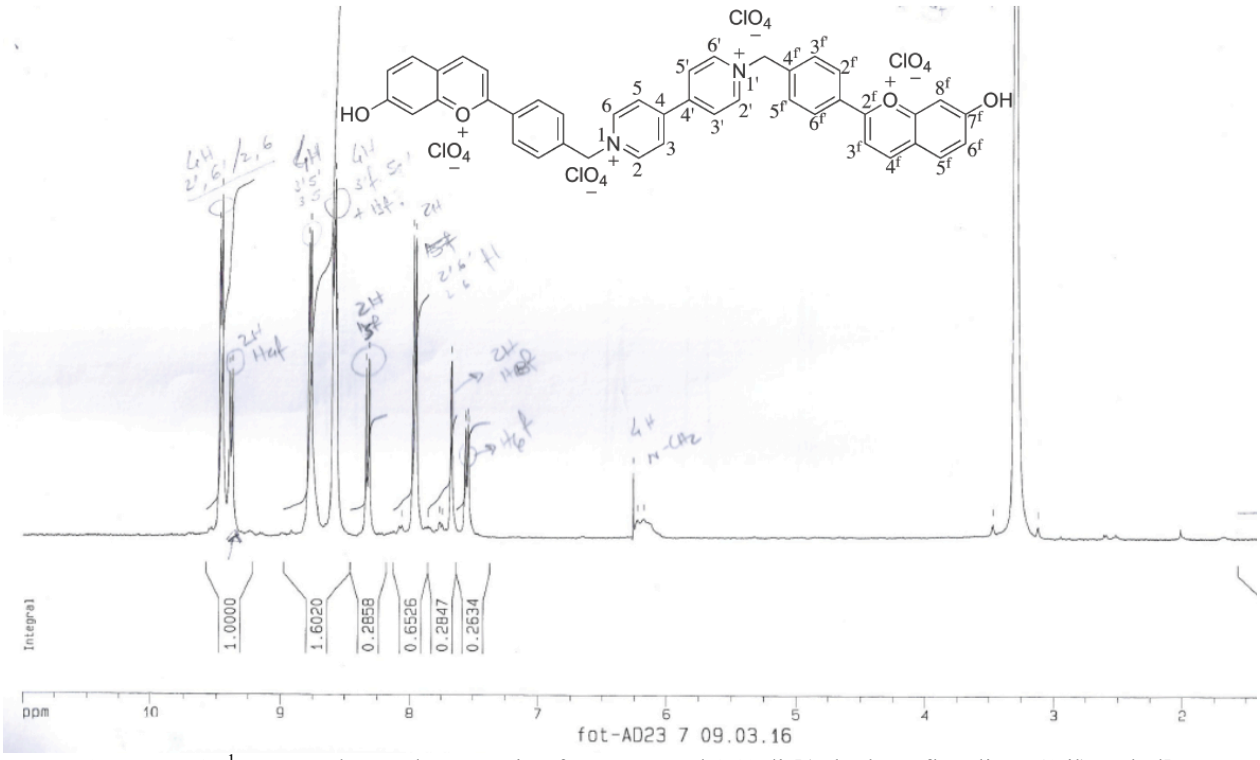


**Figure VI.6 -** $^{1}$H-NMR data and numeration for compound 1,1'-di-[(7-hydroxyflavylium-4'-il)methyl]-4,4'-bipyridinium perchlorate **(3)**

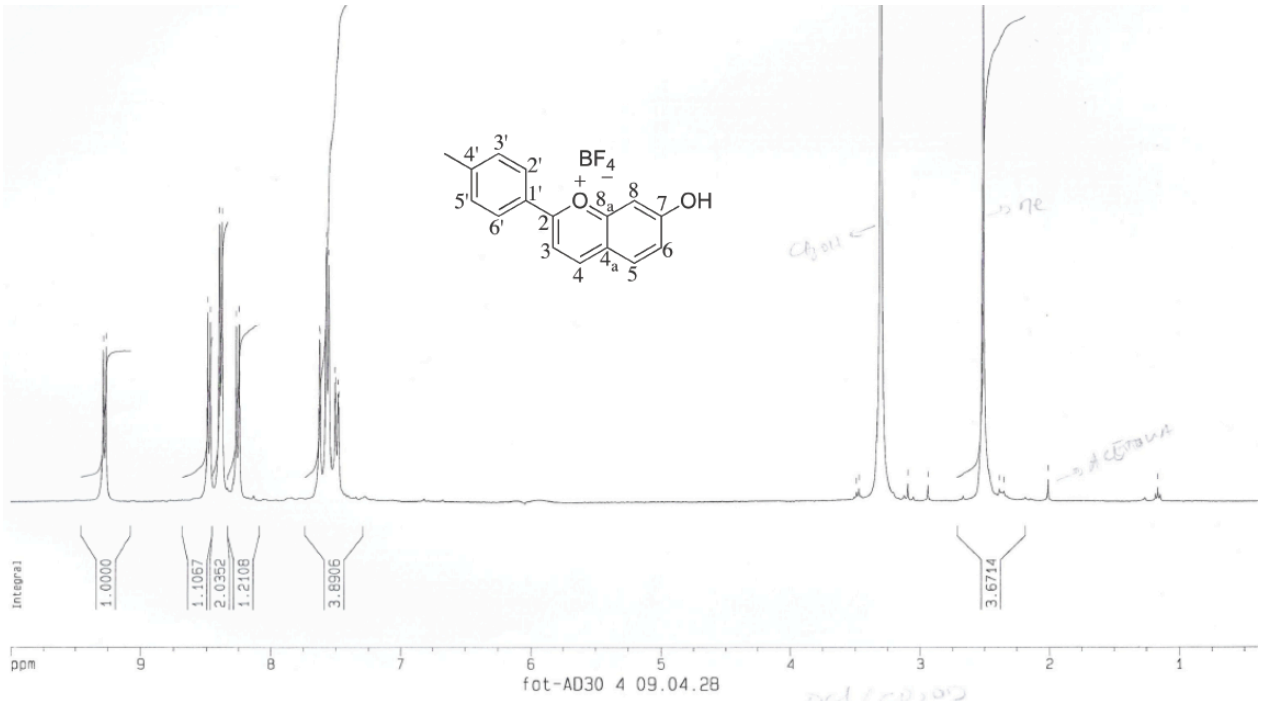


**Figure VI.7 -** $^{1}$H-NMR data and numeration for compound 7-hydroxy-4'-methylflavylium tetrafluorborate **(6)**

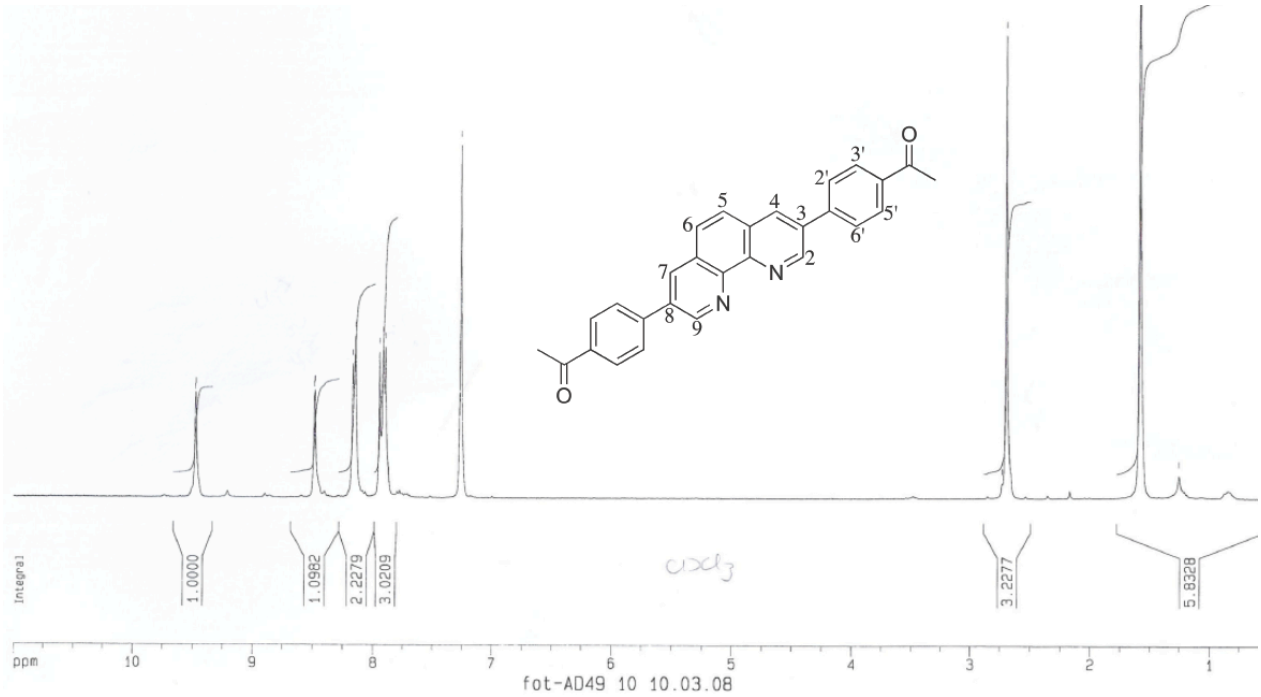


**Figure VI.8 -** $^{1}$H-NMR data and numeration for compound 3,8-bis(p-oxophenyl)-1,10-phenanthroline **(8)**

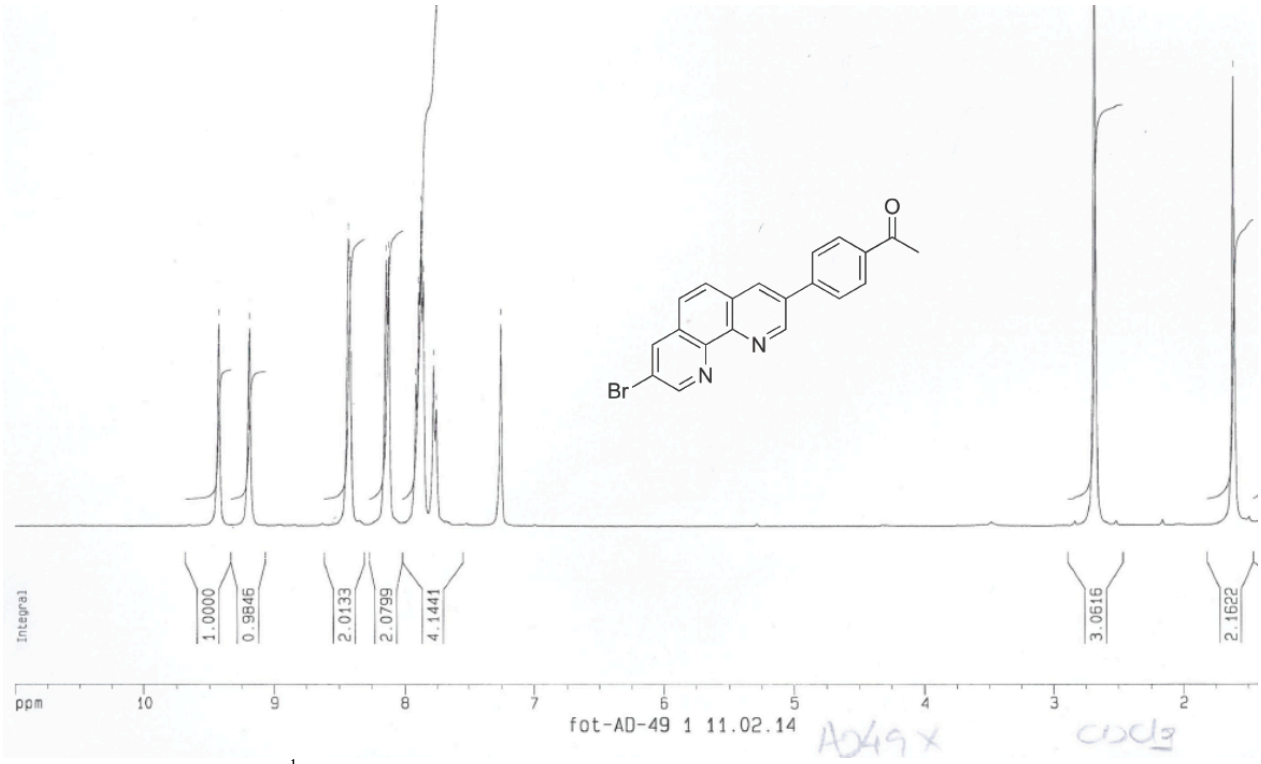


**Figure VI.9 -** $^{1}$H-NMR data and numeration for compound (3-Bromo-8-p-oxophenyl)-1,10-phenanthroline **(12)**

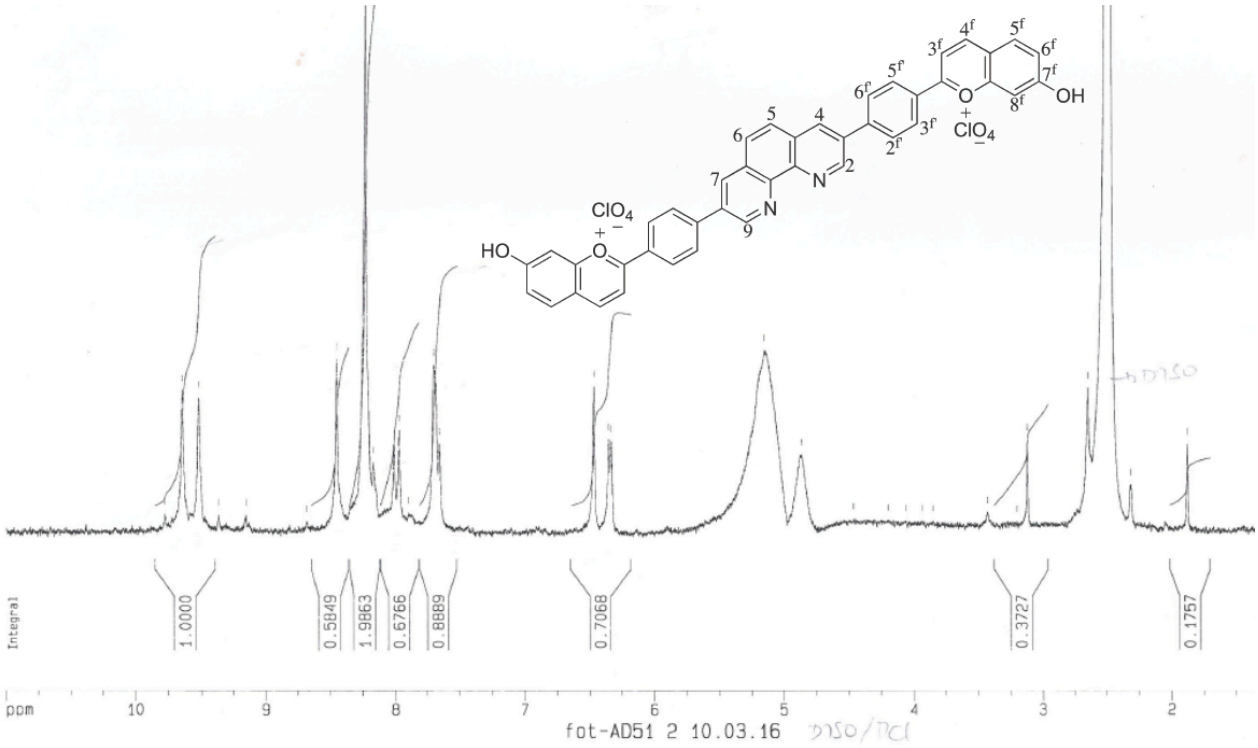


**Figure VI.10 -** $^{1}$H-NMR data and numeration for compound 3,8-Bis(7-dihydroxiflavylium)-1,10-phenanthroline perchlorate **(9)**

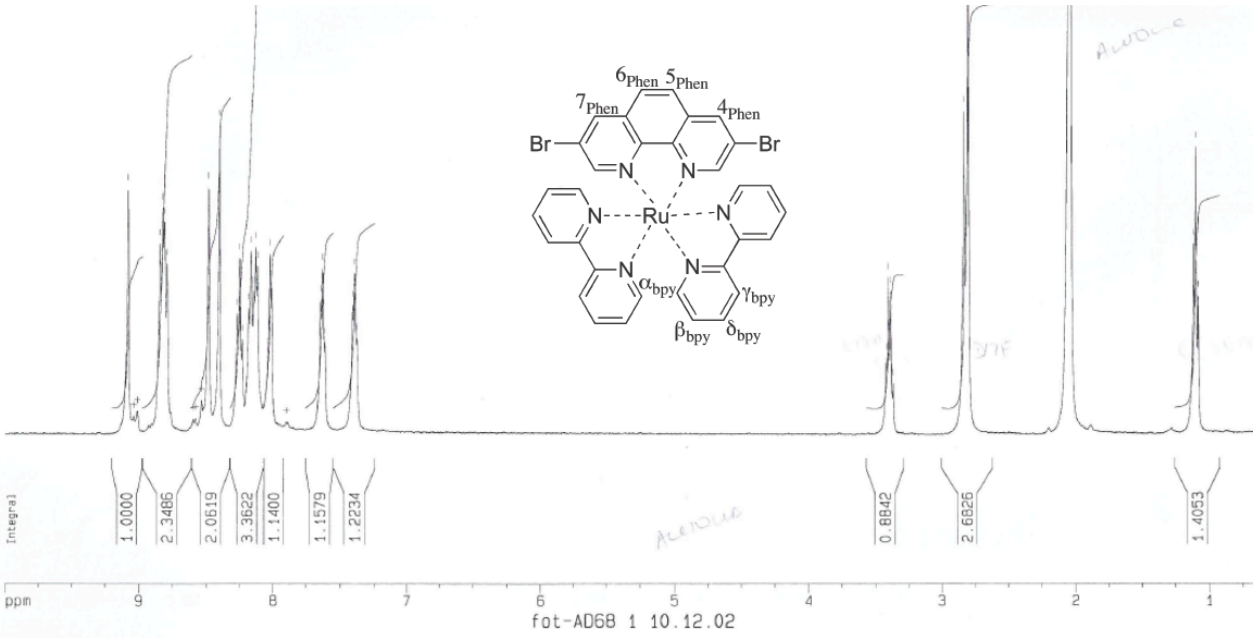


**Figure VI.11 -** $^{1}$H-NMR data and numeration for compound [(3,8-dibromo-1,10-phenanthroline)Ru(bpy)$_2$](PF$_6$)$_2$ **(14)**

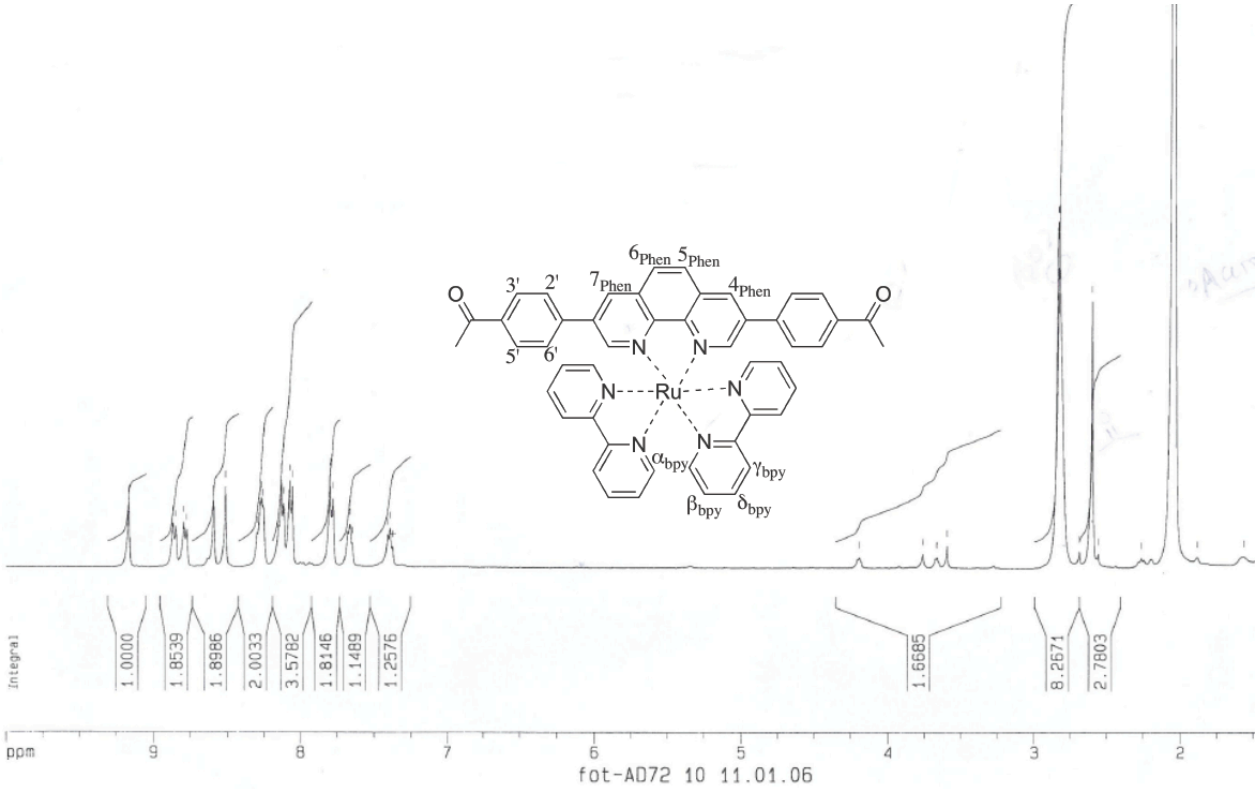


**Figure VI.12 -** $^{1}$H-NMR data and numeration for compound [(3,8-Bis(p-oxophenyl-1,10-phenanthroline))Ru(bpy)$_2$](PF$_6$)$_2$ **(10)**

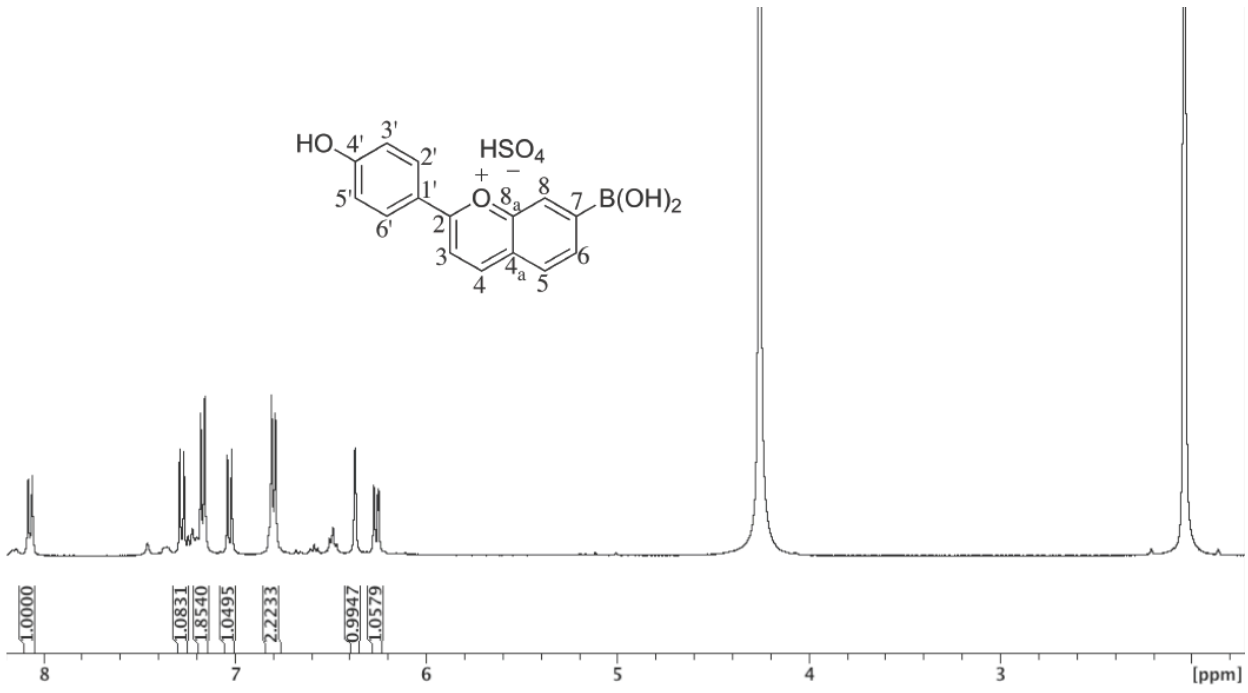


**Figure VI.13 -** $^{1}$H-NMR data and numeration for compound 4'-boronic acid-7-hydroxyflavylium hydrogensulphate **(15)**

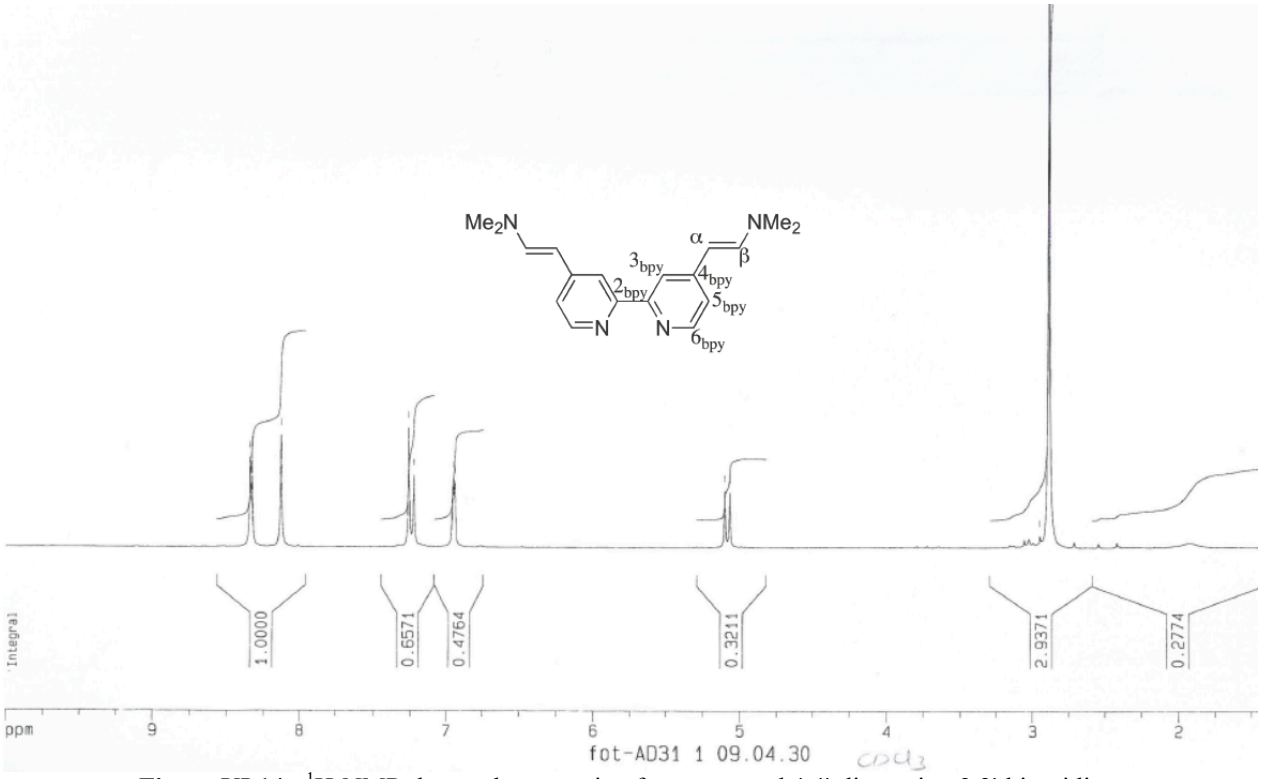


**Figure VI.14 -** $^{1}$H-NMR data and numeration for compound 4,4'-dienamine-2,2'-bipyridine

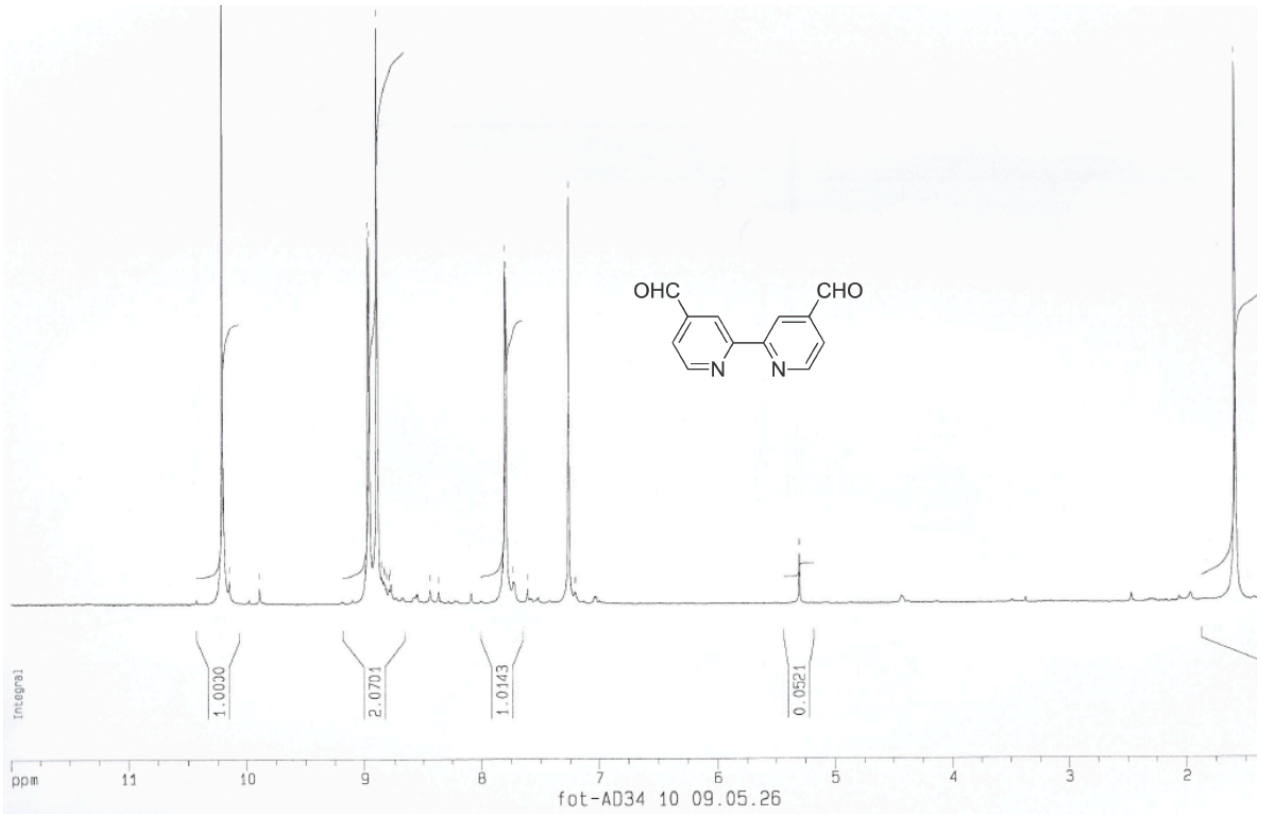


**Figure VI.15 -** $^{1}$H-NMR data for compound 4,4'-diformyl-2,2'bipyridine

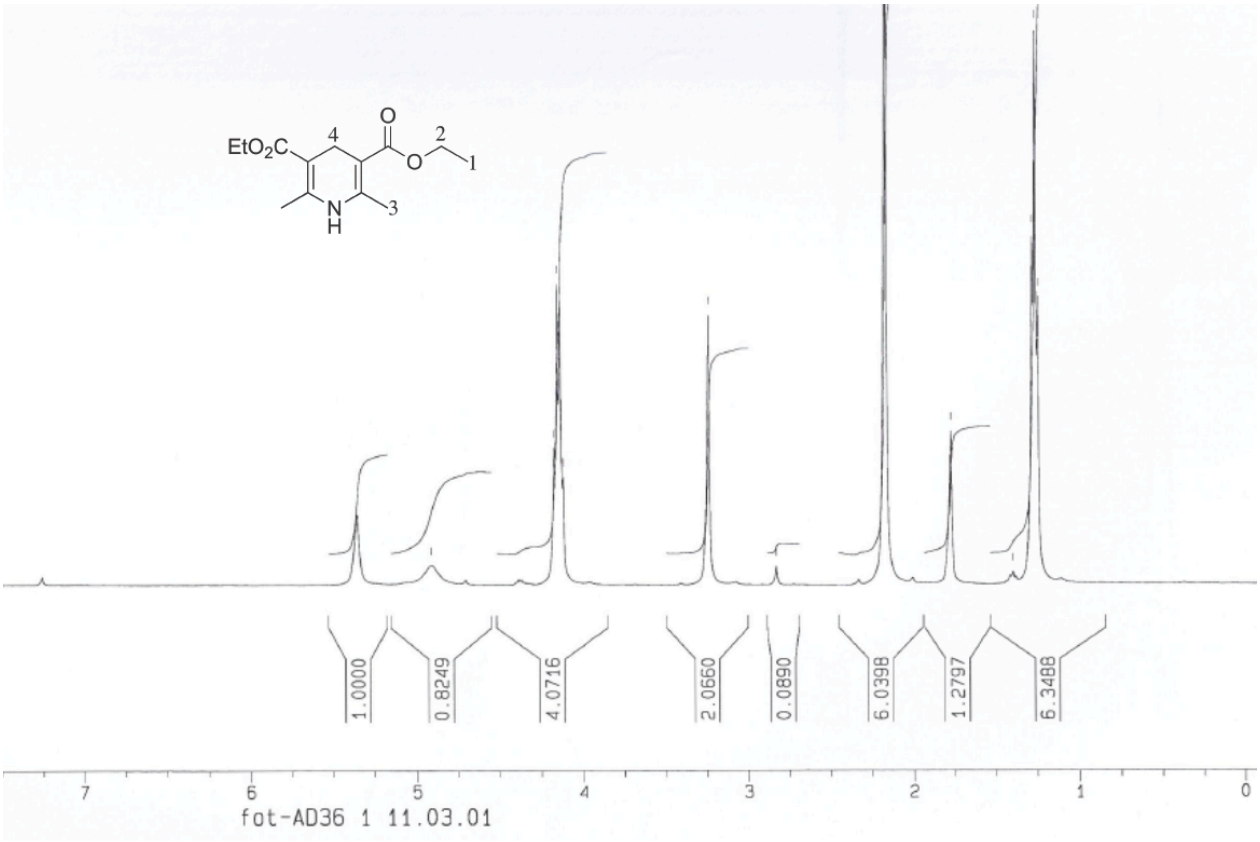


**Figure VI.16 -** [1]H-NMR data and numeration for compound Hantzsch 1,4-DHP **(17)**

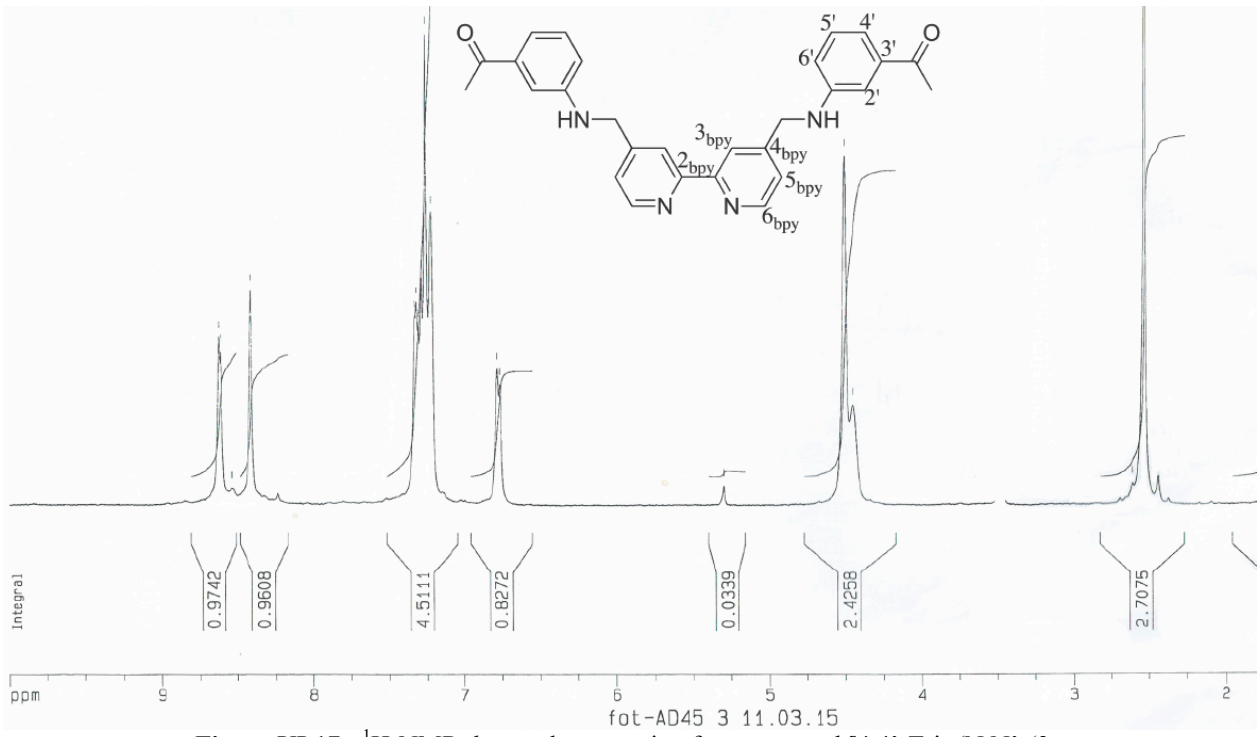


**Figure VI.17 -** [1]H-NMR data and numeration for compound [4,4'-Tri- (N,N'-(3-methylamino)acetophenone)-2,2'-bipyridine) **(18)**

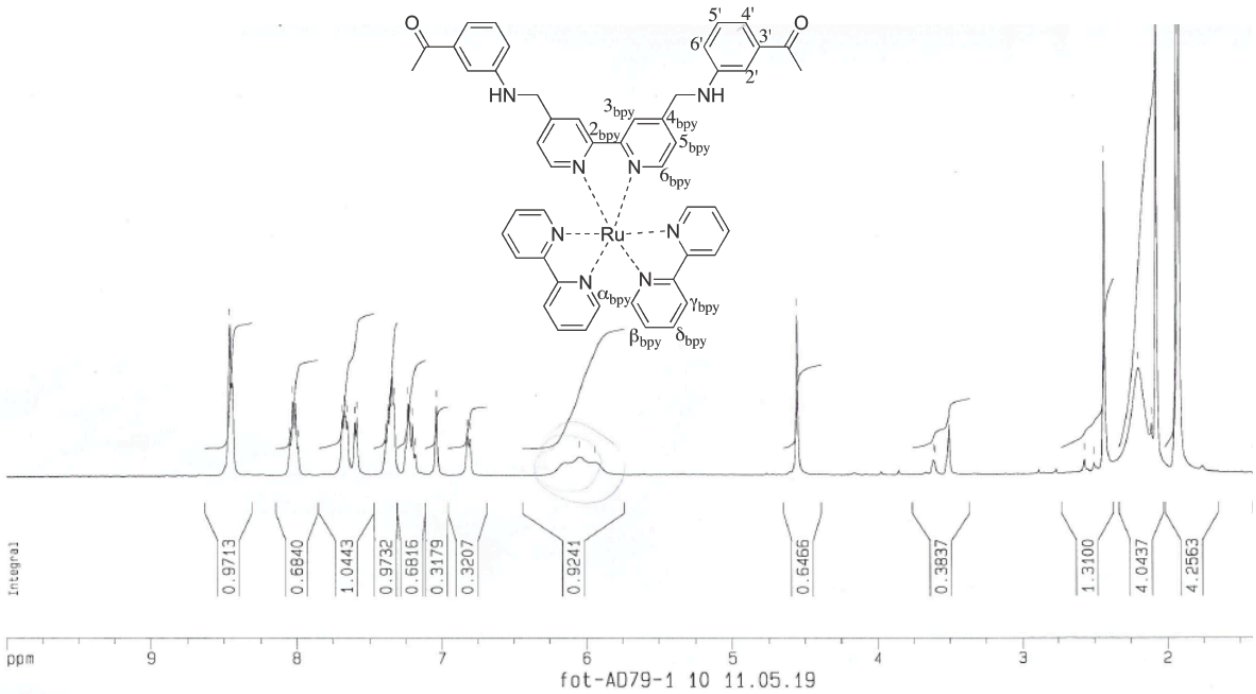


**Figure VI.18 -** $^{1}$H-NMR data and numeration for compound [4,4'-Tri- (N,N'-(3-methylamino)acetophenone)-2,2'-bipyridine)Ru(bpy)$_2$](PF$_6$)$_2$ **(20)**

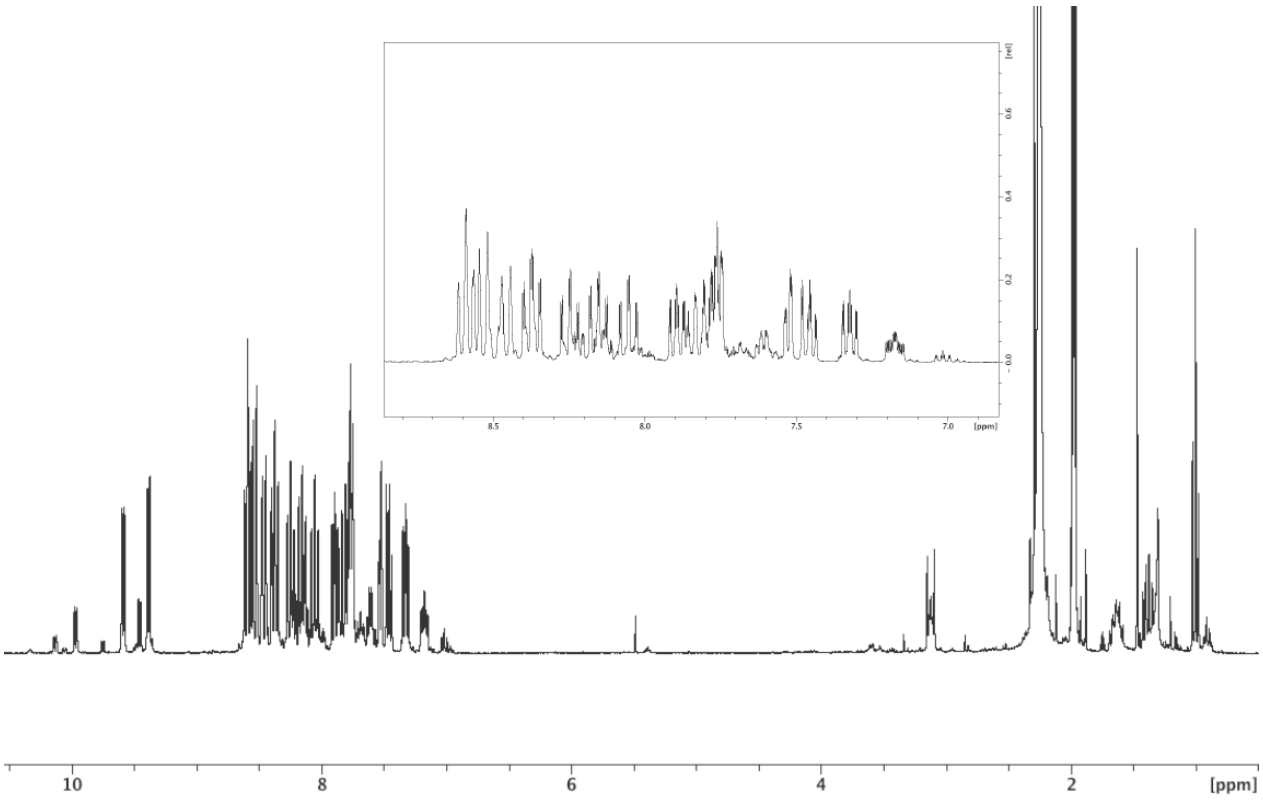


**Figure VI.19 -** $^{1}$H-NMR data obtained for complex **11**

# CHAPTER VII. References

# VII. References


[1] F. Pina, M. Maestri, V. Balzani, in *Handbook of Photochemistry and Photobiology,* American Scientific Publishers, Stevenson Ranch, CA, USA, **2003**, Chapter 9, vol. 3, 411-449.

[2] V. Balzani, *Photochem. Photobiol. Sci.* **2003**, *2*, 459-476.

[3] V. Balzani, A. Credi, M. Venturi, *Nanotoday*, **2007**, 2, 18-25.

[4] V. Balzani, A. Credi, M. Raymo, J. F. Stoddart, *Angew. Chem. Int. Ed.* **2000**, *39*, 3348.

[5] R. P. Feyman, *Engineering and Science* **1960**, 23, 22.

[6] J. M. Lehn, *Supramolecular Chemistry: Concepts and Perspectives*, VCH, Weinheim, Germany, **1995**.

[7] J. M. Lehn, *Chem. Soc. Rev*., **2007**, 36, 151-160.

[8] J. W. Steed, J. L. Atwood, *Supramolecular Chemistry*, Wiley, **2000**.

[9] V. Balzani, F. Sandola, in *Supramolecular Photochemistry*, Ellis Horwood, **1991**.

[10] V. Petrov, A. J.Parola, F. Pina, *Journal of Physical Chemistry* 116, **2012,** 8107-8118.

[11] F. Pina, M. J. Melo, C. A. T. Laia, A. J. Parola and J. C. Lima, *Chemical Society Reviews*, 41, **2012**, 869-908.

[12] V. Balzani, L. Moggi, F. Sandola, in *Supramolecular Photochemistry*, ed. V. Balzani, Reidel, Dordrecht, **1987**.

[13] F. Pina, M. Maestri, V. Balzani, *in Molecular Switches*, ed. B. L. Feringa, Wiley-VCH, Weinheim, Germany, **2001**, Chapter 10, 309-337 and references therein.

[14] P. Dewick, *Medicinal Natural Products, A Biosynthetic Approach*, Wiley VCH, **2002**, New York, USA, Chapter 4, 121-166.

[15] K. Springob, J.-I. Nakajima, M. Yamazaki, K. Saito, *Nat. Prod. Rep.* **2003**, 20, 288-303.

[16] G. A. Iacobucci, J. G. Sweeney, *Tetrahedron* **1983**, 39, 3005-3038 and references therein.

[17] R. Brouillard, in *Anthocyanins as Food Colors - A Series of Monographs Vol. chapter 1*, P. Markakis ed., Academic Press, New York, **1982**.

[18] ed. J. B. Harborne, *The Flavonoids*, Chapman and Hall, New York, **1982**.

[19] R. Willstätter and A. E. Everest, Justus Liebigs Ann. Chem., **191**3,401, 189–232.

[20] R. Willstätter and H. Mallinson, Justus Liebigs Ann. Chem., **1915**, 408, 15–41.

[21] R. Willstätter and H. Mallinson, Justus Liebigs Ann. Chem., **1915**, 408, 147–162.

[22] D. D. Pratt and R. Robinson, *J. Chem. Soc. Trans*., **1924**, 125, 188–199.

[23] D. D. Pratt and R. Robinson, *J. Chem. Soc. Trans*., **1925**, 127, 167–175.

[24] C. Timberlake, F., P. Bridle, *Food Chem*, **1997**, 58, 103-109.

[25] C. Ovando, M. L. P. Hernández, M. E. P. Hernández, J. A. Rodríguez, C. A. G.-Vidal, *Food Chemistry*, **2009**, 113, 859-871.

[26] L. Jurd*, Vol. U. S. Patent 3 301 683*, **1967**.

[27] D. Candau, F. S., *Vol. U.S. Patent 6 471 949*, L'Oreal S.A., **2002**.

[28] D. Candau, S. Forestier, I. Elguidj, *Vol. U.S. Patent 6 511 656*, L'Oreal S.A., **2003**.

[29] Y. Hirshberg, *J. Am. Chem. Soc*. **1956**, 78, 2304-2312.

[30] A. L. Roque, Dissertação thesis, FCT-UNL (Lisboa), **2001**.

[31] E. Sondheimer and Z. I. Kertesz, *J. Am. Chem. Soc*., **1948**, 70, 3476–3479.

[32] E. Sondheimer, *J. Am. Chem. Soc*., **1953**, 75, 1507–1508.

[33] L. Jurd, *J. Org. Chem.*, **1963**, 28, 987-991.

[34] L. Jurd, T. A. Geissman, *J. Org. Chem.* **1963**, 28, 2394-2397.

[35] C. Timberlake, F., P. Bridle, *Nature,* **1966**, 212, 158-159.

[36] L. Jurd, *Tetrahedron.* **1969**, 25, 2367-2380.

[37] R. Brouillard, J. E. Dubois, *J. Am. Chem. Soc.* **1977**, *99*, 1359-1364.

[38] R. Brouillard, J. Lang, *Can. J. Chem.* **1990**, *68*, 755-761.

[39] R. Brouillard, B. Delaporte, *J. Am. Chem. Soc.* **1977**, 99, 8461-8468

[40] H. Santos, D. Turner, J. C. Lima, P. Figueiredo, F. Pina and A. L. Maçanita, *Phytochemistry*, **1993**, 33, 1227–1232.

[41] R. A. McClelland, S. Gedge, *J. Am. Chem. Soc.* **1980**, *102*, 5838-5848.

[42] R. A. McClelland, G. McGall, *J. Org. Chem.* **1982**, *47*, 3730-3736.

[43] P. Figueiredo, J. C. Lima, H. Santos, M.-C. Wigand, R. Brouillard, A. L. Maçanita, F. Pina, *J. Am. Chem. Soc* **1994**, 116, 1249-1254.

[44] F. Pina, M. Maestri, V. Balzani, *Chem. Commun.* **1999**, 107-114.

[45] A. Roque, C. Lodeiro, F. Pina, M. Maestri, S. Dumas, P. Passaniti, V. Balzani, *J. Am. Chem. Soc.* **2003**, 125, 987-994.

[46] F. Pina, M. J. Melo, R. Balardini, L. Flamigni, M. Maestri, *New J Chem*, **1997**, 21, 969-976.

[47] F. Pina, V. Petrov, C. A. T. Laia *Dyes and Pigments,* 92, **2012**, 877-889.

[48] F. Pina, *J. Chem. Soc. Faraday Trans.* **1998**, 94, 2109-2116.

[49] D. Fernandez, F. Folgosa, A. J. Parola, F. Pina, *New J. Chem*. **2004**, 28, 1221-1226.

[50] C. A. T. Laia, A. J. Parola, F. Folgosa, F. Pina, *Org. Biomol. Chem.* **2007**, 5, 69-77.

[51] V. Petrov, R. Gomes, A. J. Parola, A. Jesus, C. A. T. Laia , F. Pina, *Tetrahedron* **2008**, 64, 714-720.

[52] V. Petrov, R. Gomes, A. J. Parola, F. Pina*, Dyes and Pigments* **2009***,* 80, 149-155.

[53] F. Pina, M. J. Melo, A. J. Parola, M. Maestri, V. Balzani, *Chem. Eur. J.* **1998**, 4, 2001-2007.

[54] F. Pina, M. J. Melo, M. Maestri, P. Passaniti, N. Camaioni, V. Balzani, *Eur. J. Org. Chem*. **1999**, 3199-3277.

[55] M. Montalti, A. Credi, L. Prodi, M. T. Gandolfi, *Handbook of Photochemistry*, CRC Press, Boca Raton, FL, **2006**, 3rd ed, Chapter 12, 601-616.

[56] C. G. Hatchard, C. A. Parker, *Proc. R. Soc. (London), Ser. A* **1956**, 235, 518-536.

[57] F. Pina, A. Hatton, *Langmuir* **2008**, *24*, 2356-2364.

[58] M. Maestri, R. Ballardini, F. Pina, M. J. Melo, *J. Chem. Educ.* **1997**, 74, 1314-1316.

[59] Y. Hirshberg, *New Scientist*, **1960**, 7, 1243.

[60] A. Roque, C. Lodeiro, F. Pina, M. Maestri, R. Ballardini, V. Balzani, Eur. *J. Org. Chem*. **2002**, 16, 2669-2709.

[61] F. Pina, J. C. Lima, A. J. Parola, C. A. M. Afonso, *Angew.* Chem. Int. Ed. **2004**, 43, 1525-1527.

[62] M. C. Moncada, D. Fernández, J. C. Lima, A. J. Parola, C. Lodeiro, F. Folgosa, M. J. Melo, F. Pina, *Org. Biomol. Chem*. **2004**, 4, 2802-2808.

[63] L. Giestas, F. Folgosa, J. C. Lima, A. J. Parola, F. Pina, Eur. *J. Org. Chem*. **2005**, 43, 4187-4200.

[64] F. Pina, J. C. Lima, A. J. Parola, A. Roque, *Photochem. Photobiol. Sci*. **2007**, 6, 381-385.

[65] F. Pina, A. Roque, M. J. Melo, M. Maestri, L. Belladelli, V. Balzani, *Chem. Eur. J.* **1998**, 4, 1184-1191.

[66] F. Pina, M. J. Melo, M. Maestri, R. Ballardini, V. Balzani, *J. Am. Chem. Soc.,* **1997**, 119, 5556-5561.

[67] M. Maestri, F. Pina, A. Roque, P. Passaniti, *J. Photochem. Photobiol. A,* **2000**, 137, 21-28.

[68] M. C. Moncada, A. J. Parola, C. Lodeiro, F. Pina, M. Maestri, V. Balzani, *Chem. Eur. J.* **2004**, *10*, 1519-1526.

[69] A. Roque, C. Lodeiro, F. Pina, M. Maestri, S. Dumas, P. Passaniti, V. Balzani, *J. Am. Chem. Soc*. **2003**, 125, 987-994.

[70] A. Roque, F. Pina, S. Alves, R. Ballardini, M. Maestri, V. Balzani, *J. Mater. Chem.* **1999**, 9, 2265-2269.

[71] A. P. de Silva and C. P. McCoy, *Chem. Ind*., **1994**, 992–996.

[72] A. P. de Silva, H. Q. N. Gunaratne and C. P. McCoy, *Nature*, **1993**, 364, 42–44.

[73] A. P. de Silva and N. D. McClenaghan, *J. Am. Chem. Soc*., **2000**, 122, 3965–3966.

[74] A. P. de Silva, H. Q. N. Gunaratne, T. Gunnlaugsson, A. J. M. Huxley, C. P. McCoy, J. T. Rademacher, T. E. Rice, *Chem. Rev*. **1997**, 97, 1515-1566.

[75] F. Pina, M. J. Melo, M. Maestri, P. Passaniti, V. Balzani, *J. Am. Chem. Soc.,* **2000**, 122, 4496.

[76] A. M. Diniz, R. Gomes, A. J. Parola, C. A. T. Laia, F. Pina, *Journal of Physical Chemistry B*, 113, **2009**, 719-727.

[77] R. Gomes, A. M. Diniz, A. Jesus, A. J. Parola, F. Pina, *Dyes and Pigments* 81, **2009**, 69-79.

[78] S. Gago, V. Petrov, Ana M. Diniz, A J. Parola, L. Cunha-Silva, F. Pina, *J. Phys Chem A*, **2011**, 11(1):372-380.

[79] A. Jimenez, C. Pinheiro, A. J. Parola, M. Maestri, Fernando Pina, *Photochem. Photobiol. Sci.* **2007**, 6, 372-380.

[80] A. M. Diniz, C. Pinheiro, V. Petrov, A. J. Parola, F. Pina, *Chem. Eur. J.* **2011**, 17, 6359−6368.

[81] G. Calogero, A. Sinapoli, I. Citro, G.D. Marco, V. Petrov, A.M. Diniz, A.J. Parola, F. Pina, *Photochem. Photobiol. Sci*., **2013**, 12, 883-894.

[82] T. Swain in The Flavonoids (Eds.: J. B. Harborne, T. J. Mabry, H. Mabry), Chapman and Hall, London, **1975**, 1096-1129.

[83] D. Amic, N. Trinajstic, D. Davidovic-Amic, *J. Chem. Soc. Perkin Trans. 2* **1992**, 11, 1933-1938.

[84] F. Pina, A. J. Parola, R. Gomes, M. Maestri, V. Balzani " Multistate/Multifunctional Molecular-Level Systems: Photochromic Flavylium Compounds", in "Molecular Switches", Vol.1, second edition, eds. Ben Feringa and W. R. Browne, Wiley-VCH, Weinheim, Germany, Chapter 6, **2011,** 181-226.

[85] F. Pina, M. J. Melo, M. Maestri, P. Passaniti, N. Camaioni, V. Balzani, *Eur. J. Org. Chem.* **1999**, 3199-3207.

[86] R. Gavara, C. A.T. Laia, A. J. Parola, F. Pina, *Chem. Eur. J.*, **2010**, *16*, 7760-7766.

[87] F. H. Allen, *Acta Cryst. B,* **2002,** 58, 380-388.

[88] F. H. Allen, W. D. S. Motherwell, *Acta Cryst. B,* **2002,** 58, 407-422.

[89] D. Amic, N. Trinajstic, *J. Chem. Soc. Perkin Trans. 2* **1991**, 891-895.

[90] J. G. Sweeny, G. A. Iacobucci, *J. Agric. Food Chem*. **1983**, 31, 531-533.

[91] M. C. Moncada, S. Moura, M. J. Melo, A. Roque, C. Lodeiro, F. Pina, *Inorg. Chim. Acta*, 365, **2003**, 51-61.

[92] F. Pina, *Journal of the Chemical Society Faraday Transactions.* **1998**,94, 2109-2116.

[93] R. Gavara, Y. Leydet, V. Petrov, F. Pina, *Photochemical and Photobiological Sciences,* 11, **2012**, 1691-1699.

[94] R. Gavara, C. A.T. Laia, A. J. Parola, F. Pina, *Chem. Eur. J.*, **2010**, *16*, 7760-7766.

[95] C. A.T. Laia, A. J. Parola, F. Folgosa, F. Pina, *Organic and Biomolecular Chemistry* **2007**, 5, 69 -77.

[96] J. C. Lima, C. Vautier-Giongo, A. Lopes, E. Melo, F. H. Quina, A. L. Maçanita, *J. Phys. Chem. A,* **2002**, 106, 5851-5859.

[97] R. Gomes, A. J. Parola, C. A. Laia, F. Pina, *J. Phys. Chem. B*, **2007**, 111, 12059-12065.

[98] http://www.abrf.org/ABRFNews/1997/December1997/dec97Table.htmlThe, in *ABRF-Association of Bimolecular Resource Facilities, Table of Detergents*.

[99] R. Gomes, A. J. Parola, C. A. Laia, F. Pina, *Photochem. Photobiol. Sci*. **2007**, 6, 1003-1009.

[100] Küster F.W., Thiel A., Tabelle per le analisi chimiche e chimico-fisiche. 12th Ed Milano: Hoepli; **1982**. P157-160

[101] O. Gia, A. Anselmo, M. T. Conconi, C. Antonello, E. Uriarte, S. Caffieri, *J. Med. Chem*. **1996**, 39, 4489-4496.

[102] Apparently the compound precipitated as a mixture of 90% dication (protonation of the diethylamino group) and 10% monocation.

[103] T. Kottke, D. Stalke, *J. App. Cryst*. **1993**, 26, 615-619.

[104] APEX2. Data Collection Software Version 2.1-RC13, Bruker AXS, Delft, The Netherlands **2006**.

[105] Cryopad. Remote monitoring and control, Version 1.451, Oxford Cryosystems, Oxford, United Kingdom **2006**.

[106] SAINT+. Data Integration Engine v. 7.23a © 1997-2005, Bruker AXS, Madison, Wisconsin, USA.

[107] Sheldrick, G. M. SADABS v.2.01, Bruker/Siemens Area Detector Absorption Correction Program **1998**, Bruker AXS, Madison, Wisconsin, USA.

[108] Sheldrick, G. M. *Acta Cryst. A* **2008**, 64, 112-122.

[109] Sheldrick, G. M. SHELXS-97, Program for Crystal Structure Solution, University of Göttingen **1997**.

[110] Sheldrick, G. M. SHELXL-97, Program for Crystal Structure Refinement, University of Göttingen **1997**.

[111] C. L. Bird, A. T. Kuhn, *Chem. Soc. Rev*. **1981**, 10, 49-83.

[112] C. P. Wilde, D. Pisharodi, *Journal of Electroanalytical Chemistry* **1995**, *398*, 135-142.

[113] L. Michaelis, E. S. Hill, *J. Gen. Physiol.* **1933**, *16*, 859-873.

[114] P. M. S. Monk, *The Vialogens - Physicochemical Properties, Synthesis and Aplications of the Salts of 4'4-bypiridine*, Wiley, West Sussex, England, **1998.**

[115] R. Robinson and D. D. Pratt, *J. Chem. Soc*., **1922**, 1577–1585.

[116] A. R. Katritzky, P. Czerney, J. R. Levell, W. Du, *Eur. J. Org.Chem*., **1998**, 2623–2629.

[117] W. W. Porter, T. P. Vaid, A. L. Rheingold, *J. Am. Chem. Soc*. **2005**, 16559-16566.

[118] F. Pina, M. J. Melo, A. J. Parola, M. Maestri, V. Balzani, *Chem. Eur. J.* **1998**, 4, 2001-2007.

[119] F. Galindo, J. C. Lima, S. V. Luis, A. J. Parola, F. Pina, *Adv. Funct. Mat*., **2005**, 15, 541-545.

[120] M. Maestri, F. Pina, A. Roque, P. Passaniti, *J. Photochem. Photobiol A: Chem* **2000**, 137, 21-28.

[121] J. T. Edsall, J. Wyman, "Biophysical Chemistry", Academic Press, New York, **1958**, Vol 1

[122] A. Bencini, M. A. Bernardo, A. Bianchi, M. Ciampolini, V. Fusi, A. J. Parola, F. Pina, B. Valtancoli, *J. Chem. Soc., Perkin Trans. 2*, **1998**, 413-418.

[123] K. A. Conners, "Chemical Kinetics The Study of Reaction Rates in Solution", Chapter III, **1990** VCH Publishers, Inc., ISBN 3-527-28037-5.

[124] V. Petrov, F. Pina, *J. Math. Chem*. **2010**, 47, 1005-1026.

[125] L. D. Hicks, A. J. Fry, V. C. Kurzweil, *Electrochim. Acta,* **2004**, 50, 1039–1047.

[126] N. Cotelle, P. Hapiot, J. Pinson, C. Rolando, H. Vézin, *J. Phys. Chem. B*, **2005**, 109, 23720-23729.

[127] See Supplementary material NMR data and numeration of hydrogens and carbons.

[128] F.W. Küster, A. Thiel, Tabelle per le analisi chimiche e chimico-fisiche. 12th Ed Milano: Hoepli; **1982**, 157-160.

[129] N. Leventis, C. Sotiriou-Leventis, A. M. M. Rawashdeh, G. Zhang, *Electrochim. Acta* 50 **2003**, 48, 2799-2806.

[130] V. Balzani, G. Bergamini, F. Marchioni, P. Ceroni, *Coordin. Chem Rev*. **2006**, 250, 1254-1266.

[131] N. Armaroli, G. Accorsi, A. Listorti, K. Yoosaf, *Chem. Soc Rev*, **2009**, 38, 1690-1700.

[132] Y. Tor, H. Joshi, R. Jamshidi, Angew. *Chem. Int. Ed*. **1999**, 38, 19, 2721-2725.

[133] R. Kumar, D. Kumar, A. K. Chakraborti, *Synthesis***, 2007**, 299-303.

[134] H. Le Bozec, P. Dupau, T. Renouard, *Tet. Lett.,* **1996**, 37, 42, 7503-7506.

[135] A. Ohsawa, T. Itoh, K. Nagata, A. Kurihara, M. Miyazaki, *Tett*., **2002**, 43, 3105-3108.

[136] A. Ohsawa, T. Itoh, K. Nagata, M. Miyazaki, H. Ishikawa, A. Kurihara, *Tett.*, **2004**, 60, 6649-6655.

[137] Y. Tor, D. Tzalis, *J. Am. Chem. Soc*., **1997**, 119, 852-853.

[138] J.P. Sauvage, C. Dietrich-Buchecker, M. C. Jiménez, *Tetrah. Letters*, **1999**, 40, 3395-3396.

[139] J.P. Sauvage, C. Dietrich-Buchecker, M. C. Jimenez-Molero, *Chem. Eur. J.* **2002**, 8, 6, 1456-1466.

[140] P. T. Perumal, M. Anniyappan, D. Muralidharan, *Synthetic Communications*, **2002**, 32 (4), 659-663.

[141] J. Alvarez-Builla, R. Alajarin, P. Jordán, J. J. Vaquero, *Synthesis*, **1995**, 4, 389-391.